Electronic Supplementary Material (ESI) for Organic & Biomolecular Chemistry.


# Supporting Information for

# A Molecular Chemodosimeter to Probe "Closed Shell" Ions in Kidney Cells

Amine Assel[a], Meagan Stanley[b], Rashid Mia[b&c] Besma Boulila[a], Peter J. Cragg[d], Iyanuoluwani Owolabie[e], Meredith Hetrick[e], Alex Flynt[e], Karl J Wallace[b]* and Hichem Ben Jannet[a]

[a]Laboratory of Heterocyclic Chemistry, Natural Products and Reactivity (LR11ES39), Team: Medicinal Chemistry and Natural Products, Faculty of Science of Monastir, University of Monastir, Avenue of Environment, 5019 Monastir, Tunisia.

[b]Department of Chemistry and Biochemistry, School of Mathematics and Natural Science, The University of Southern Mississippi, 118 College Drive, Hattiesburg, MS 39406, USA.

[c]Department of Chemistry and Biochemistry, Stephen F. Austin State University, P.O. Box 13006 SFA Station, Nacogdoches, TX 75962, USA.

[d]School of Applied Chemical Sciences, University of Brighton, Brighton, BN2 4GJ, UK.

[e]Department of Cellular and Molecular Biology, The University of Southern Mississippi, 118 College Drive, Hattiesburg, MS 39406, USA.

Table of Contents

# 1.0 General Methods and Instrumentation

One-dimensional $^{1}H$, and C NMR spectra were recorded on a Bruker *Avance 400* spectrometer operating at a proton frequency of 400.13 MHz and equipped with a standard BFO 5 mm two-channel probe in the appropriate deuterated solvents or were recorded on a Bruker *Ultrashield plus* 400 or 600 MHz spectrometer. Chemical shifts are reported in parts per million (ppm) downfield from tetramethylsilane (0 ppm) as the internal standard, and coupling constants (*J*) are recorded in hertz (Hz). The multiplicities in the $^{1}H$ NMR spectra are reported as (br) broad, (s) singlet, (d) doublet, (dd) doublet of doublets, (ddd) doublet of doublet of doublets, (*t*) triplet, (*sp*) septet and (*m*) multiplet. All spectra were recorded at ambient temperature (298 K) unless otherwise stated. UV-Vis experiments were performed on an Evolution 220 (ThermoFisher Scientific) UV-Vis spectrometer. Low-resolution mass spectra were measured with Finnigan TSQ70. High-resolution mass spectra (HRMS) were recorded at the College of Sciences Major Instrument Cluster in the Department of Chemistry and Biochemistry at Old Dominion University. The analysis was completed using positive-ion mode electrospray ionization (ESI) Apollo II ion source on a Bruker 10 Tesla APEX -Qe FTICR-MS. IR spectra were recorded on a Nicolet *Summit* FT-IR paired with an Everest *Smart Orbit* ATR attachment. The characteristic functional groups are reported in wavenumbers ($cm^{-1}$) and are described as weak (w), medium (m), strong (s), and very strong (vs). Fluorescence steady-state experiments were carried out on a QuantaMaster™ 40 Intensity Based spectrofluorometer from PTI technologies in the steady-state mode. Lifetime fluorescence were carried out on a Deltaflex TCSPC (Horbia Scientific) and the data fitted to the appropriate exponential. DFT calculations were carried out using Spartan '20.[1] All chemical reagents were purchased from commercial sources and used as received. Precursors 3-acetyl-4-hydroxcoumarin (**A**) and 2-((2-quinolin-8-yl) oxy)acetohydrazide (**B**) were prepared according to published procedures.[2, 3]

## 2.0 Synthesis and characterization of QHC1 and QHC2:

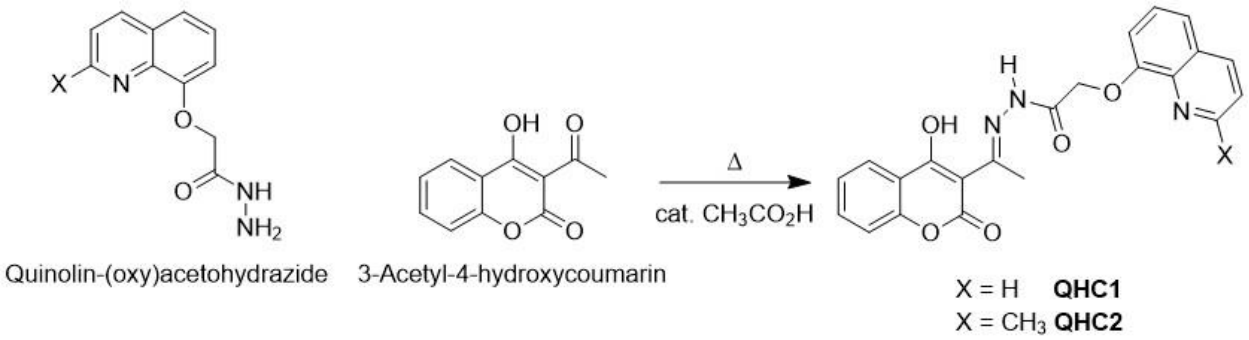


The quinolin-(oxy)acetohydrazide (X = H, $CH_3$) (1.0 mmol) was dissolved in ethanol (60 mL), and then 3-acetyl-4-hydroxycoumarin (1.1 mmol) was added in the presence of a catalytic amount of acetic acid and refluxed for 3 hours, the precipitate was filtered and washed with ethanol. The solid was dried under vacuum. and the compounds **QHC1** and **QHC2** were obtained with 88% and 79% yields, respectively.

(*E*)-N'-(1-(4-hydroxy-2-oxo-2H-chromen-3-yl)ethylidene)-2-(quinolin-8-yloxy)acetohydrazide **(QHC1)**: (0.87 g, 2.15 mmol, yield 88 %) mp: 223–226 °C $^1$H NMR (300 MHz, DMSO-$d_6$) δ 15.81 (s, 1H, OH), 8.94 (d, $J$ = 5.686 Hz, 1H, H15), 8.42 (dd, $J$ = 8.350, 1.726 Hz, 1H, H17), 7.97 (dd, $J$ = 7.860, 1.712 Hz, 1H, H5), 7.62 (m, 4H, H7,18,16,20), 7.33 (m, 3H, H19,8,6), 5.08 (s, 2H, H12), 2.69 (s, 3H, H10). $^{13}$C NMR (75 MHz, DMSO) δ 179.3(C4), 171.9(C9), 166.8(C11), 161.8(C2), 154.1(C13), 153.6(C8a), 149.8(C15), 134.0(C13a), 137.0(C17), 134.9(C7), 129.7(C17a), 127.4(C20), 126.1(C5), 124.4(C6), 122.6(C16), 122.0(C18), 119.9(C4a), 116.8(C8), 113.0(C19), 95.8(C3), 68.5(C12),17.9(C10). ESI-MS (negative mode) m/z $[M-H]^-$ = 402.1; IR (ATR solid); 3525(w) $NH_{amide}$, 3224(w) $OH_{enol}$, 3025(w) $CH_{\nu\text{-}Ar}$, 2763(w) $CH_{\nu\text{-}methyl/methylene}$, 1685(m) $NH_{\nu\text{-}amideI}$, 1608(m) $CN_{imine}$, 1557(m), $NCO_{amideII}$; 1254(m) $CO_{ester}$, 1117(m) $CO_{\delta\text{-}lactone}$, 752(s) $CH_{\delta\text{-}oopAr}$ $cm^{-1}$; HRMS-ESI; Exact Mass $[C_{22}H_{17}N_3O_5 + H]^+$ m/z = 404.124097 Observed Mass Found for $[C_{22}H_{17}N_3O_5 + H]^+$; m/z = 404.124018

(*E*)-N'-(1-(4-hydroxy-2-oxo-2H-chromen-3-yl)ethylidene)-2-((2-methylquinolin-8-yl)oxy)acetohydrazide **QHC2:** (0.81 g, 1,93 mmol, yield 79 %); mp: 234–237 °C, $^1$H NMR (400 MHz, DMSO-$d_6$ ): δ(ppm) = 15.61 (1H, s, OH), 8.27 (1H, d, J = 8.44, H17), 7.96 (1H, dd,J = 7.88, 1.47, H5), 7.66 (1H, td, J = 7.67, 1.56, H7), 7.58 (1H, d, J = 8.10, H18), 7.47 (1H, d, J = 8.64,

H20), 7.47 (1H, d, J = 8.45, H16), 7.30 (1H, t, J = 7.61, H6), 7.30 (1H, m, H8), 7.30 (1H, m, H19), 5.04 (2H, s, H12), 2.67 (3H, s, H21), 2.65 (3H, s, H10). $^{13}$C NMR (100 MHz, DMSO-$d_6$): δ(ppm) = 178.9 (C4), 172.1 (C2), 172.1 (C9), 166.6 (C11), 161,3 (C2), 157.7 (C15), 153.2 (C13), 153.1 (C8a), 139.0 (C13a), 136.5 (C17), 134.3 (C7), 127.5 (C17a), 125.8 (C20), 125.6 (C5), 123.9 (C6), 122.7 (C16), 121.3 (C18), 119.4 (C4a), 116.3 (C8), 112.8 (C19), 95.4 (C3), 68.3 (C12), 24.8 (C21), 17.3 (C10). ESI-MS (positive mode) m/z $[M+H]^+$ = 418.1; IR (ATR solid) 3536(m) $NH_{\nu\text{-amide}}$, 3293(w), $OH_{\nu\text{-enol}}$, 3076(w) $CH_{\nu\text{-Ar}}$, 2743(w) $CH_{\nu\text{-methyl/methylene}}$,1669(s) $NH_{\nu\text{-amideI}}$, 1605(s) $CN_{\nu\text{-imine}}$, 1540(m) $NCO_{\nu\text{-amideII}}$, 1218-1262(s) $CO_{\nu\text{-ester}}$, 1116(s) $CO_{\delta\text{-lactone}}$, 752(s) $CH_{\delta\text{-oopAr}}$ $cm^{-1}$; HRMS-ESI; Exact Mass $[C_{23}H_{19}N_3O_5 + H]^+$ m/z = 418.139747, Observed Mass Found for $[C_{23}H_{19}N_3O_5 + H]^+$; m/z = 418.139619.

## 3.0 NMR studies

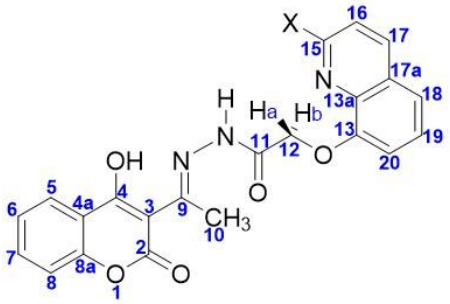


**Fig. S1** The numbering scheme used for the NMR assignments for **QHC1** and **QHC2**.

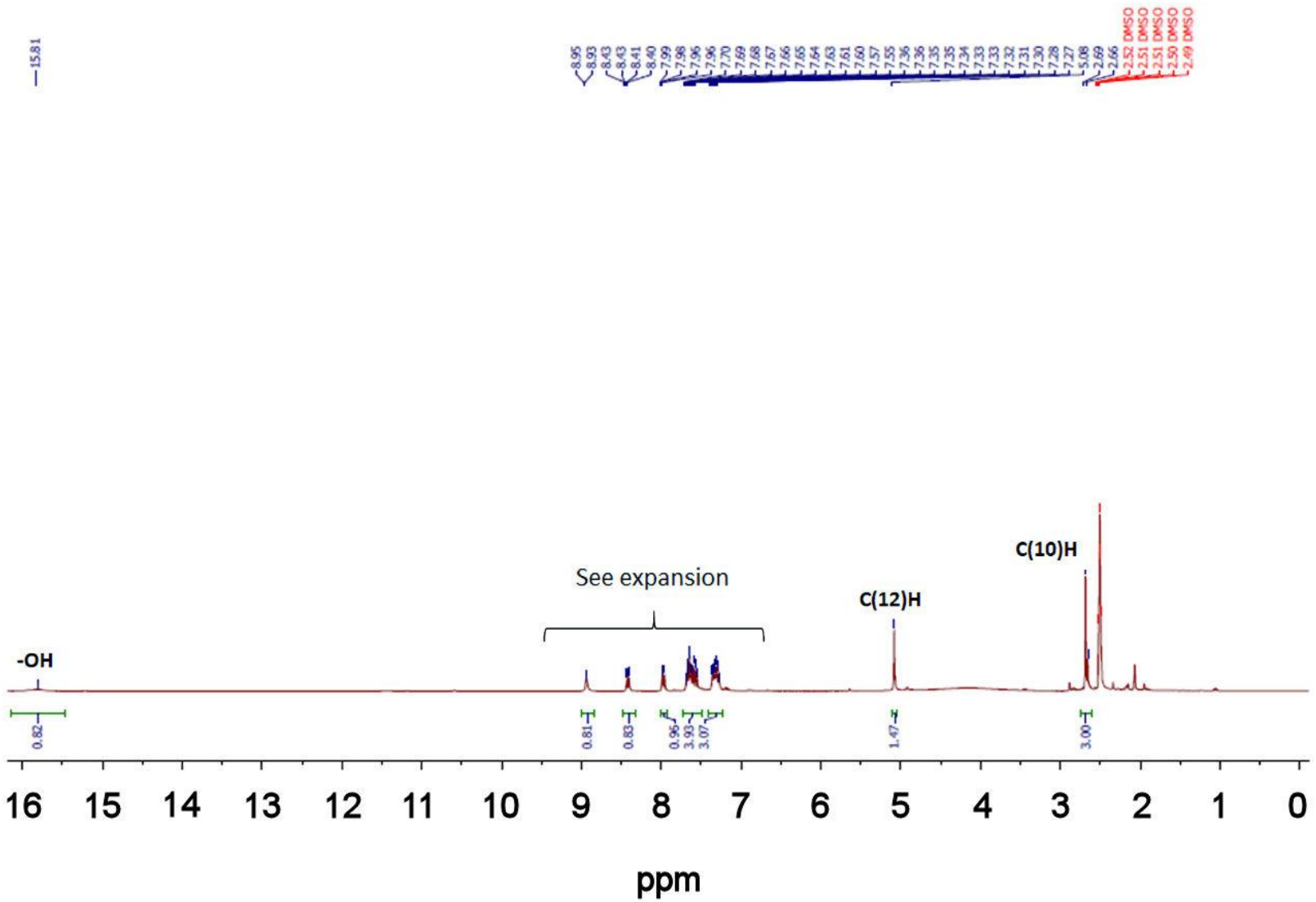


**Fig. S2** The $^{1}$H-NMR spectrum of **QHC1** in DMSO-$d_6$, 298 K (full spectrum).

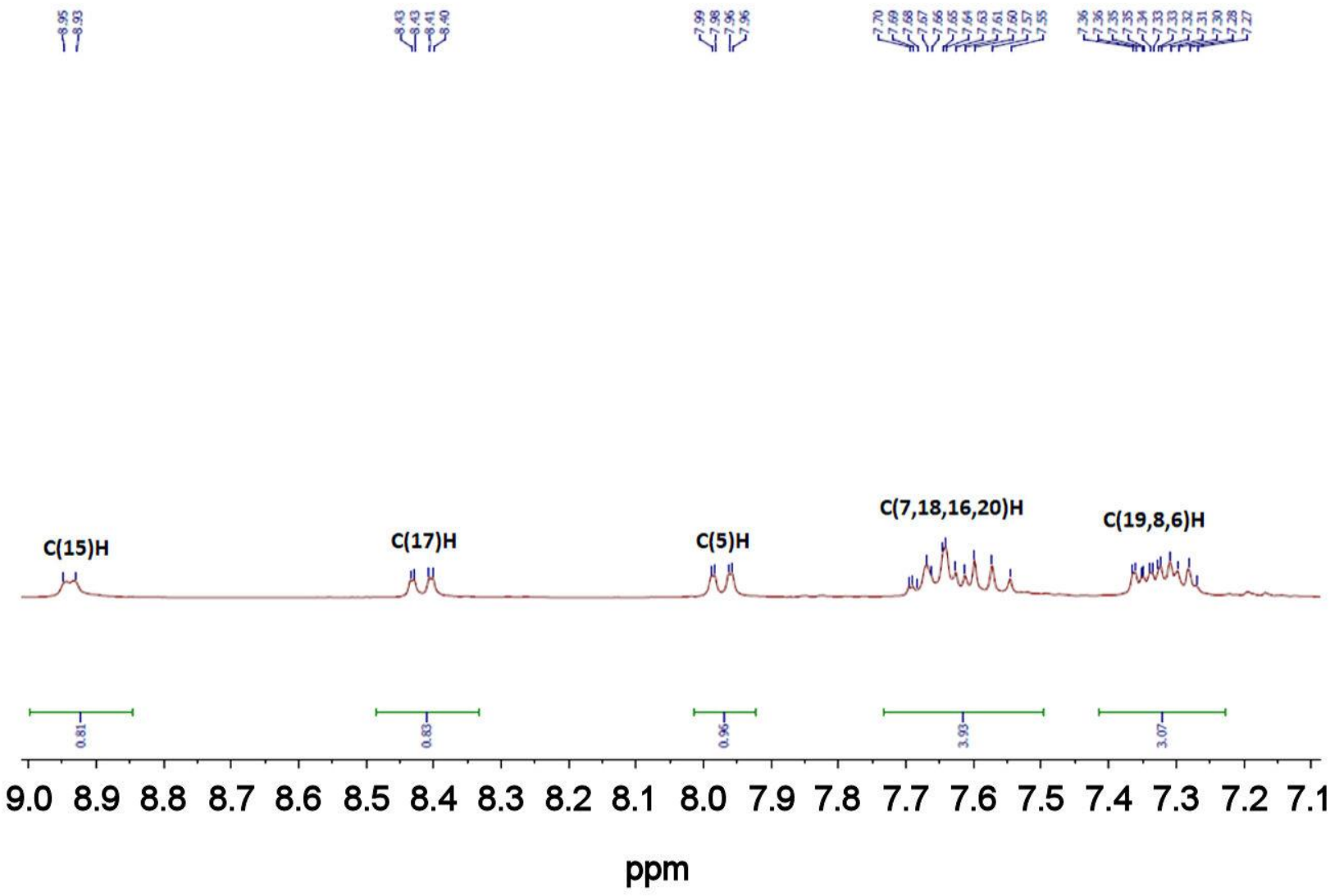


**Fig. S3** The $^{1}$H-NMR spectrum of **QHC1** in DMSO-$d_6$ 298 K (expansions).

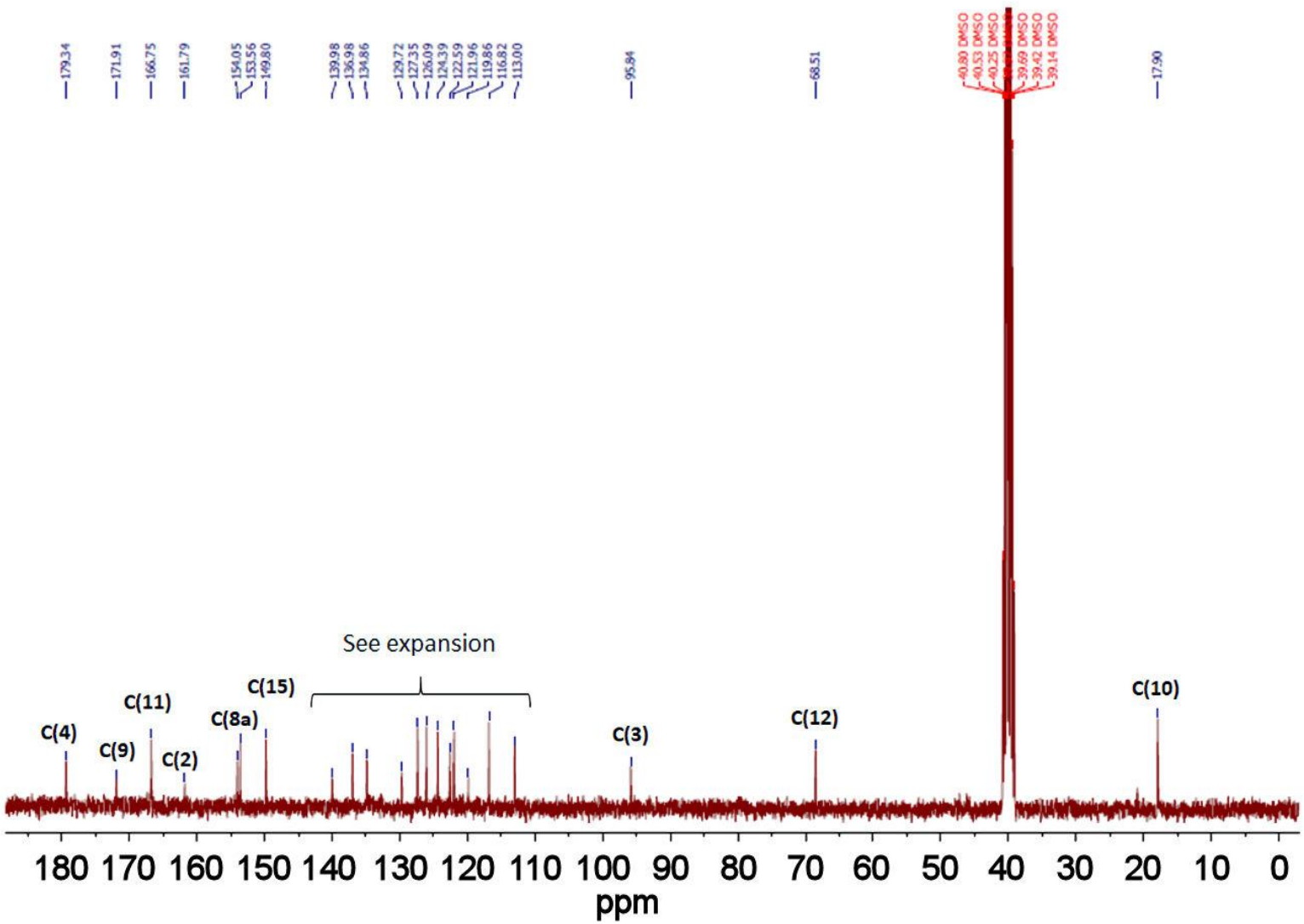


**Fig. S4** The $^{13}$C-NMR spectrum of **QHC1** in DMSO-$d_6$, 298 K.

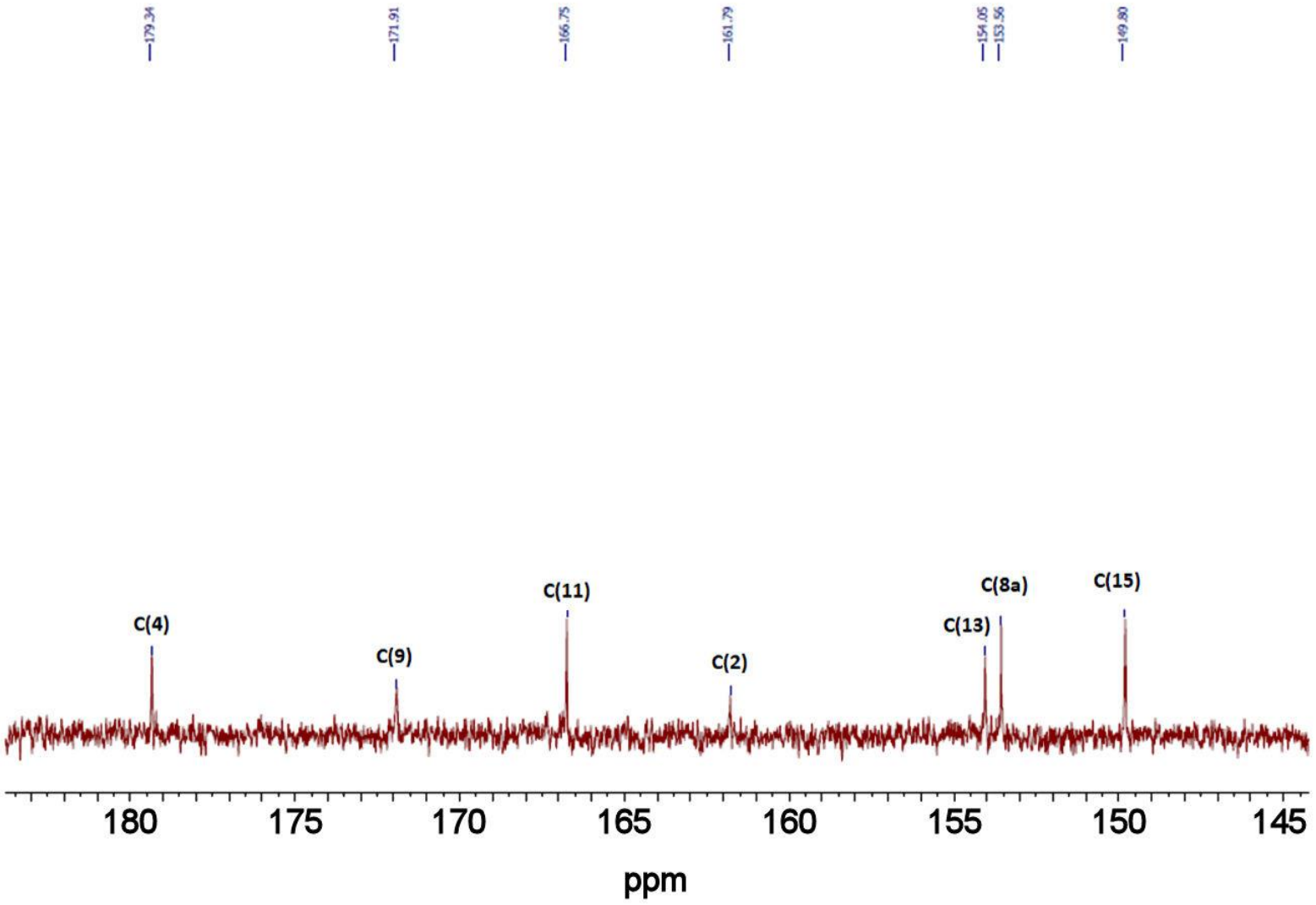


**Fig. S5** The $^{13}$C-NMR spectrum of **QHC1** in DMSO-$d_6$, 298 K.

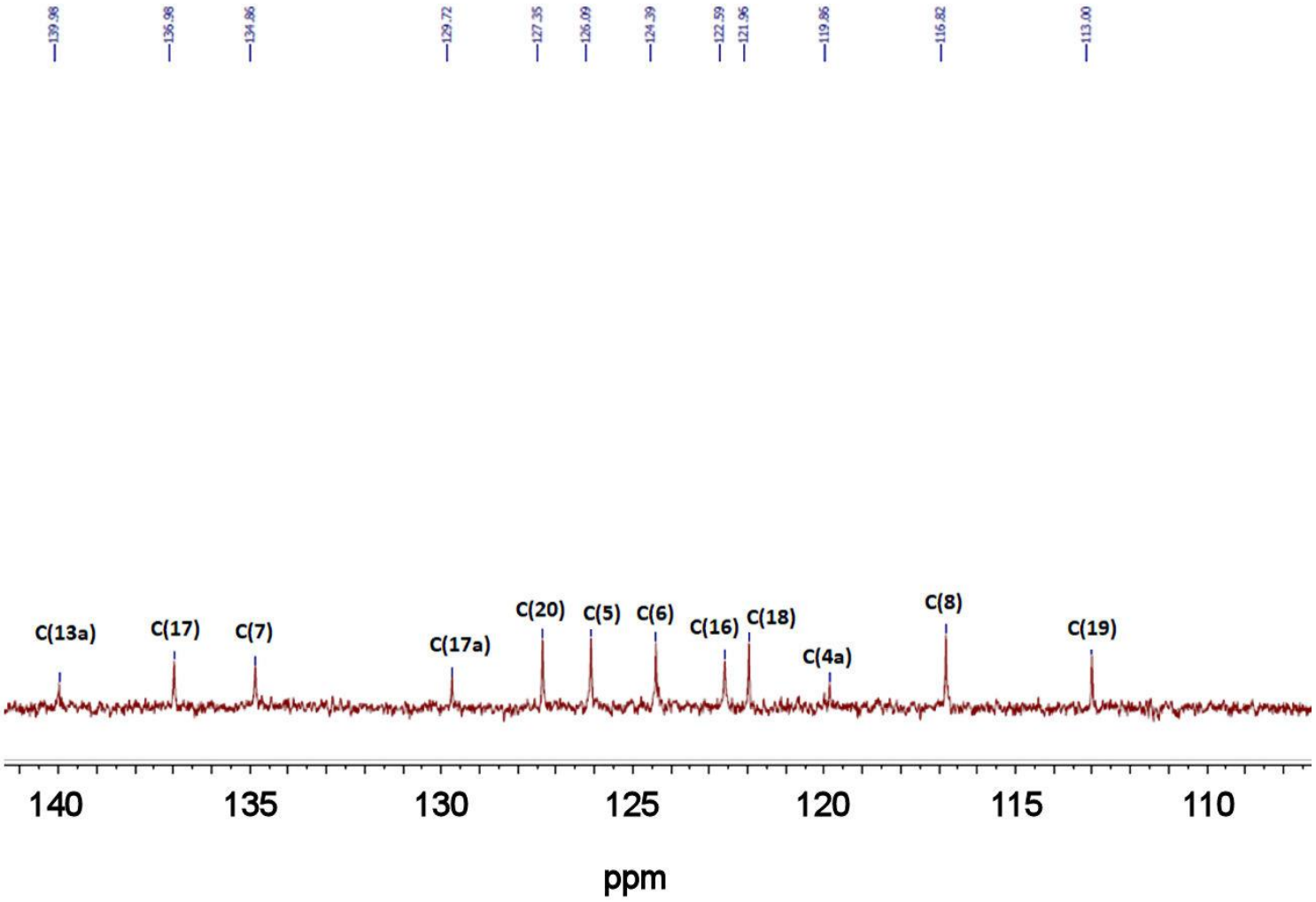


**Fig. S6** The $^{13}$C-NMR spectrum of **QHC2** in DMSO-$d_6$, 298 K.

**Table S1** Chemical shifts $^{1}H$ and $^{13}C$ for **QHC2**.

| | **$^{1}H$ NMR** | **$^{13}C$ NMR** |
|---|---|---|
| 2 | NA | 161.3 |
| 3 | NA | 95.4 |
| 4 | NA | 178.9 |
| 4a | NA | 119.4 |
| 5 | 7.96 (1H dd *J* = 7.88, 1.47) | 125.6 |
| 6 | 7.30 (1H, t *J* = 7.61) | 123.9 |
| 7 | 7.66 (1H td *J* = 7.67, 1.56) | 134.3 |
| 8 | 7.30 (1H, m) | 116.3 |
| 8a | NA | 153.1 confirmed by HMBC ($^{3}J$ C(8)H and C(7)H |
| 9 | NA | 172.1 |
| 10 | 2.65 (3H, s) | 17.3 |
| 11 | NA | 166.6 |
| 12 | 5.04 (2H, s) | 68.3 |
| 13 | NA | 153.2 confirmed by HMBC ($^{4}J$ C(12)H; $^{2}J$ C(20)H); $^{3}$J C(19)H & $^{5}$J C(16)H |
| 13a | NA | 139.0 |
| 15 | NA | 157.7 confirmed by HMBC ($^{2}J$ C(21)H) |
| 16 | 7.47 (1H, d *J* = 8.45) | 122.7 confirmed by HMBC ($^{3}J$ C(21)H) |
| 17 | 8.27 (1H d *J* = 8.44) | 136.5 |
| 17a | NA | 127.5 |
| 18 | 7.58 (1H d *J* = 8.10) | 121.3 |
| 19 | 7.30 (1H, m) | 112.8 |
| 20 | 7.47 (1H *d J* = 8.64) | 125.8 |
| 21 | 2.67 (3H, s) | 24.8 |
| OH | 15.61 | NA |

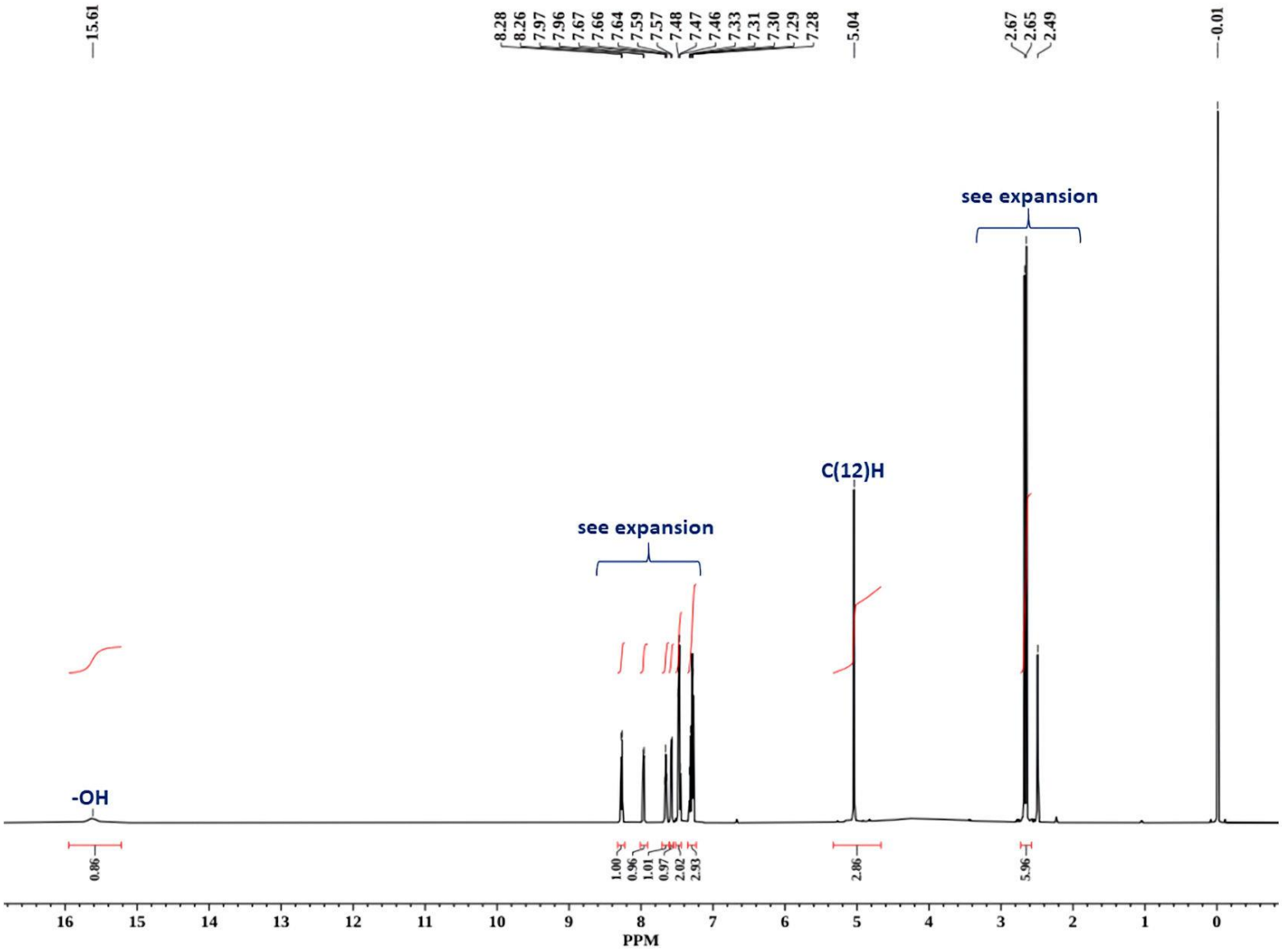


**Fig. S7** The $^{1}$H-NMR spectrum of **QHC2** in DMSO-$d_{6,}$ 298 K (full spectrum).

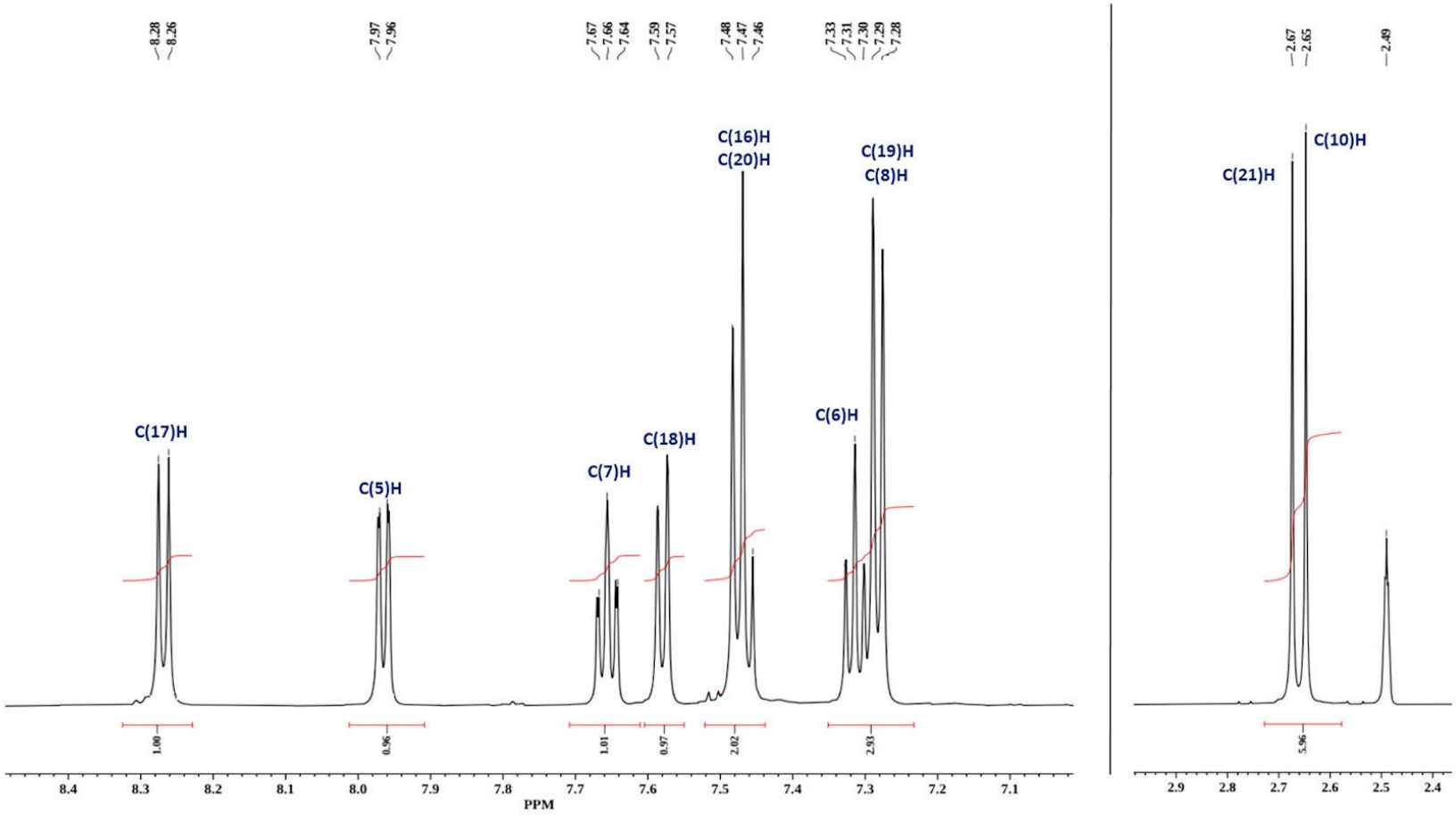


**Fig. S8** The $^{1}$H-NMR spectrum of **QHC2** in DMSO-$d_6$ 298 K (expansions).

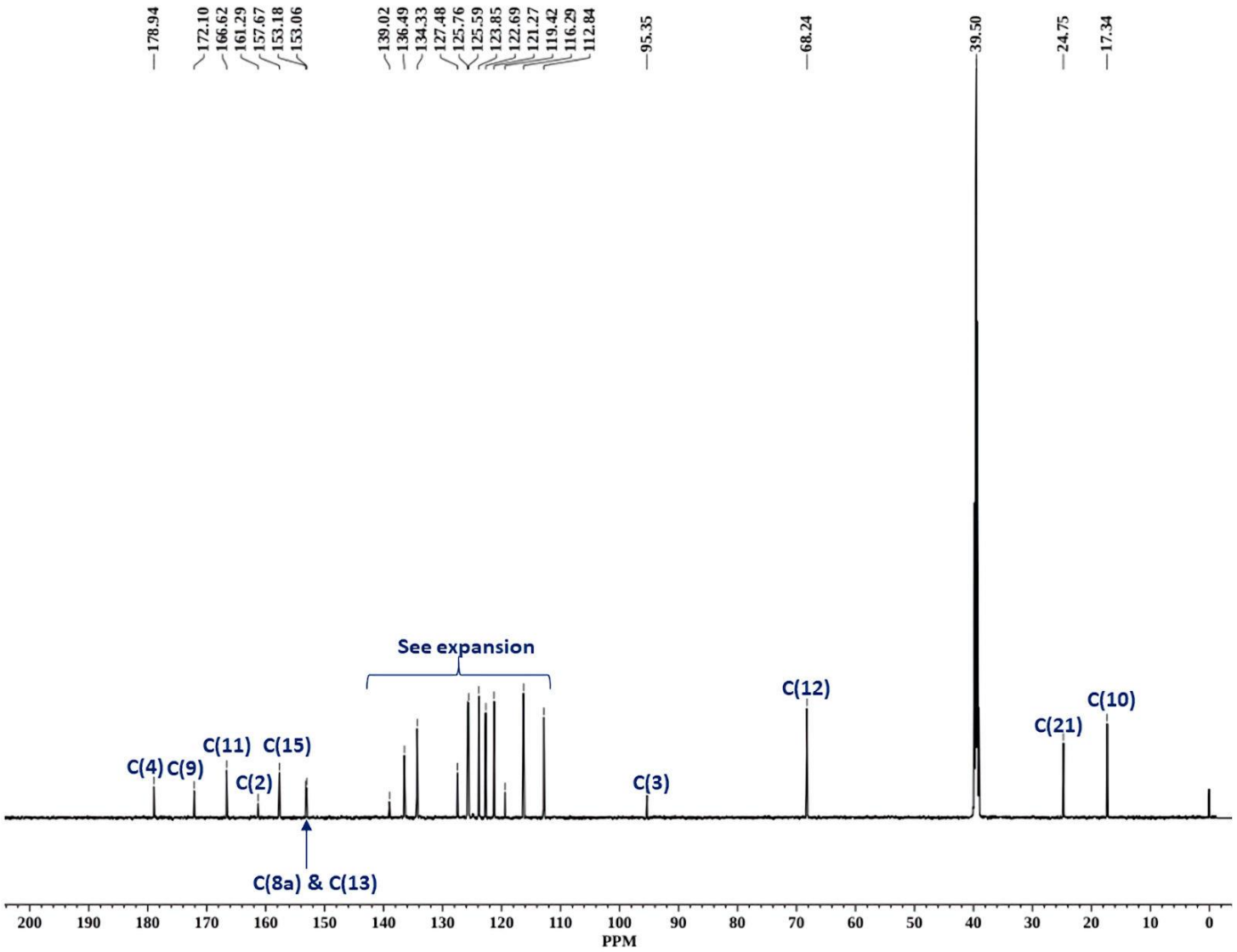


**Fig. S9** The $^{13}$C-NMR spectrum of **QHC2** in DMSO-$d_6$, 298 K

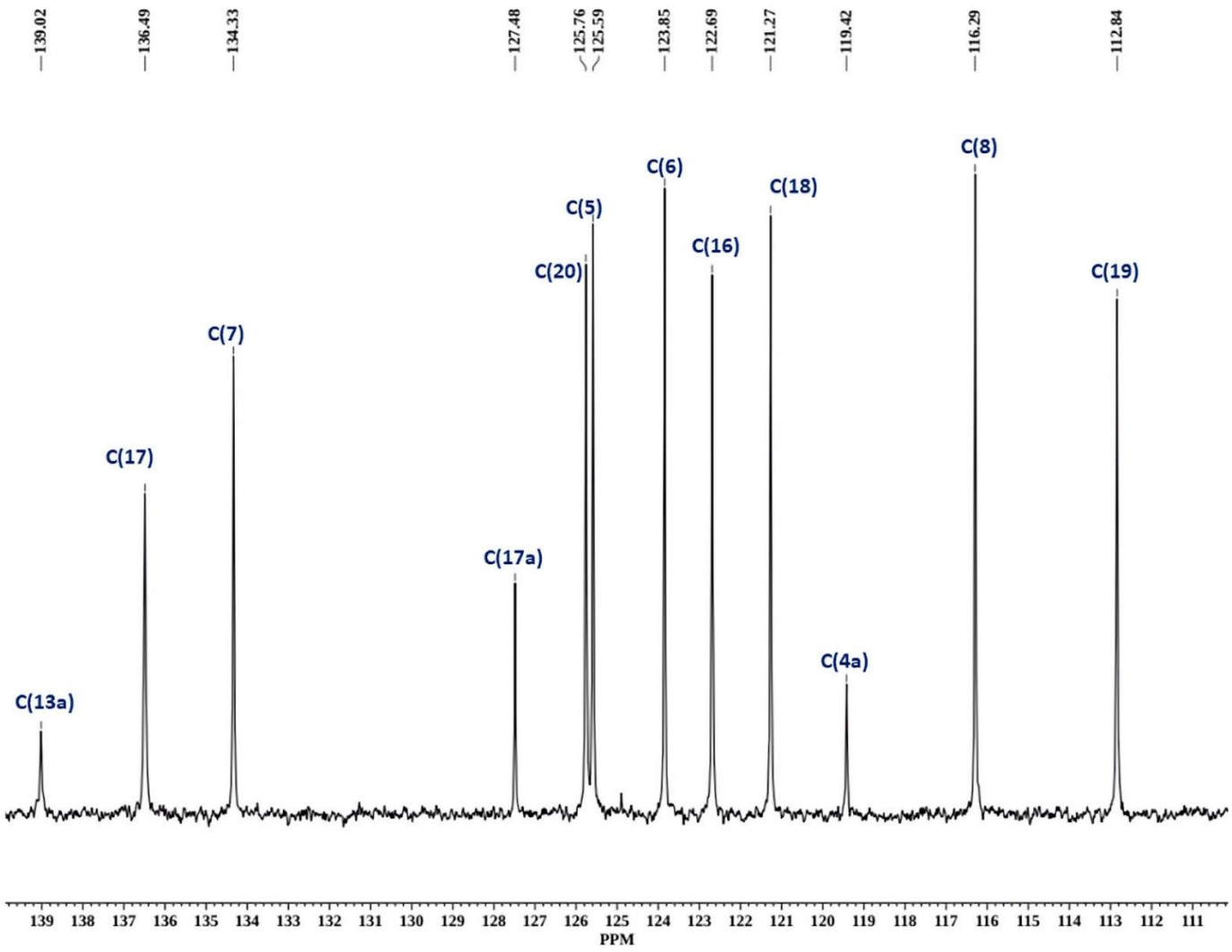


**Fig. S10** The $^{13}$C-NMR spectrum of **QHC2** in DMSO-$d_6$, 298 K (expansion).

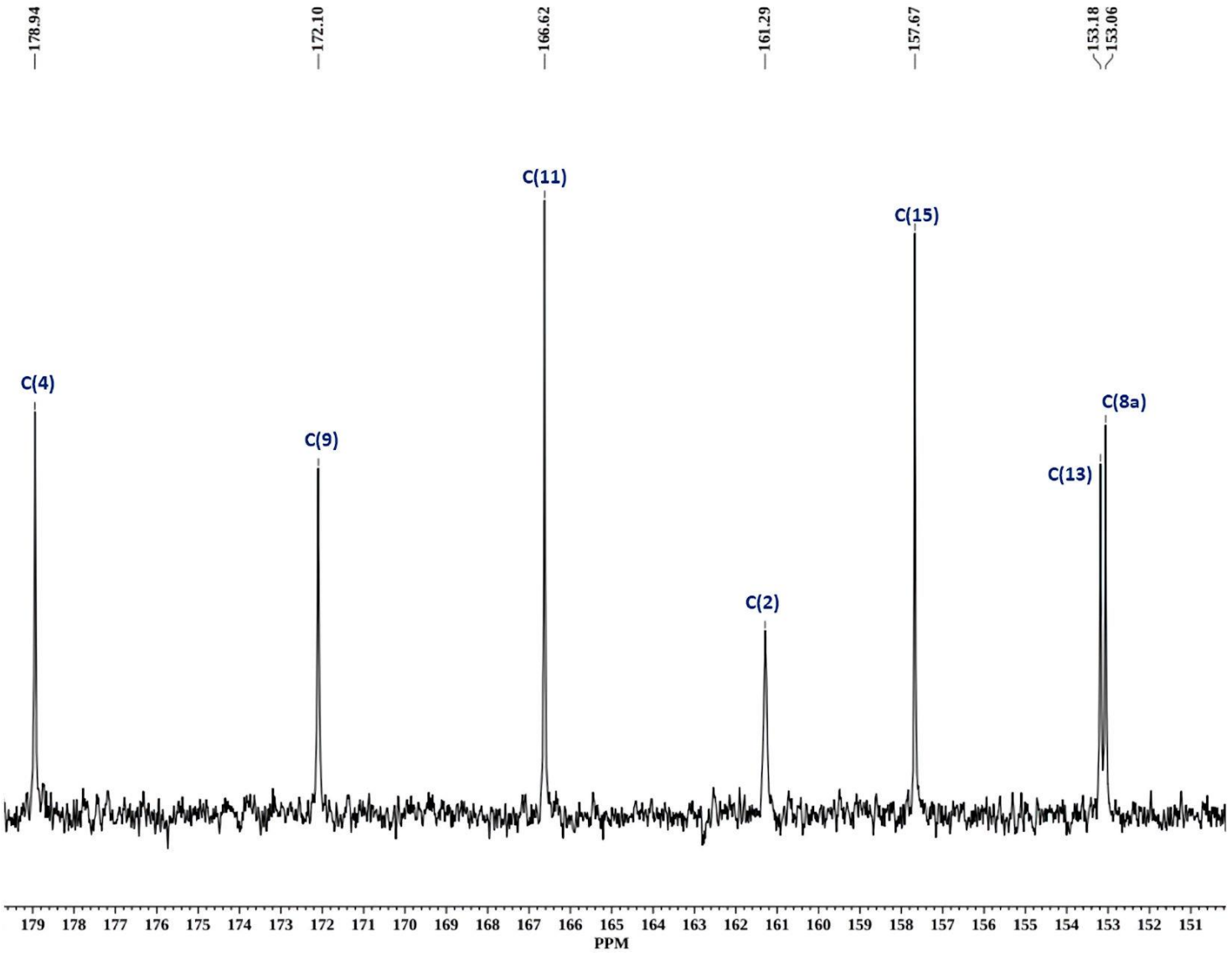


**Fig. S11** The $^{13}$C-NMR spectrum of **QHC2** in DMSO-$d_6$, 298 K (expansion).

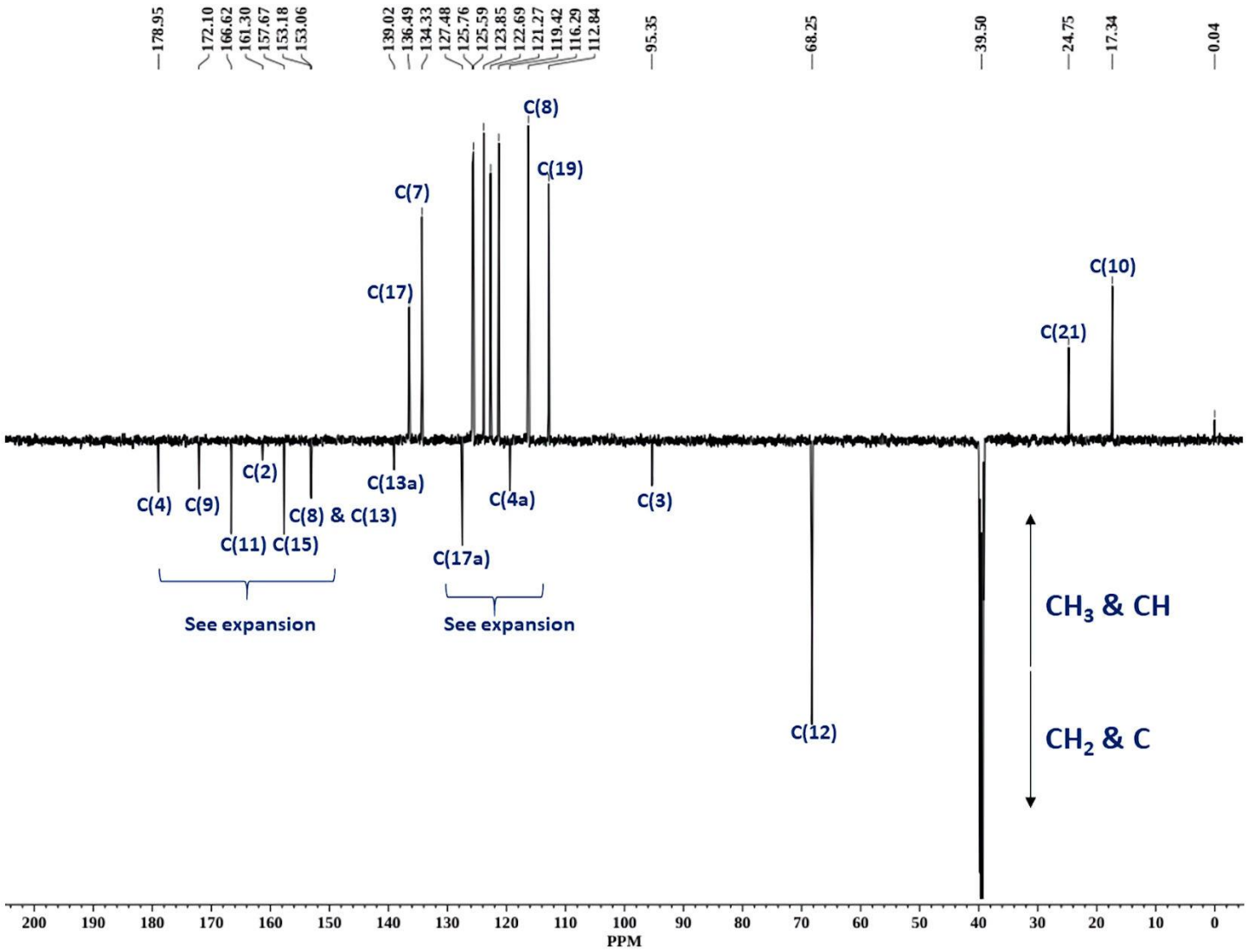


**Fig. S12** The $^{13}C$ APT-NMR spectrum of **QHC2** in DMSO-$d_6$, 298 K

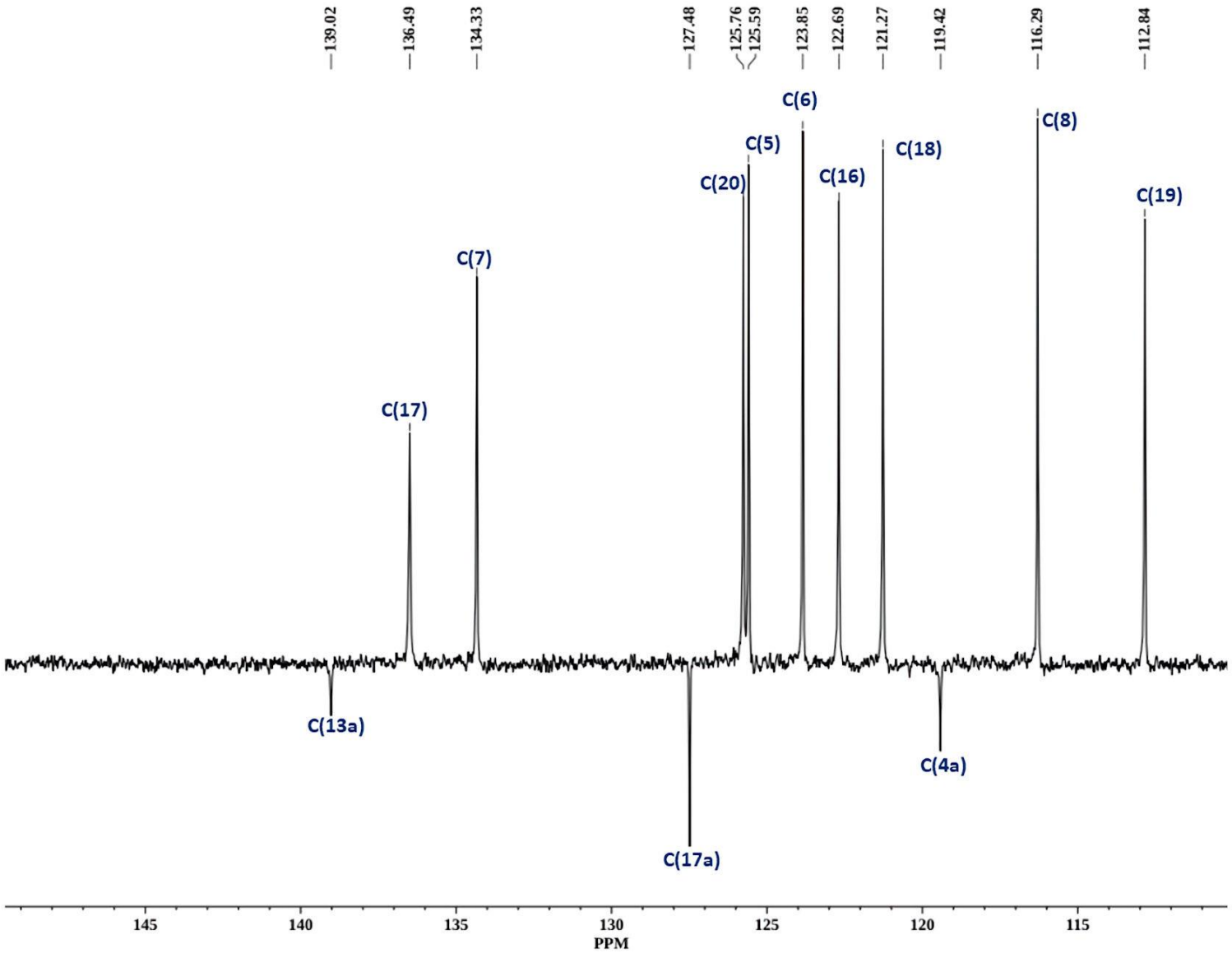


**Fig. S13** The $^{13}$C APT-NMR spectrum of **QHC2** in DMSO-$d_6$, 298 K (expansion).

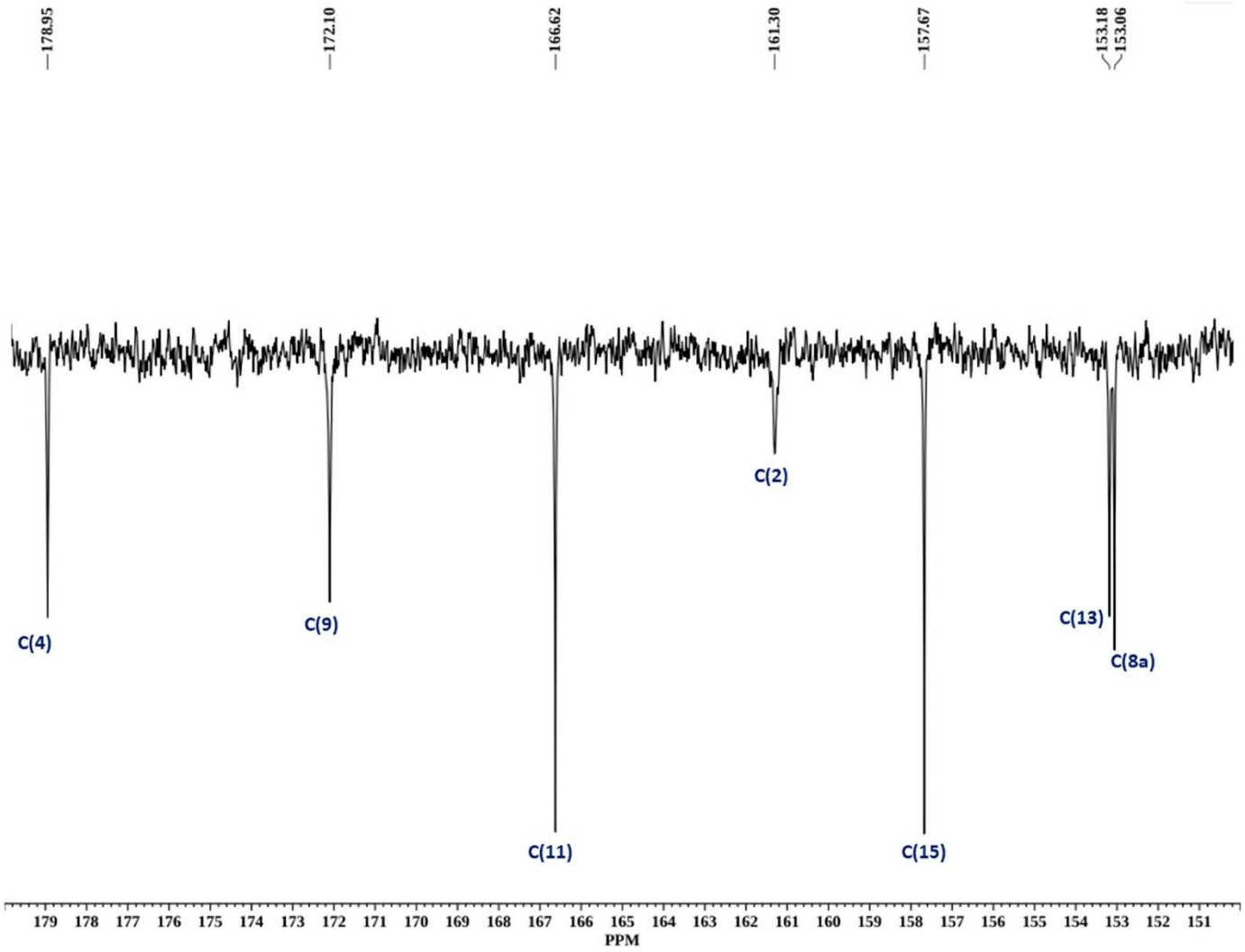


**Fig. S14** The $^{13}$C APT-NMR spectrum of **QHC2** in DMSO-$d_6$, 298 K (expansion).

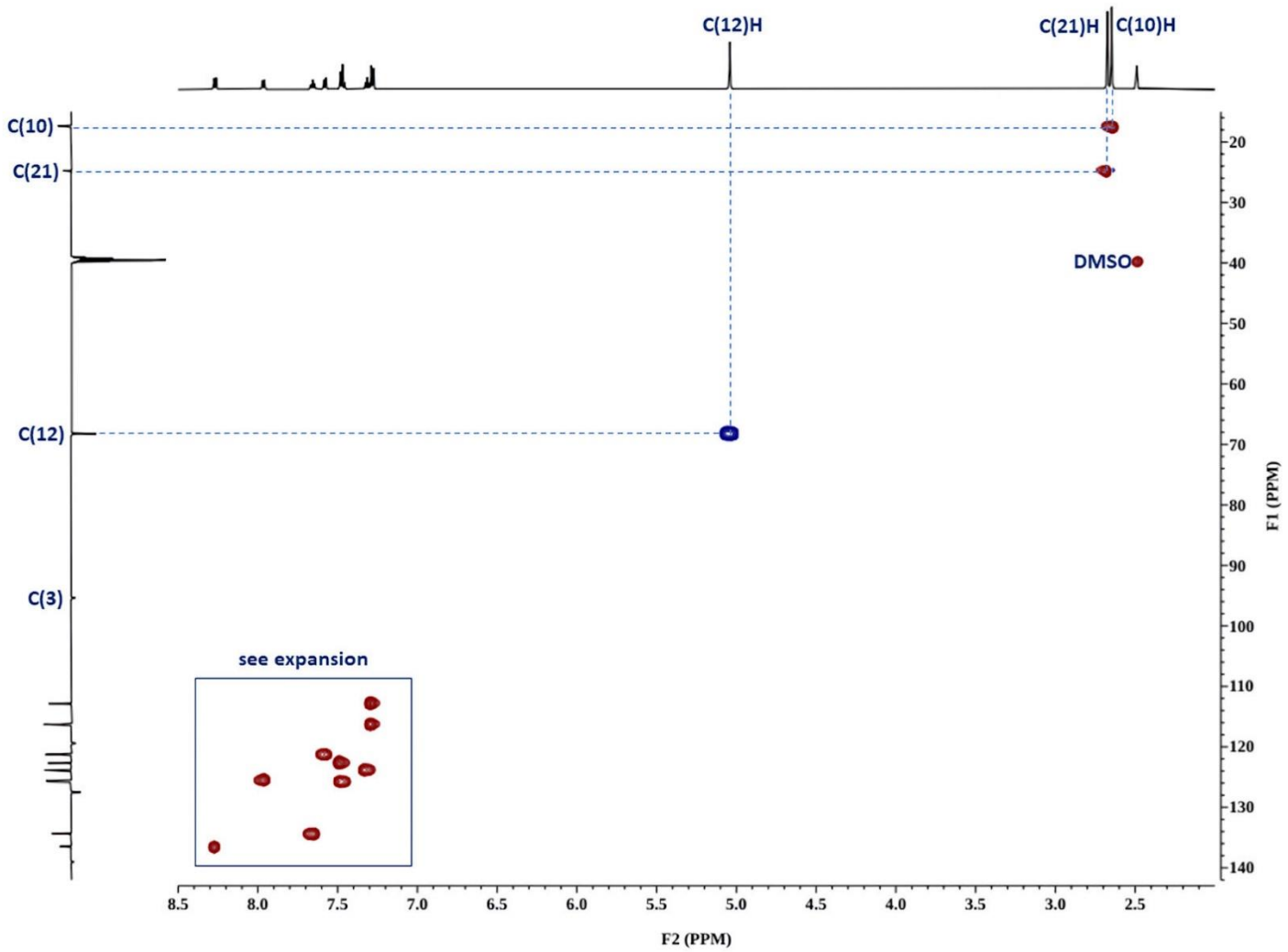


**Fig. S15** The HSQC spectrum of **QHC2** in DMSO-$d_6$, 298 K.

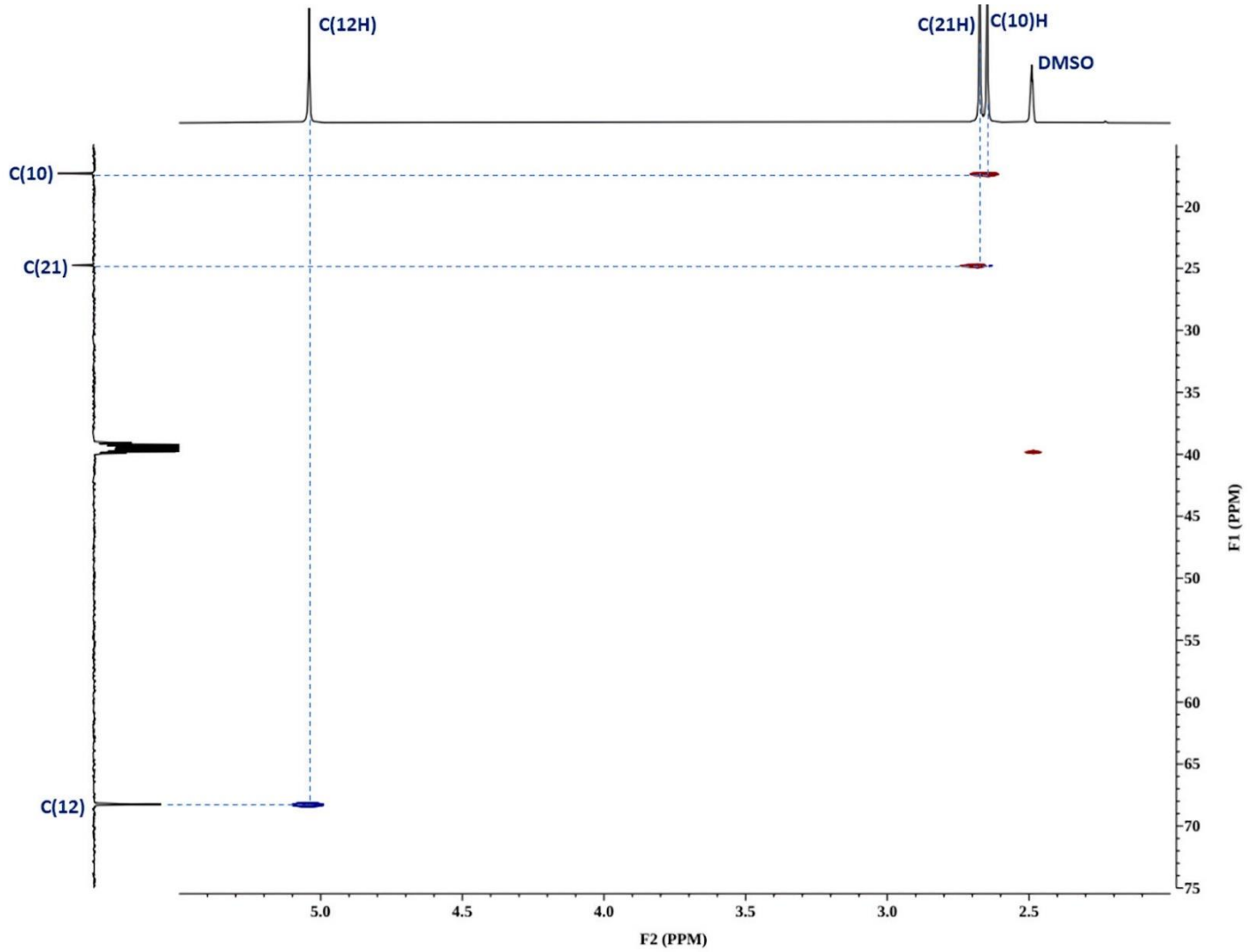


**Fig. S16** The HSQC spectrum of **QHC2** in DMSO-$d_6$, 298 K (expansion).

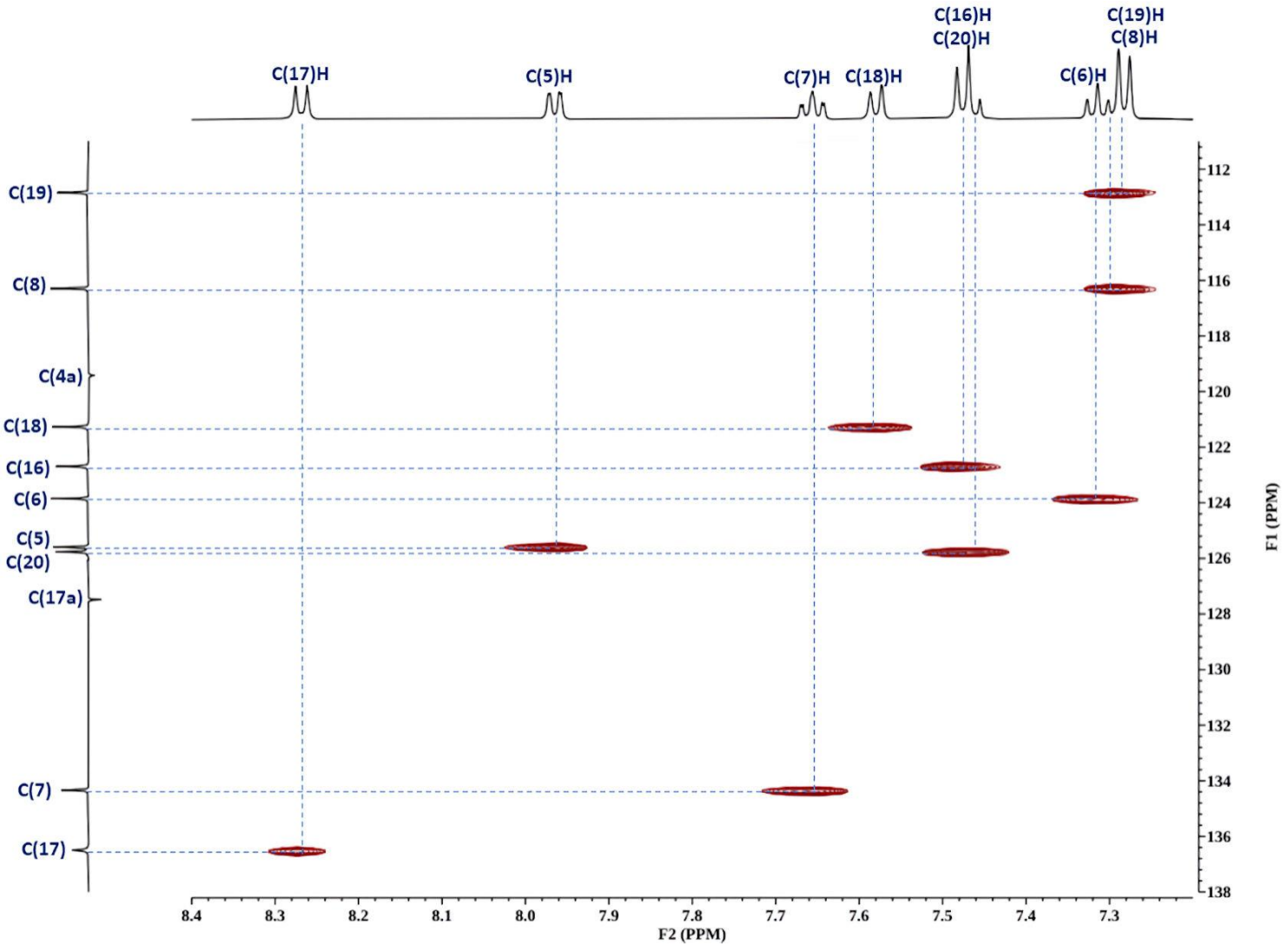


**Fig. S17** The HSQC spectrum of **QHC2** in DMSO-$d_6$, 298 K (expansion).

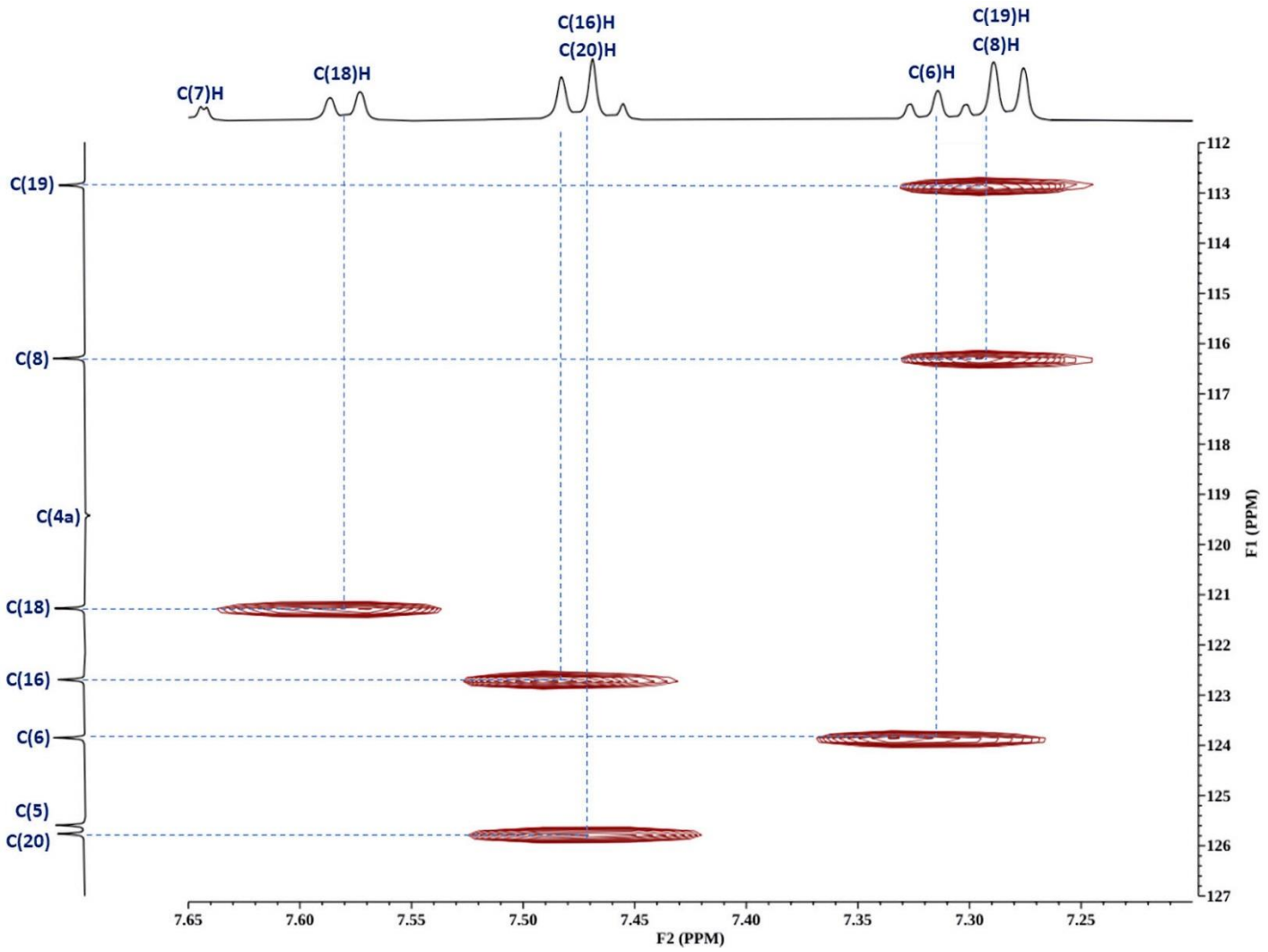


**Fig. S18** The HSQC spectrum of **QHC2** in DMSO-$d_6$, 298 K (expansion).

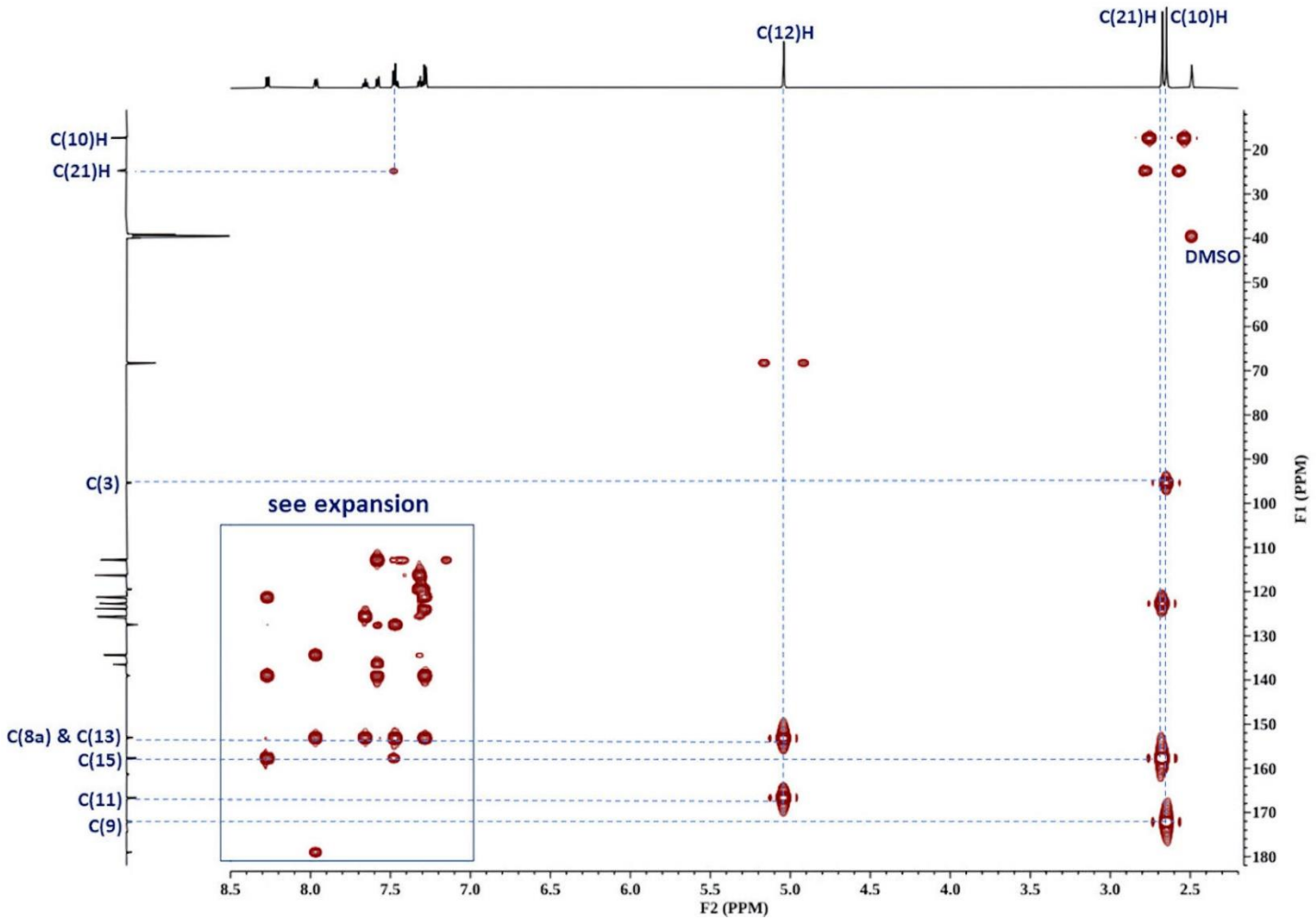


**Fig. S19** The HMBC spectrum of **QHC2** in DMSO-$d_6$, 298 K.

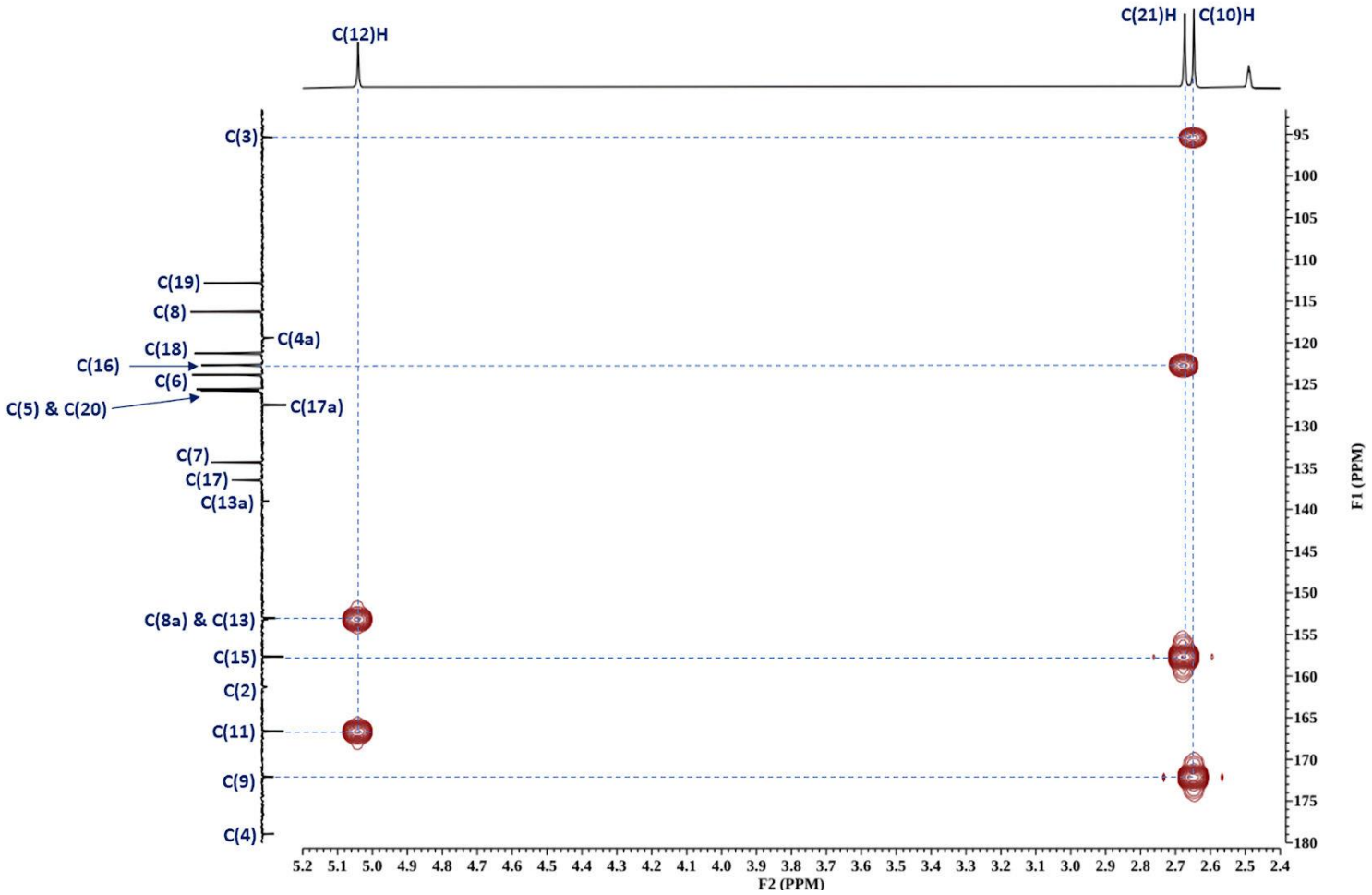


**Fig. S20** The HMBC spectrum of **QHC2** in DMSO-$d_6$, 298 K (expansion).

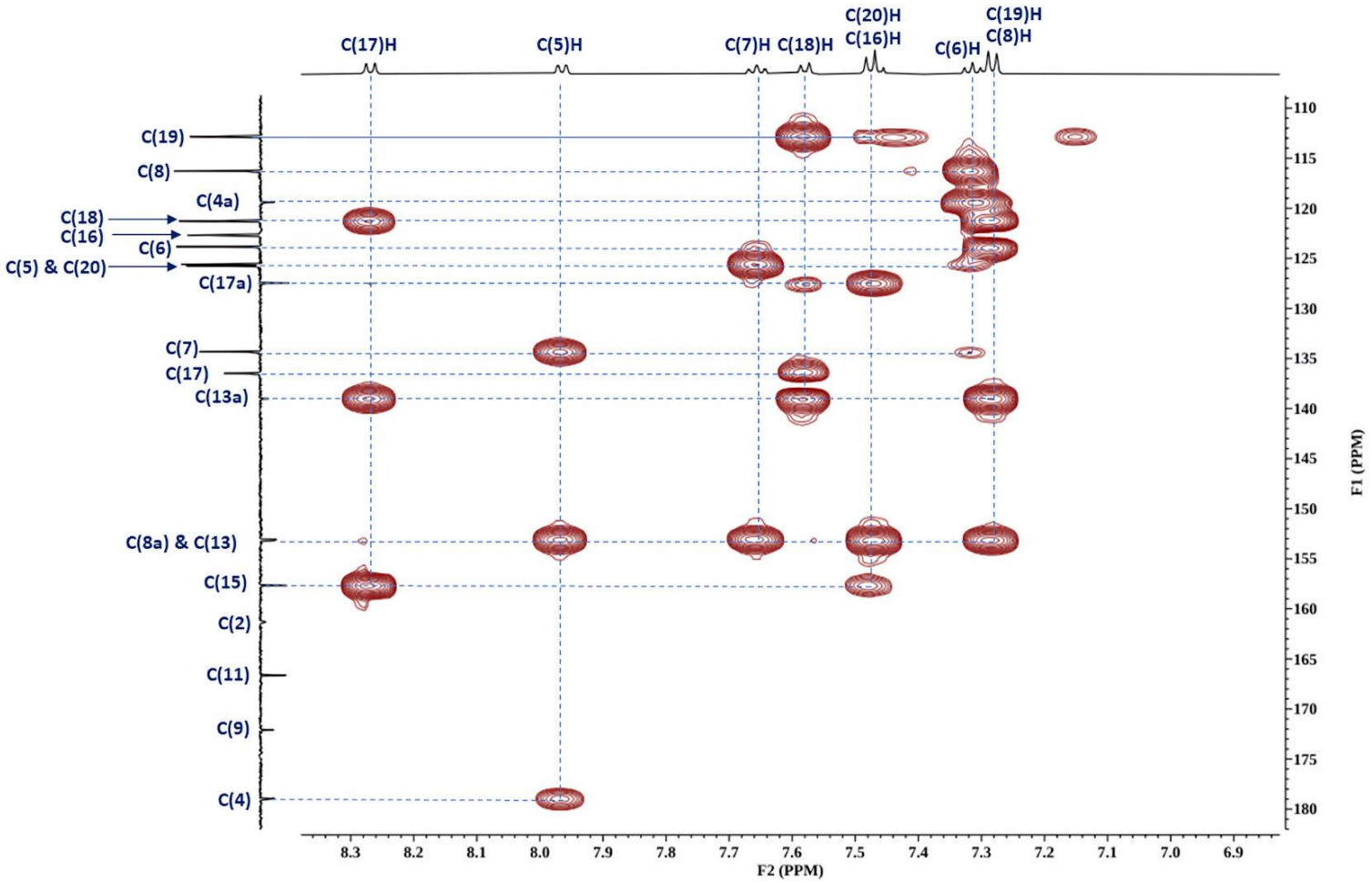


**Fig. S21** The HMBC spectrum of **QHC2** in DMSO-$d_6$, 298 K (expansion).

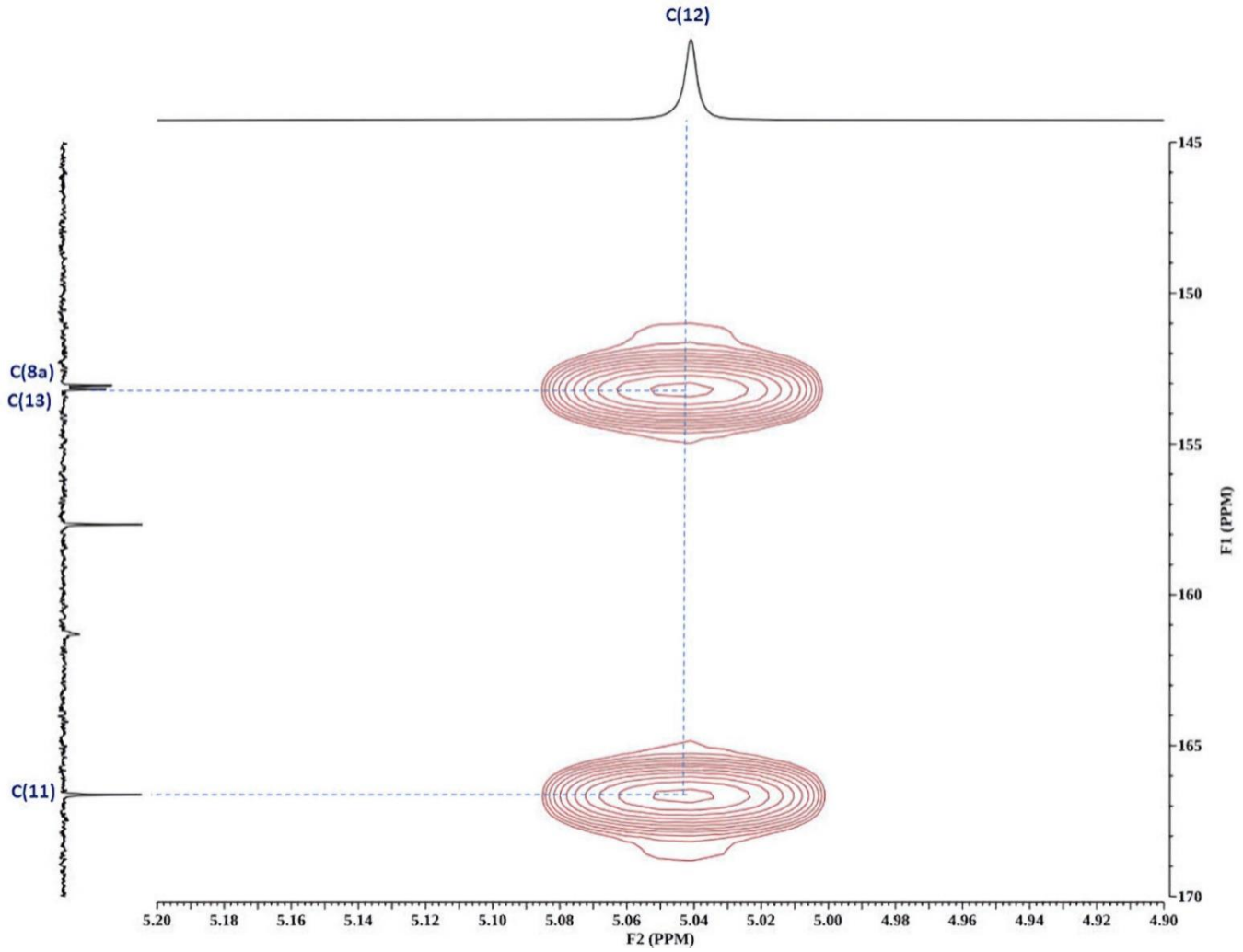


**Fig. S22** The HMBC spectrum of **QHC2** in DMSO-$d_6$, 298 K (expansion).

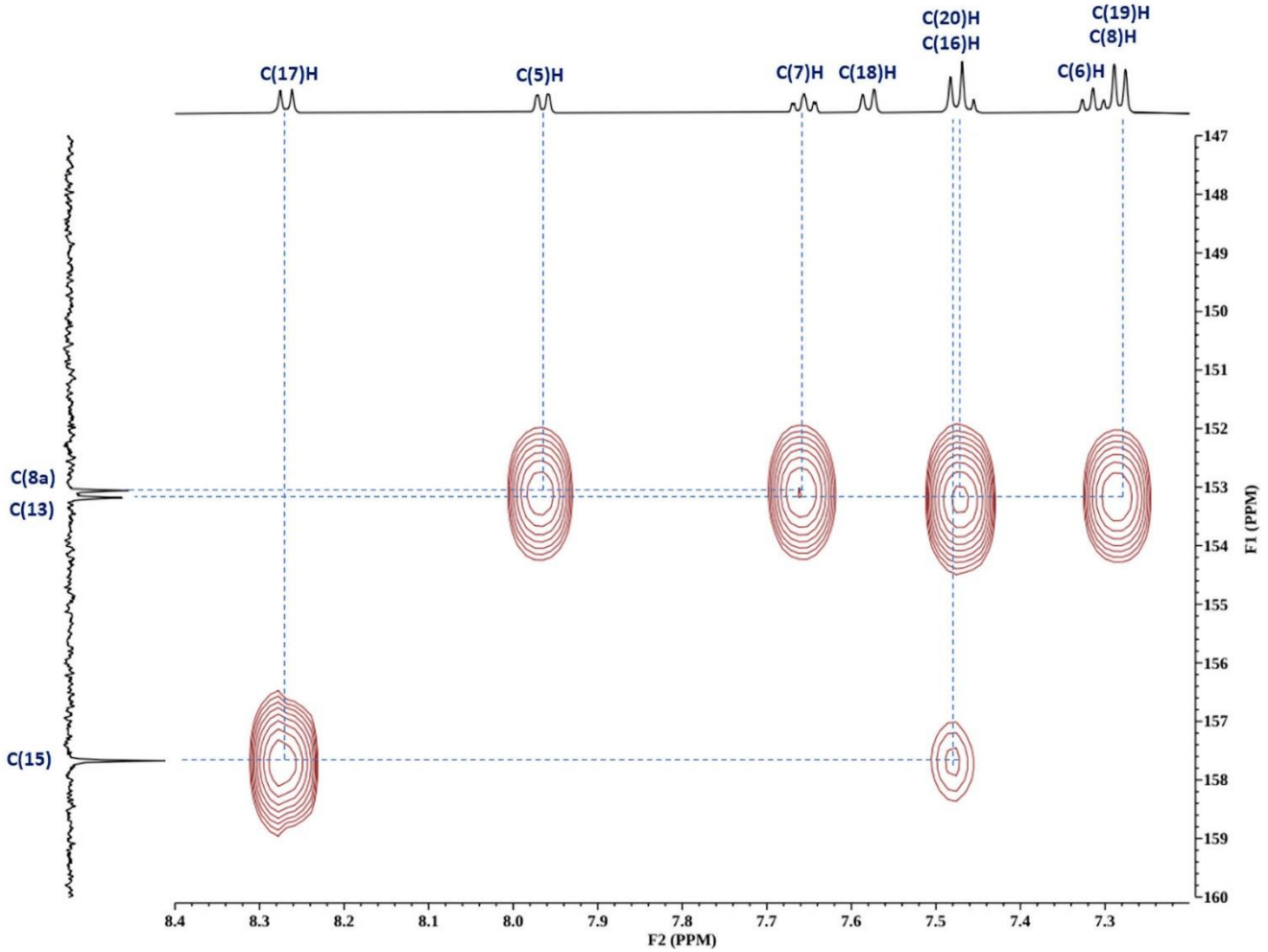


**Fig. S23** The HMBC spectrum of **QHC2** in DMSO-$d_6$, 298 K (expansion).

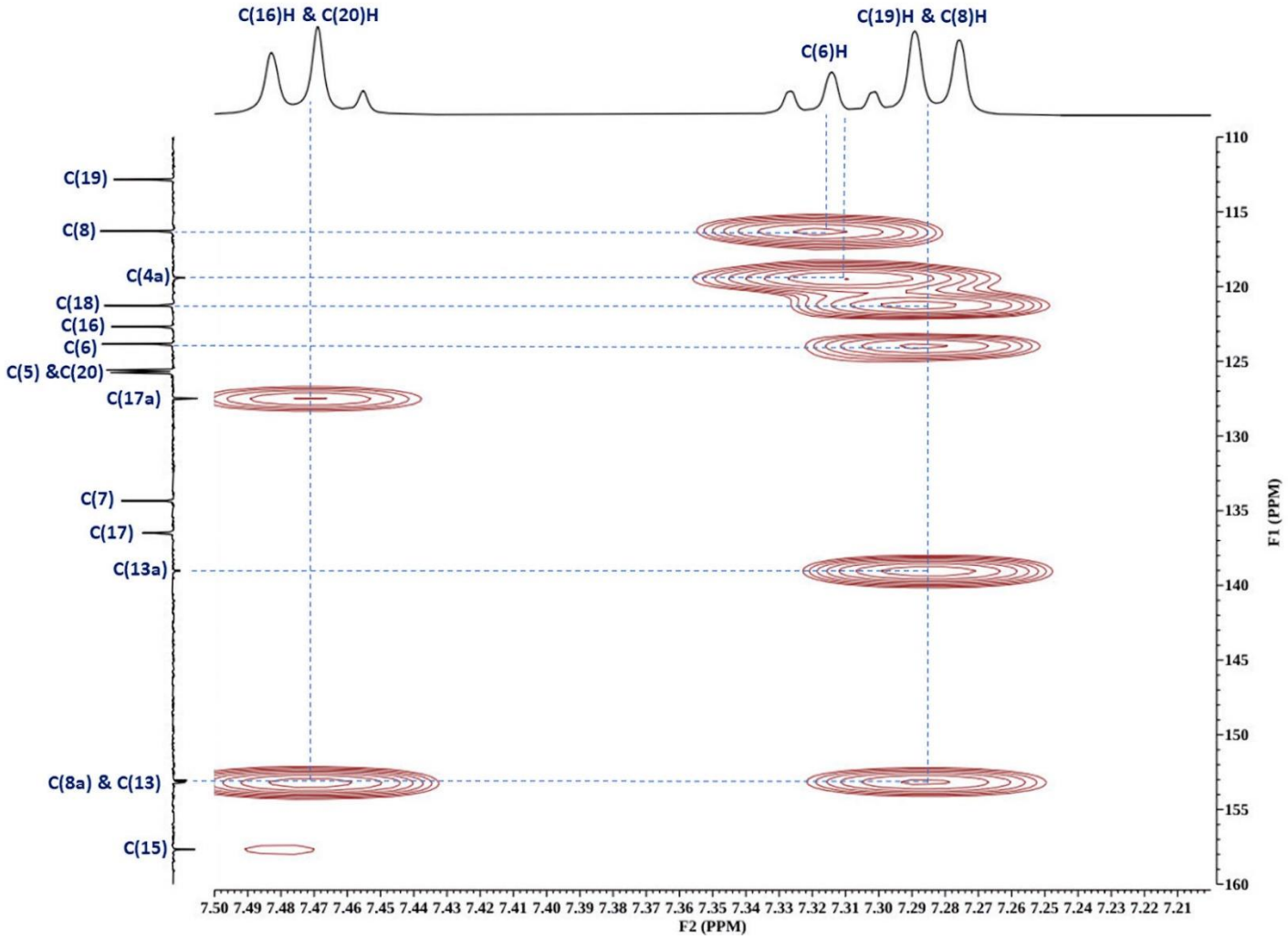


**Fig. S24** The HMBC spectrum of **QHC2** in DMSO-$d_6$, 298 K (expansion).

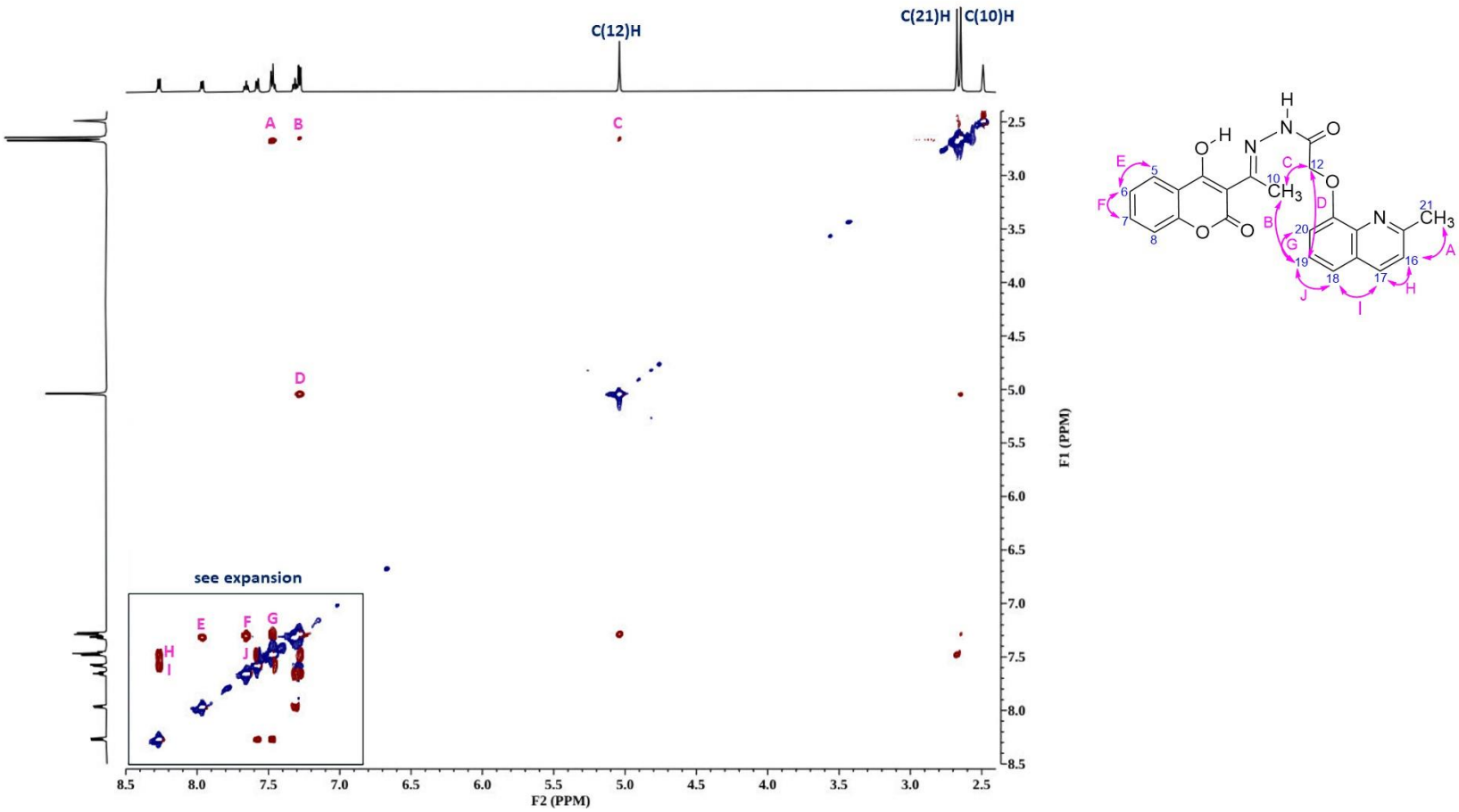


**Fig. S25** The ROESY spectrum of **QHC2** in DMSO-$d_6$, 298 K.

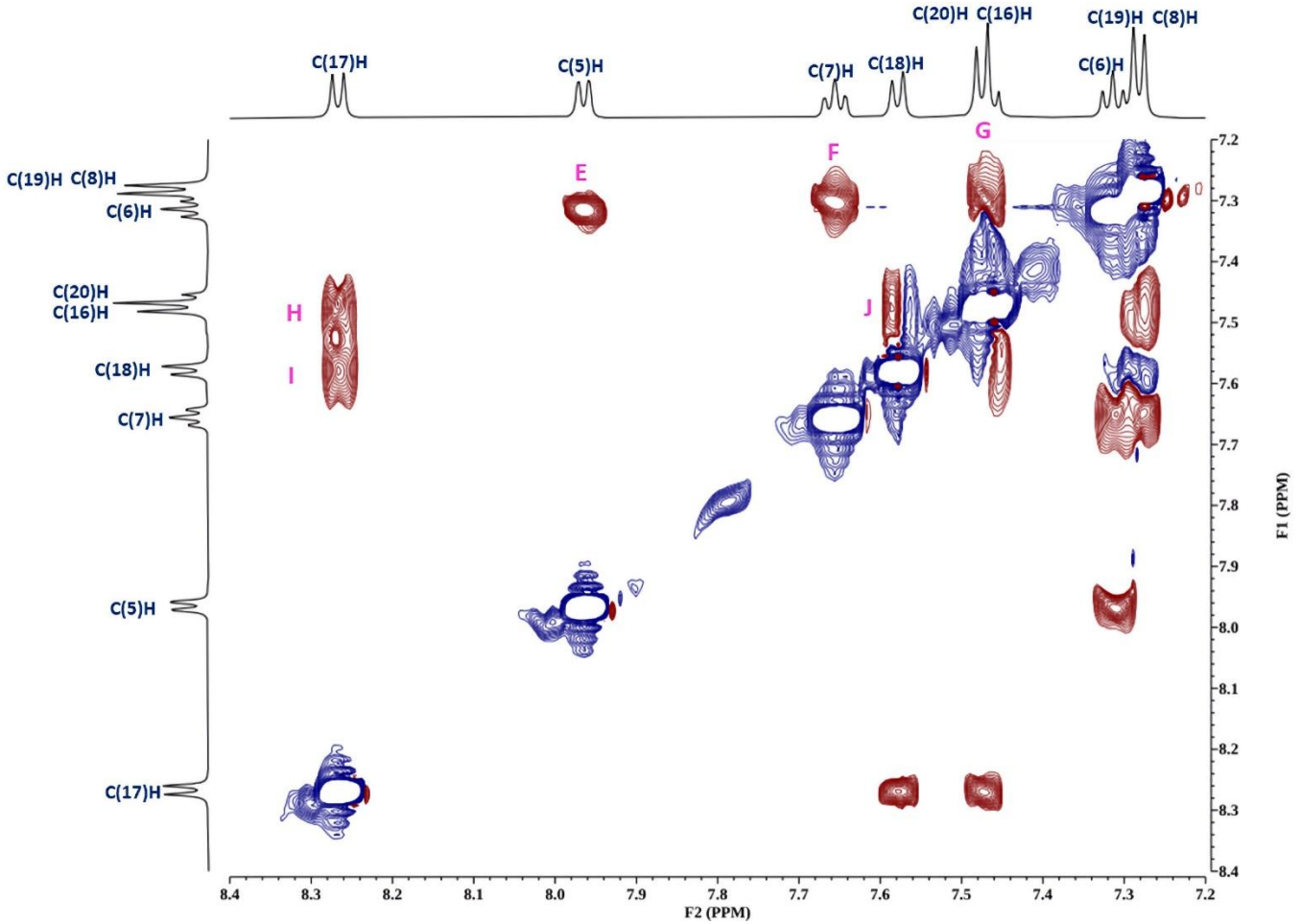


**Fig. S26** The ROESY spectrum of **QHC2** in DMSO-$d_6$, 298 K.

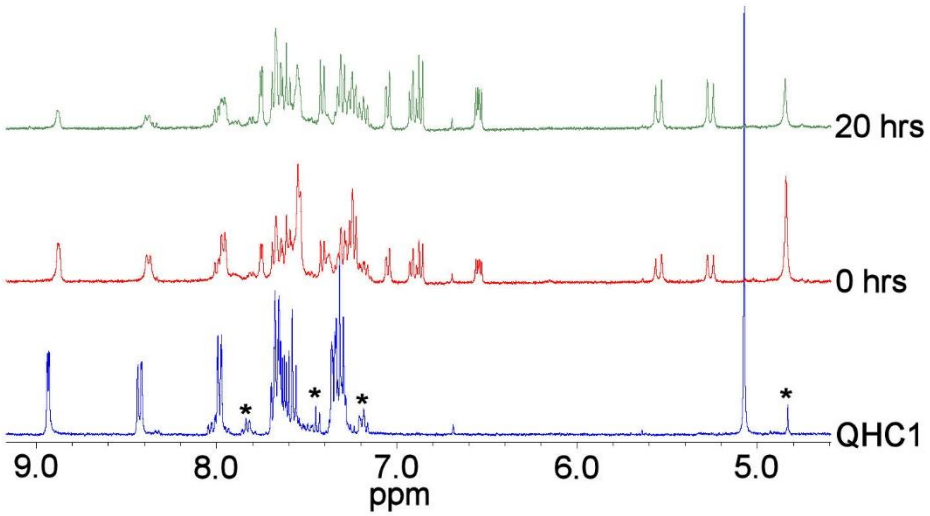


**Fig. S27** A timed $^{1}$H NMR of **QHC1** (20 mmol·dm$^{-3}$ DMSO-$d_6$, 298K) plus one equivalent of $Zn(CH_3CO_2)_2$.

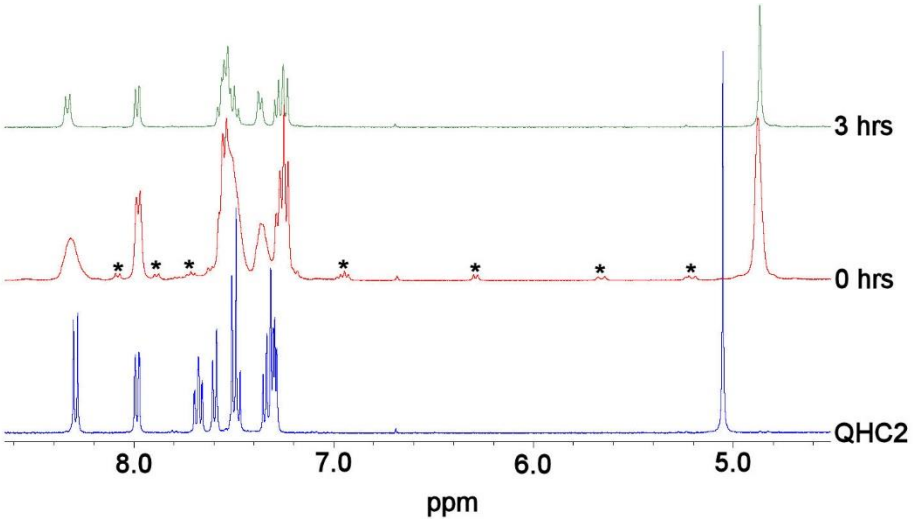


**Fig. S28** A timed $^{1}$H NMR of **QHC2** (20 mmol·dm$^{-3}$ DMSO-$d_6$, 298K) plus one equivalent of $Zn(CH_3CO_2)_2$ (* octahedral geometry)

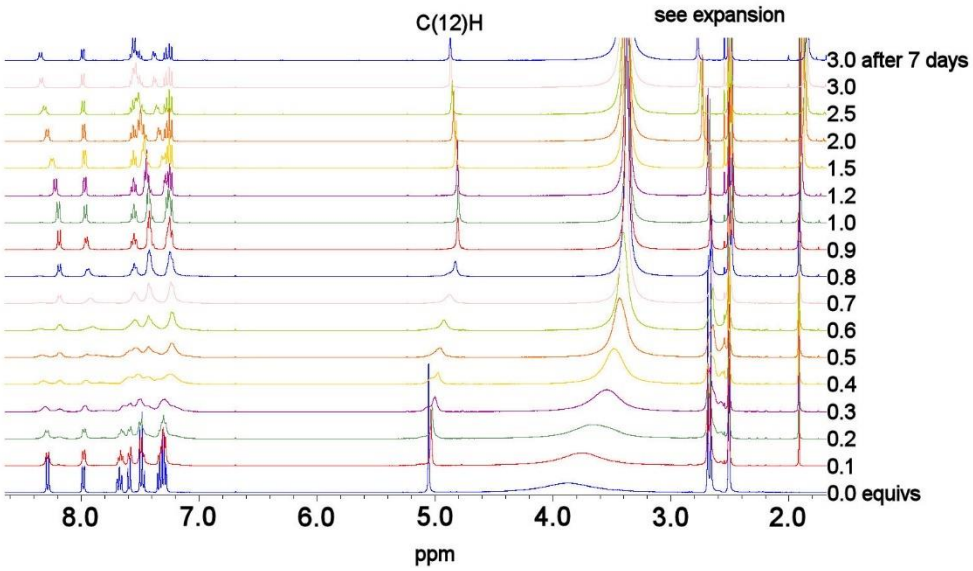


**Fig. S29** $^{1}$H NMR spectrum (20 mmol·dm$^{-3}$ DMSO-$d_6$, 298 K) of **QHC2** plus aliquots of $Zn(CH_3CO_2)_2$ were added.

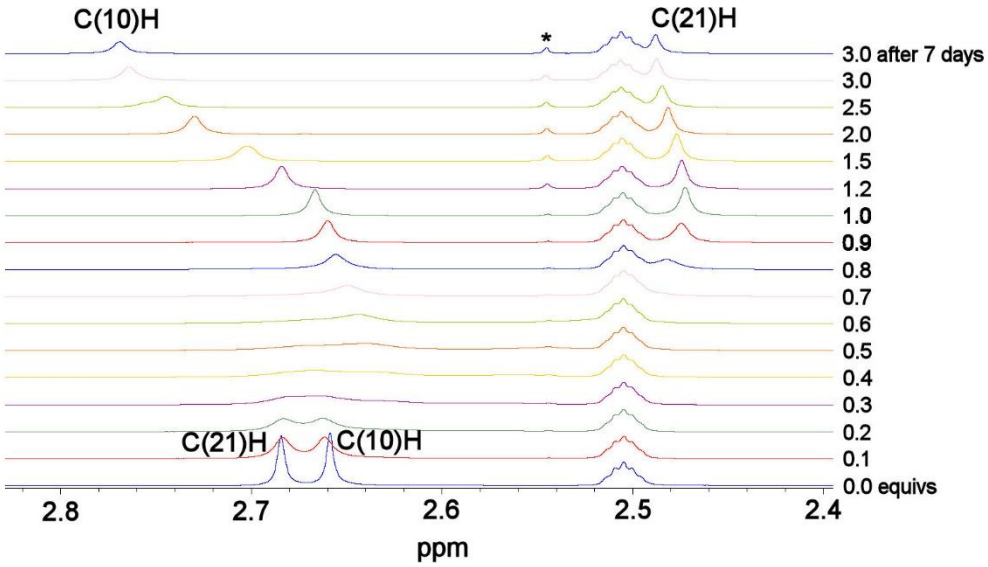


**Fig. S30** $^{1}$H NMR spectrum (20 mmol·dm$^{-3}$ DMSO-$d_6$, 298 K) of **QHC2** plus aliquots of $Zn(CH_3CO_2)_2$ were added.

# 4.0 Mass Spectrometry

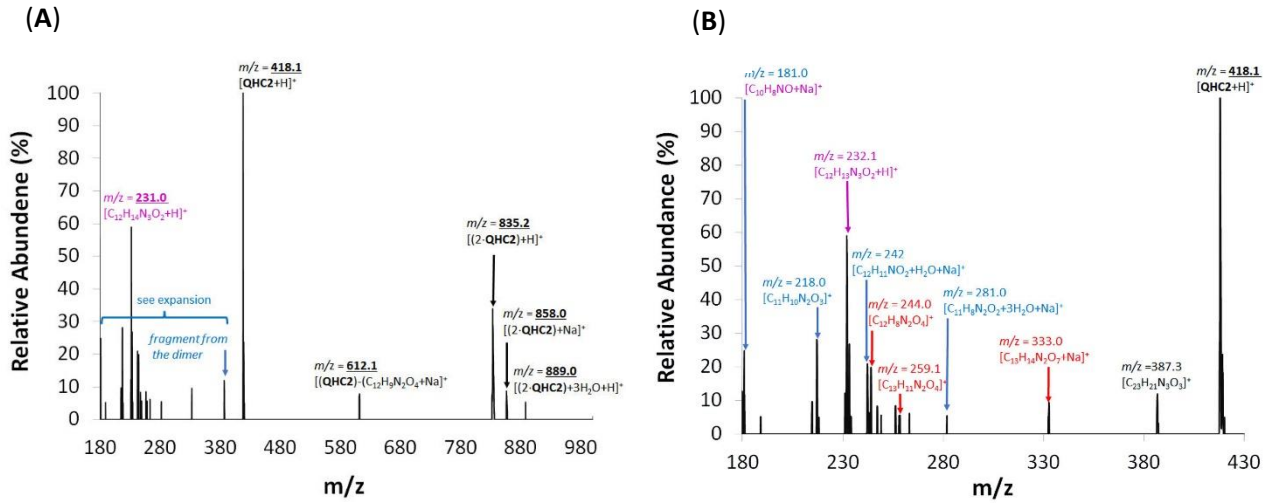


**Fig. S31** Mass spectrum (positive-mode) of **QHC2** (A) full spectrum (B) expansion

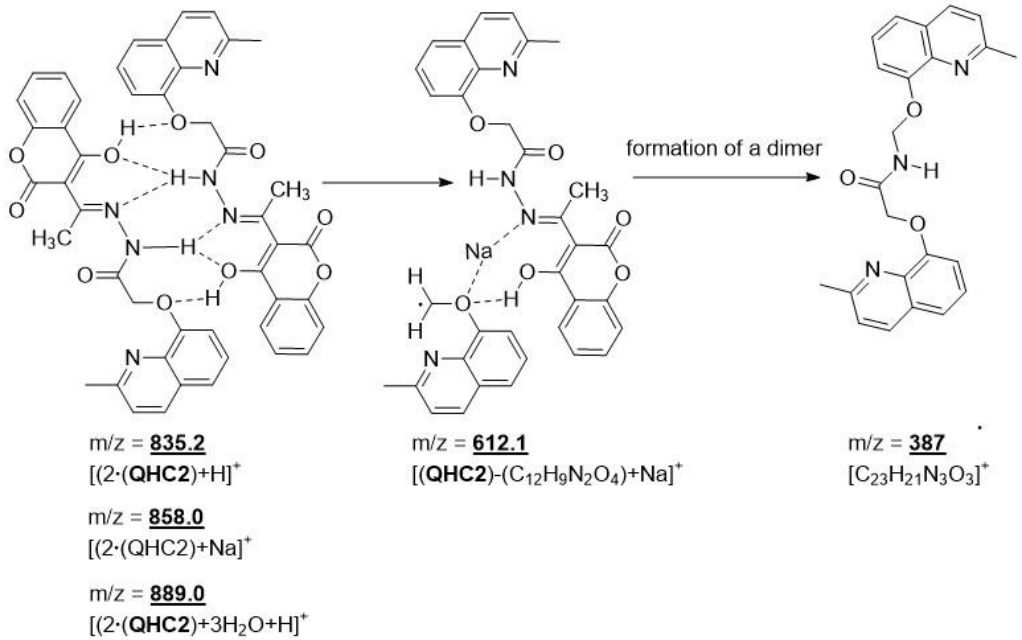


**Scheme S1** The proposed structures assigned to the m/z signals are shown in Fig S26(A).

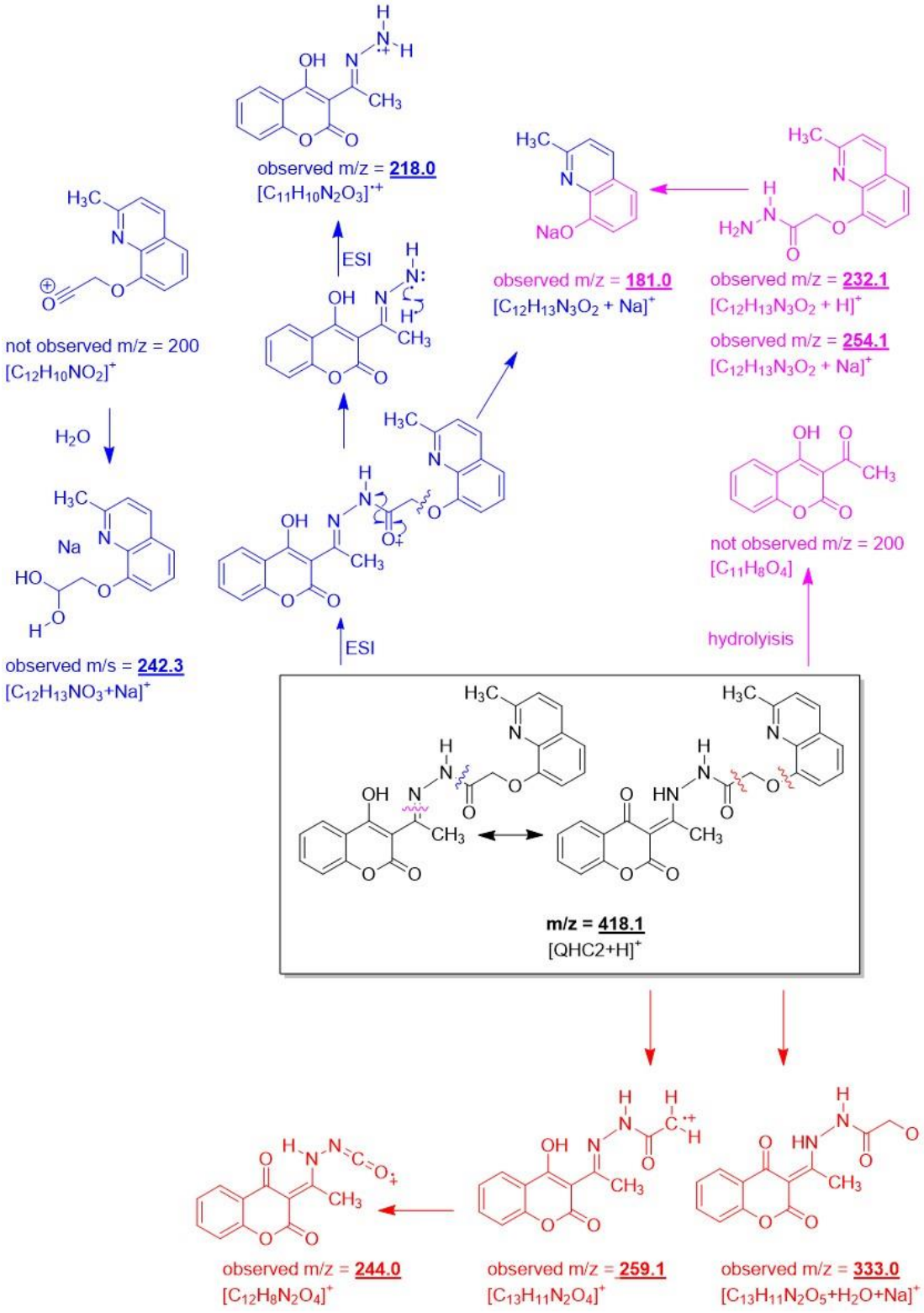


**Scheme S2** The proposed structures assigned to the m/z signals are shown in Fig 26(B).

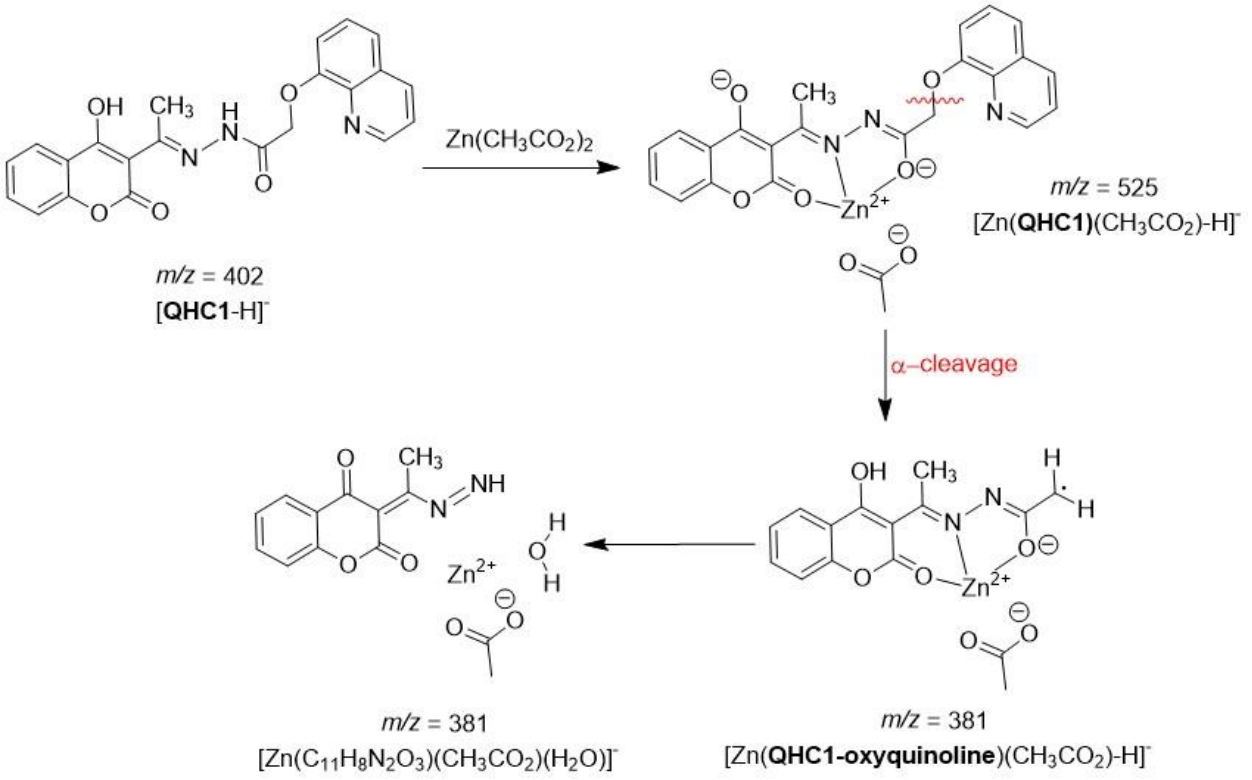


**Scheme S3** The proposed structures assigned to the m/z signals are seen in Fig 27(A).

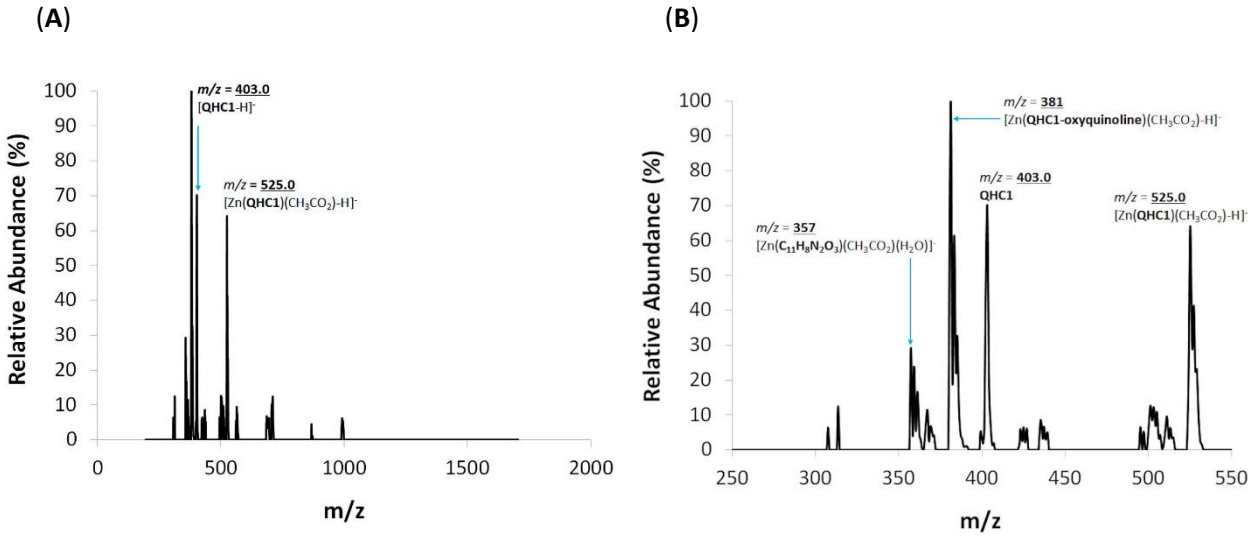


**Fig. S32** Mass spectrum (negative mode) of **QHC1** plus $Zn(CH_3CO_2)_2$ (A) full spectrum (B) expansion

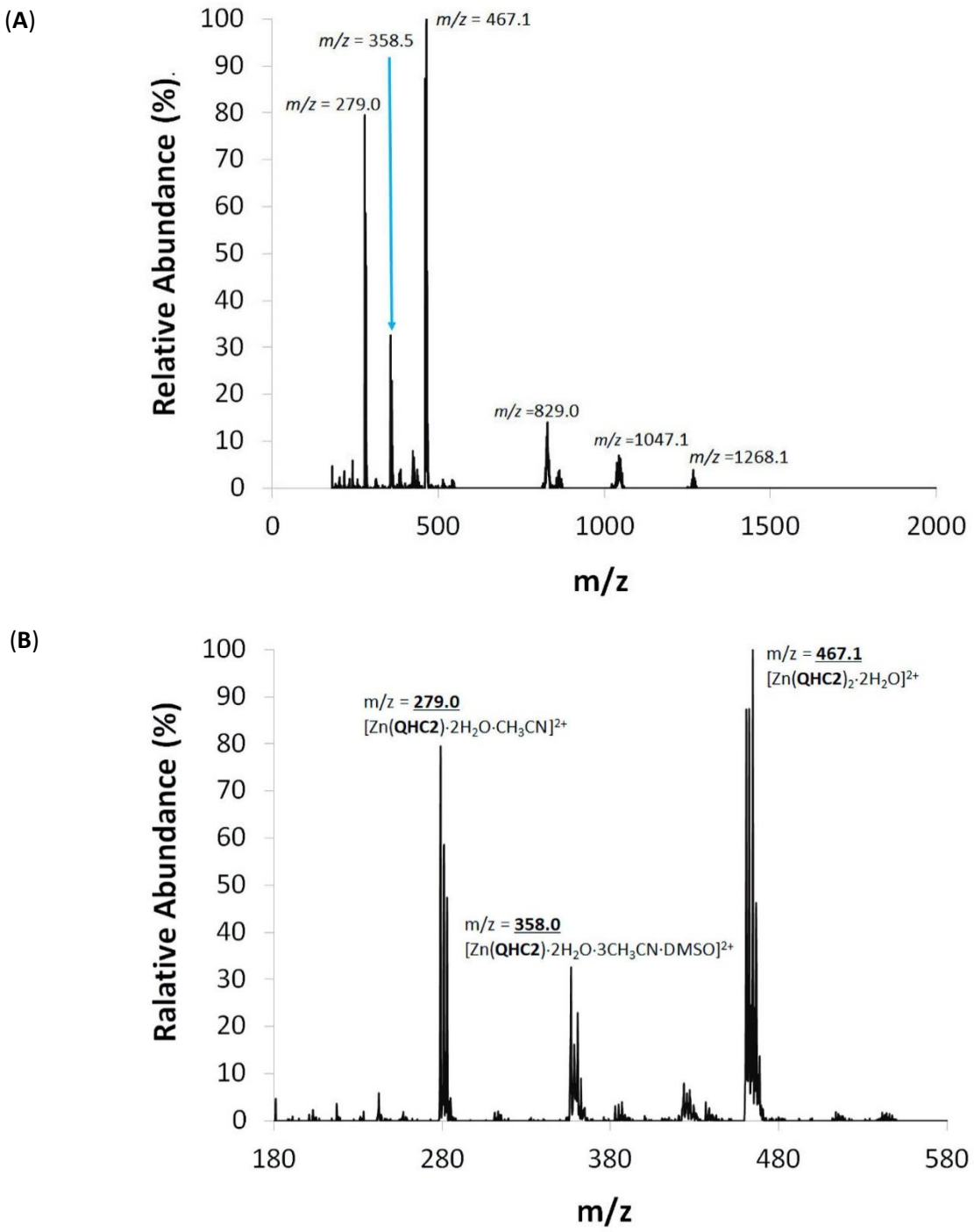


**Fig. S33** Mass spectrum (positive mode) of **QHC2** plus $Zn(CH_3CO_2)_2$ (A) full spectrum (B) expansion

# 5.0 Optical Studies (UV-Vis and Fluorescence Spectroscopy) in Organic Solutions

**Preparation of solutions: UV-vis, steady-state fluorescence, and life-time studies:** A stock solution of **HQCX** (X = 1 or 2) or **HQC2** (2.5 mM) was prepared by dissolving the appropriate weight of each compound (≈ 10.0 mg) in DMSO (10.0 mL). From the stock solutions a 50 μM working solution was prepared and transferred to a quartz cell. Stock solutions (2.0 mM) of metal acetate salts ($Cd^{2+}$, $Co^{2+}$ $Cu^{2+}$, $Fe^{2+}$ $Hg^{2+}$ $Ni^{2+}$ and $Zn^{2+}$) were prepared in DMSO. Aliquots of 5.0 μL of the metal salts were added to the UV-vis cell. Each 5.0 μL addition equates to 0.1 equivalents of the metal salts except $Cd^{2+}$ whereby the addition of 2.5 μL represents 0.05 equivalents addition. The excitation wavelength was set to 400 nm and the emission range recorded from 420 to 770 nm with a slit width set to 1.00 mm.

**Metal binding constant determination**

The following pages represent the plots (the spectra, binding isotherm, calculated mole fraction, and residuals) upon adding the metal salts to a solution of various ratios of HEPES and DMSO of **QHCX** (X = 1 or 2). Nonlinear least-squares fit isotherms were obtained using Bindfit (http://supramolecular.org)[4, 5] to fit the following binding models.

$$\mathbf{QHCX} + \mathrm{M(II)} \overset{K_{11}}{\rightleftharpoons} [\mathrm{M}(\mathbf{QHCX})]^{n+} \qquad K_{11} = \frac{[\mathrm{M}(\mathbf{QHCX})]^{n+}}{[\mathbf{QHCX}][\mathrm{M(II)}]}$$

$$\mathbf{QHCX} + [\mathrm{M}(\mathbf{QHCX})]^{n+} \overset{K_{21}}{\rightleftharpoons} [\mathrm{M}(\mathbf{QHCX})_2]^{n+} \qquad K_{21} = \frac{[\mathrm{M}(\mathbf{QHCX})_2]^{n+}}{[\mathbf{QHCX}]\,[\mathrm{M}(\mathbf{QHCX})]^{n+}}$$

$$\mathbf{2\ QHCX} + \mathrm{M(II)} \overset{\beta}{\rightleftharpoons} [\mathrm{M}(\mathbf{QHCX})_2]^{n+} \qquad \beta = \frac{[\mathrm{M}(\mathbf{QHCX})_2]^{n+}}{[\mathbf{QHCX}]^2\,[\mathrm{M(II)}]}$$

**Scheme S4** The equilibrium expression used to assign the two prominent specifies in solution (298 K).

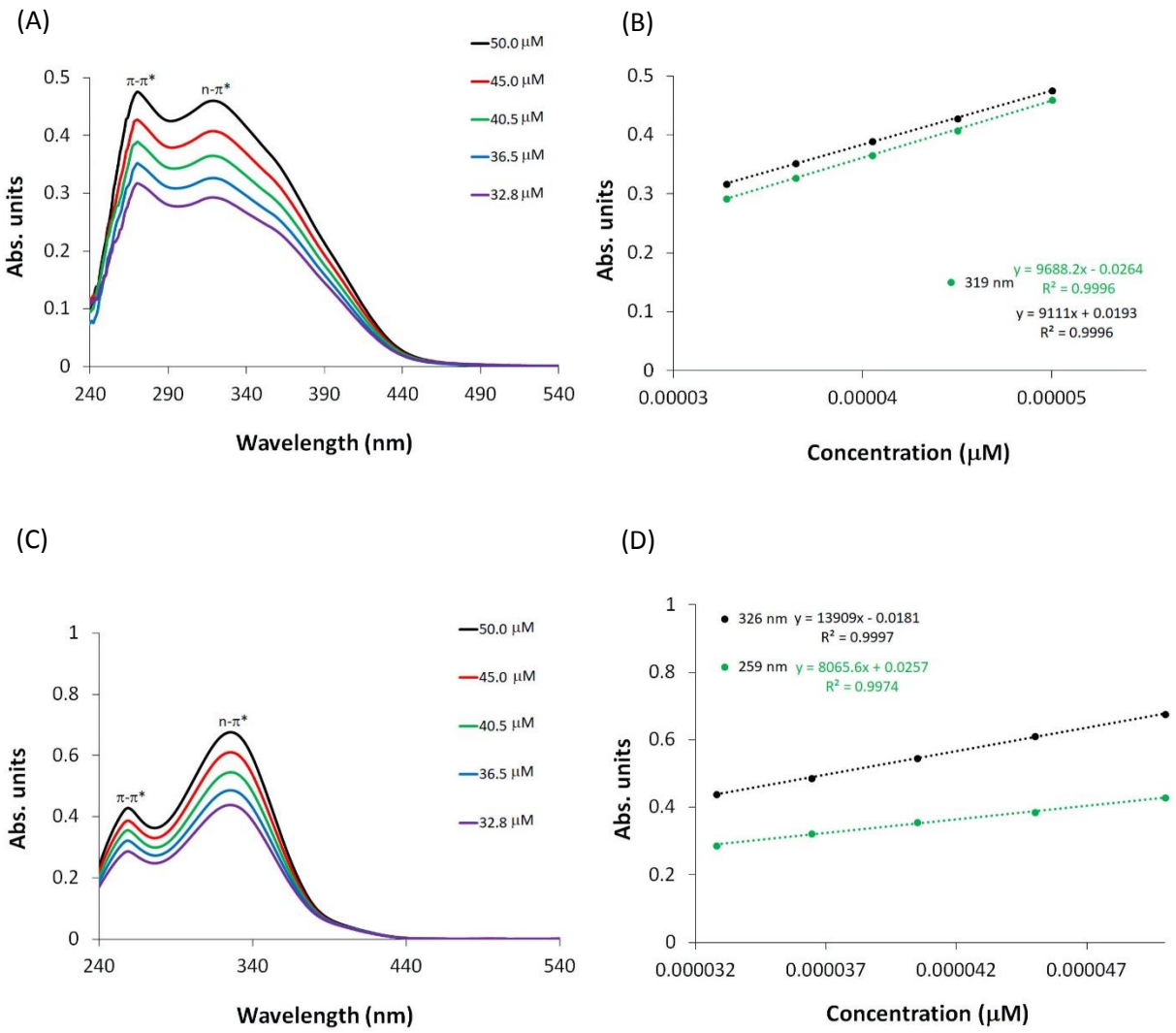


**Fig. S34** (A) UV-vis spectrum of **QHC1** and (B) Beers Law plot; (C) UV-vis spectrum of **QHC2** and (D) Beers Law plot.

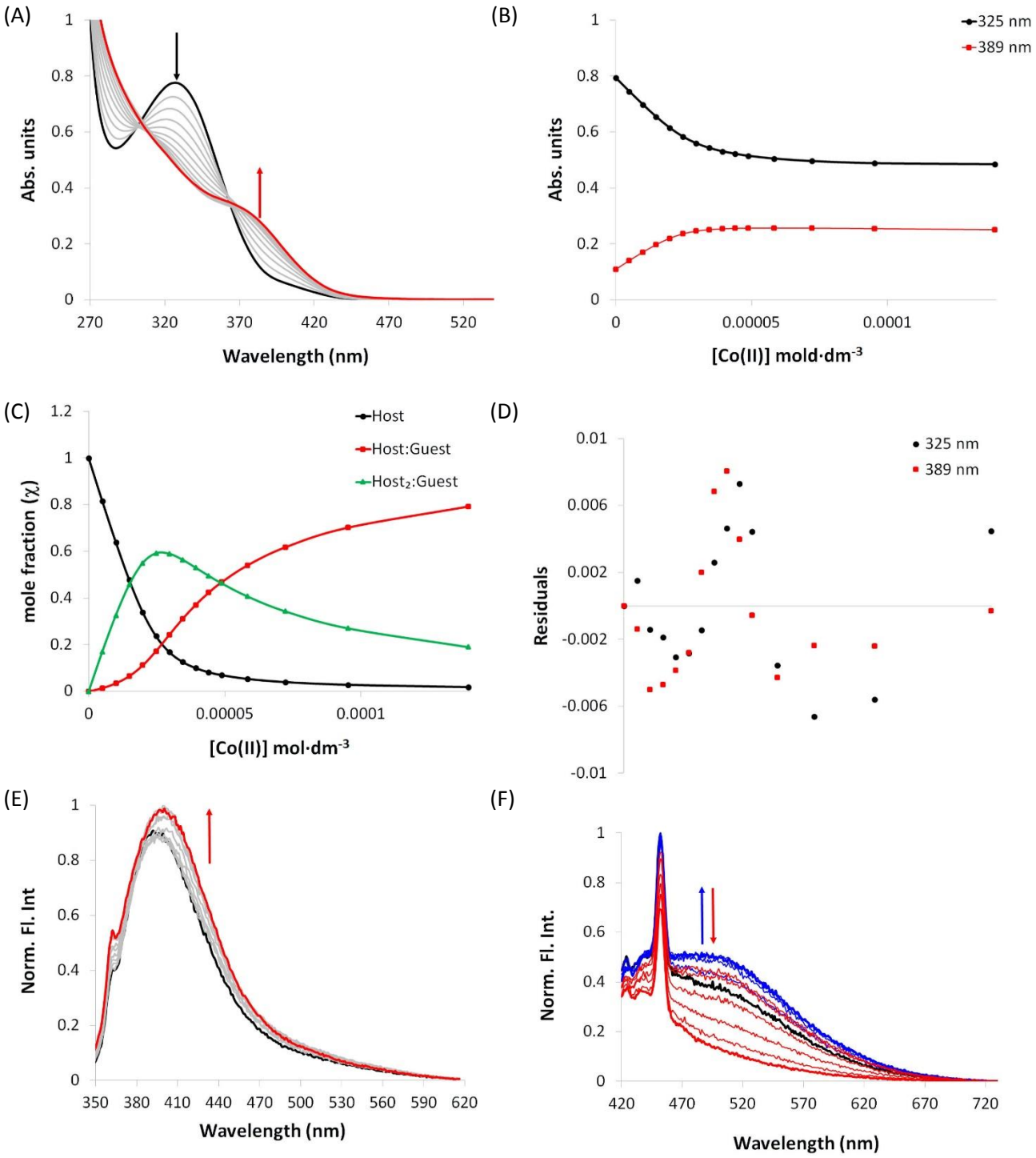


**Fig. S35** (A) Absorbance spectra of **QHC2** upon the incremental addition of $Co(CH_3CO_2)_2$, up to three equivalents in DMSO (B) Nonlinear least squares binding isotherm (C) mole fraction ($\chi$) whereby the host represents **QHC2**-black circles, the guest is $Co^{2+}$ ions and the host:guest complex ($K_{11}$), $[Co(\mathbf{QHC2})]^{2+}$-red squares and $[Co(\mathbf{QHC2})_2]^{2+}$ -green triangles (D) residual plot from the experimental data and (E) and (F) emission spectra excited at 326 and 400 nm, respectively. The data was calculated using Bindfit and the model was fitted to Nelder-Mead (full).

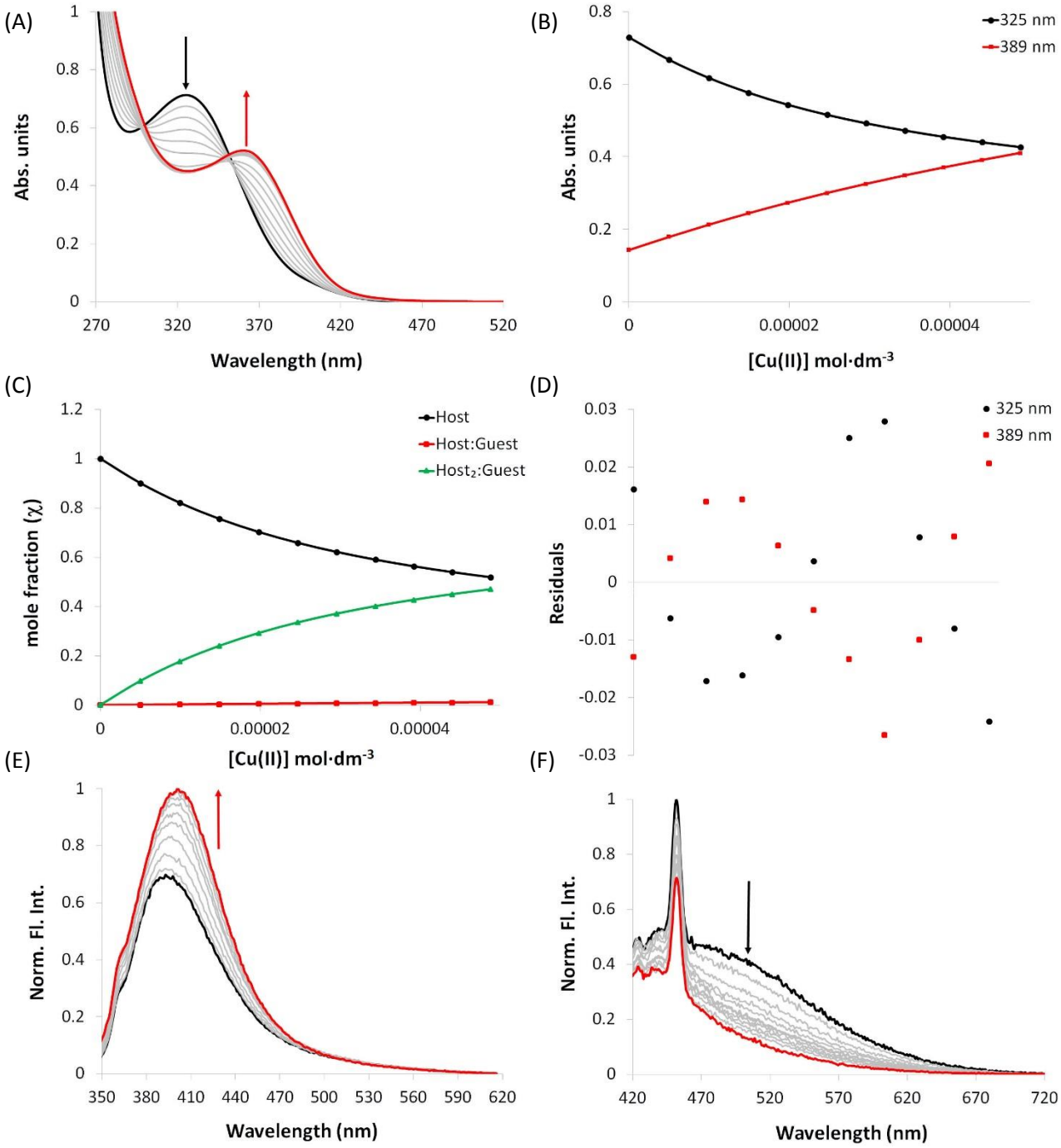


**Fig. S36** (A) Absorbance spectra of **QHC2** upon the incremental addition of $Cu(CH_3CO_2)_2$, up to one equivalent in DMSO (B) Nonlinear least squares binding isotherm (C) mole fraction ($\chi$) whereby the host represents **QHC2-**black circles, the guest is $Cu^{2+}$ ions and the host:guest complex ($K_{11}$) $[Cu(\mathbf{QHC2})]^{2+}$-red squares and $[Cu(\mathbf{QHC2})_2]^{2+}$ -green triangles (D) residual plot from the experimental data and (E) and (F) emission spectra excited at 325 and 400 nm, respectively. The data was calculated using Bindfit and the model was fitted to Nelder-Mead (full).

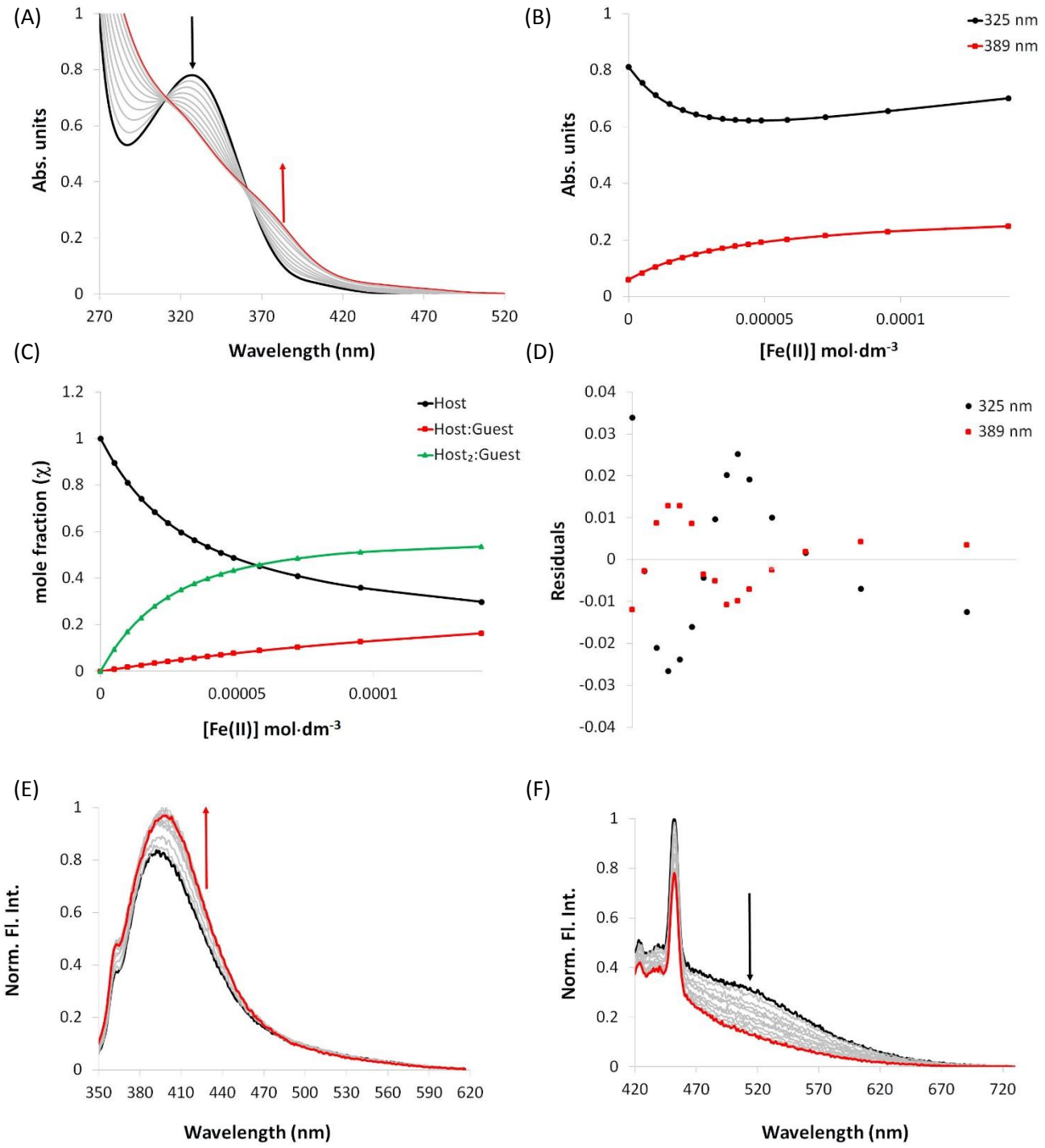


**Fig. S37** (A) Absorbance spectra of **QHC2** upon the incremental addition of $Fe(CH_3CO_2)_2$, up to three equivalents in DMSO (B) Nonlinear least squares binding isotherm (C) mole fraction ($\chi$) whereby the host represents **QHC2**-black circles, the guest is $Fe^{2+}$ ions and the host:guest complex ($K_{11}$) $[Fe(\mathbf{QHC2})]^{2+}$-red squares and $[Fe(\mathbf{QHC2})_2]^{2+}$ -green triangles (D) residual plot from the experimental data and (E) and (F) emission spectra excited at 325 and 400 nm, respectively. The data was calculated using Bindfit and the model was fitted to Nelder-Mead (full).

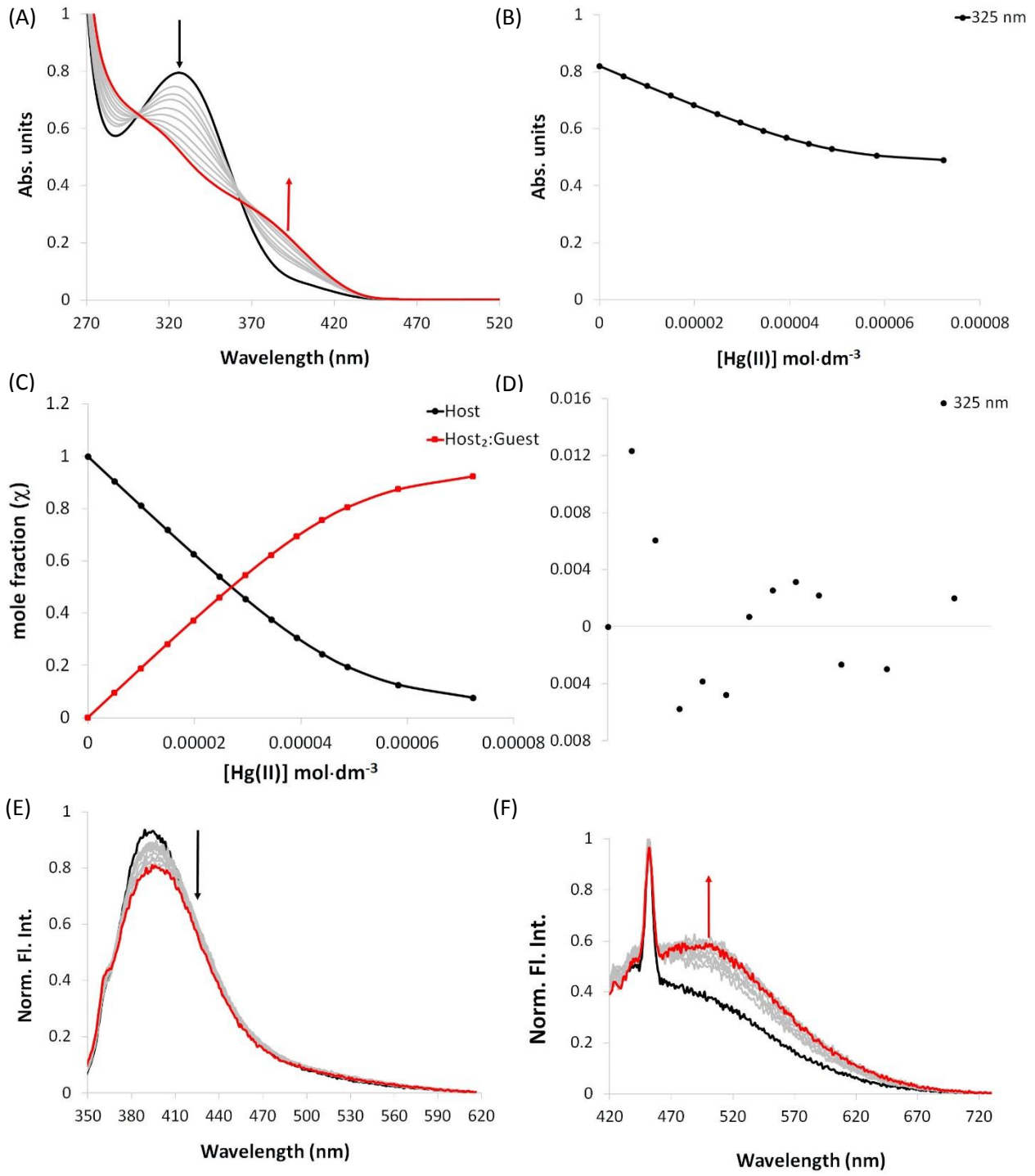


**Fig. S38** (A) Absorbance spectra of **QHC2** upon the incremental addition of $Hg(CH_3CO_2)_2$, up to one and half equivalents (B) Nonlinear least squares binding isotherm (C) mole fraction ($\chi$) whereby the host represents **QHC2**-black circles, the guest is $Hg^{2+}$ ions and the host:guest complex ($K_{11}$) $[Hg(\mathbf{QHC2})]^{2+}$-red squares and (D) residual plot from the experimental data and (E) and (F) emission spectra excited at 325 and 400 nm, respectively. The data was calculated using Bindfit and the model was fitted to Nelder-Mead (full).

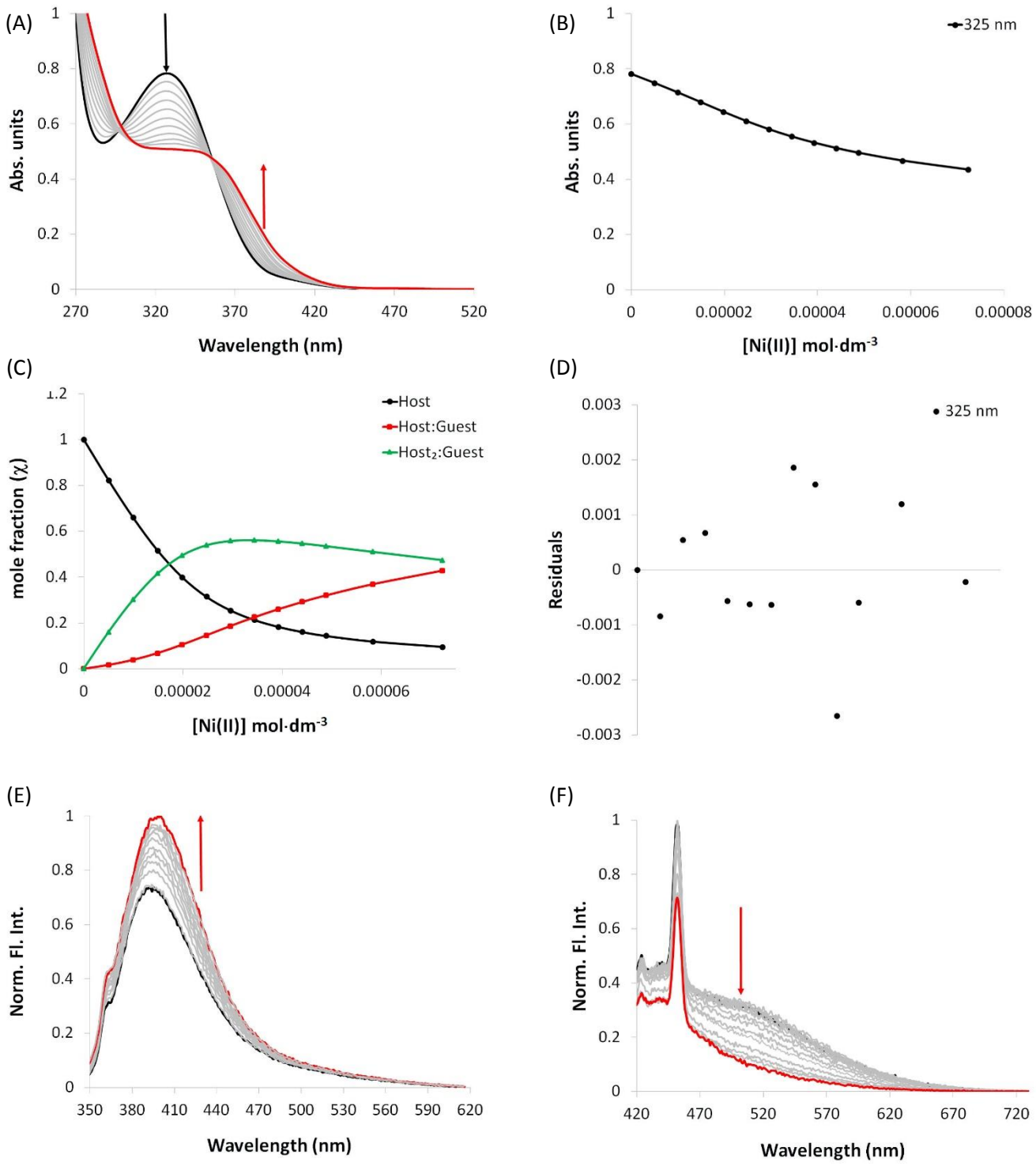


**Fig. S39** (A) Absorbance spectra of **QHC2** upon the incremental addition of $Ni(CH_3CO_2)_2$, up to one and half equivalents in DMSO (B) Nonlinear least squares binding isotherm (C) mole fraction ($\chi$) whereby the host represents **QHC2-**black circles, the guest is $Ni^{2+}$ ions and the host:guest complex ($K_{11}$) $[Ni(\mathbf{QHC2})]^{2+}$-red squares and $[Ni(\mathbf{QHC2})_2]^{2+}$ -green triangles (D) residual plot from the experimental data and (E) and (F) emission spectra excited at 325 and 400 nm, respectively. The data was calculated using Bindfit.

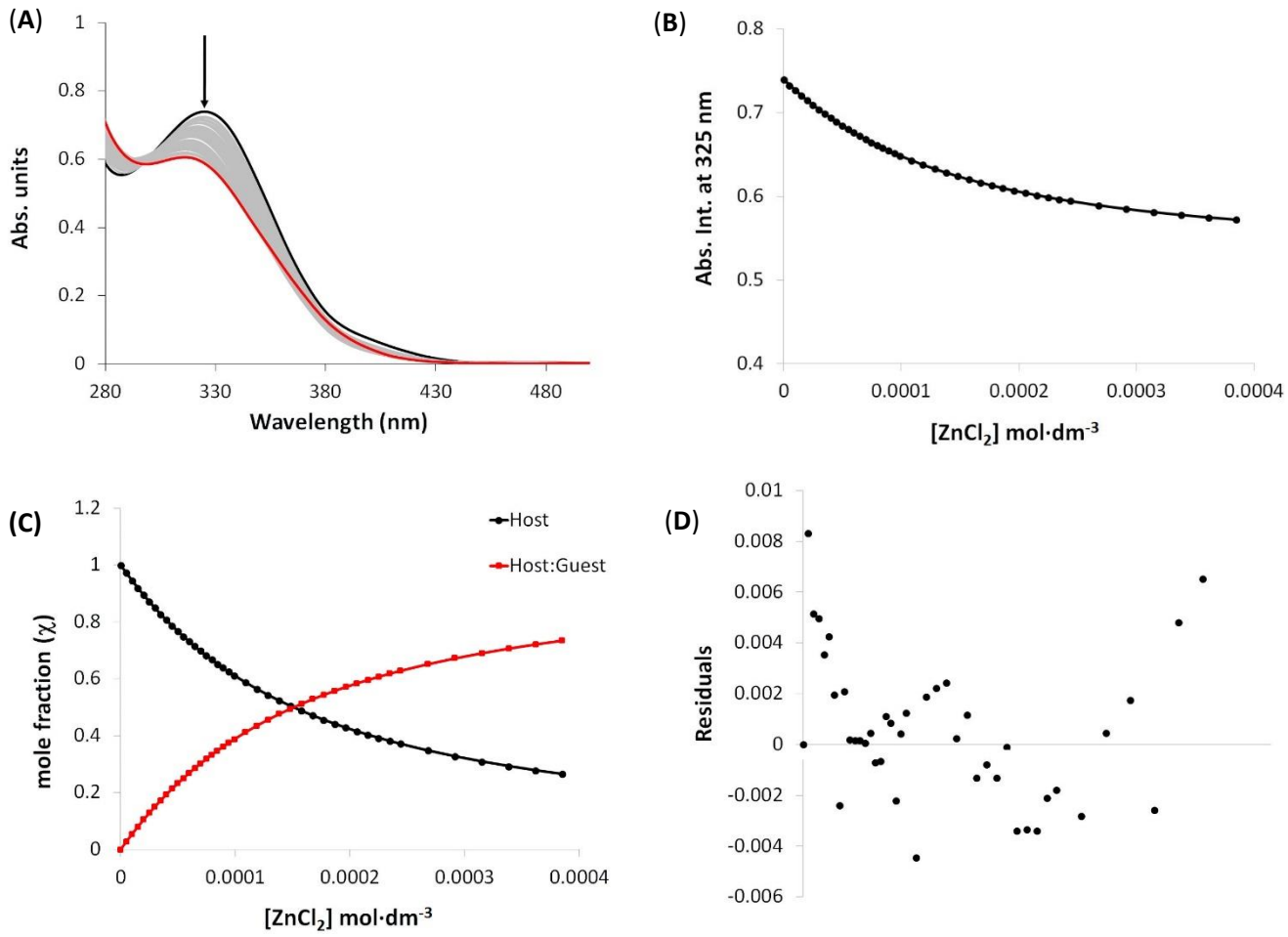


**Fig. S40** (A) Absorbance spectra of **QHC2** upon the incremental addition of $ZnCl_2$, up to 8.0 equivalents in DMSO (B) Nonlinear least squares binding isotherm (C) mole fraction ($\chi$) whereby the host represents **QHC2**-black circles, the guest is $Zn^{2+}$ ions and the host:guest complex ($K_{11}$) $[Zn(\mathbf{QHC2})]^{2+}$-red squares and (D) residual plot from the experimental data. The data was calculated using Bindfit and the model was fitted to Nelder-Mead (full).

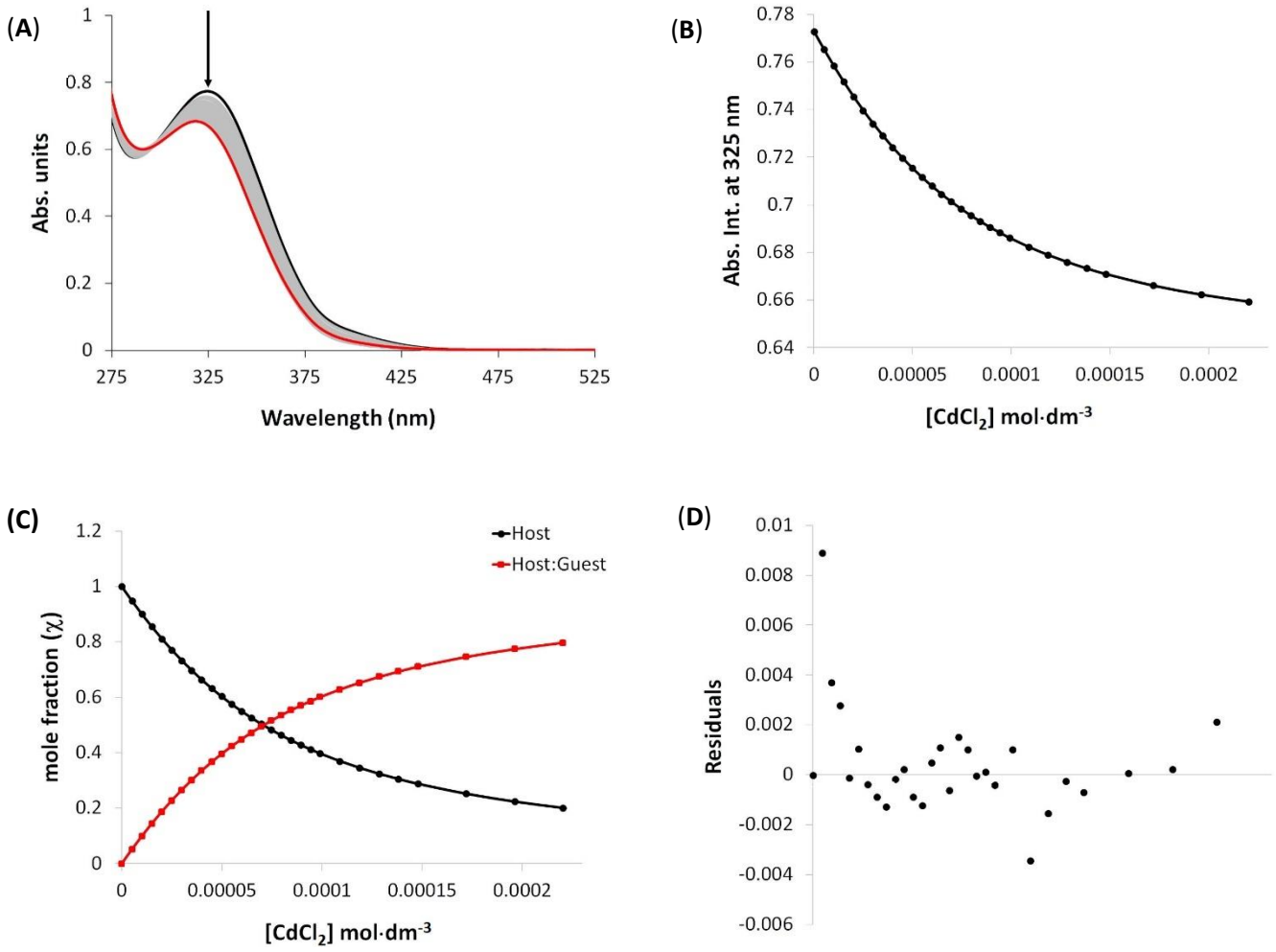


**Fig. S41** (A) Absorbance spectra of **QHC2** upon the incremental addition of $CdCl_2$, up to 5.0 equivalents in DMSO (B) Nonlinear least squares binding isotherm (C) mole fraction ($\chi$) whereby the host represents **QHC2-**black circles, the guest is $Cd^{2+}$ ions and the host:guest complex ($K_{11}$) $[Cd(\mathbf{QHC2})]^{2+}$-red squares and (D) residual plot from the experimental data. The data was calculated using Bindfit and the model was fitted to Nelder-Mead (full).

# 6.0 Fluorescence Lifetime Studies-Organic Media

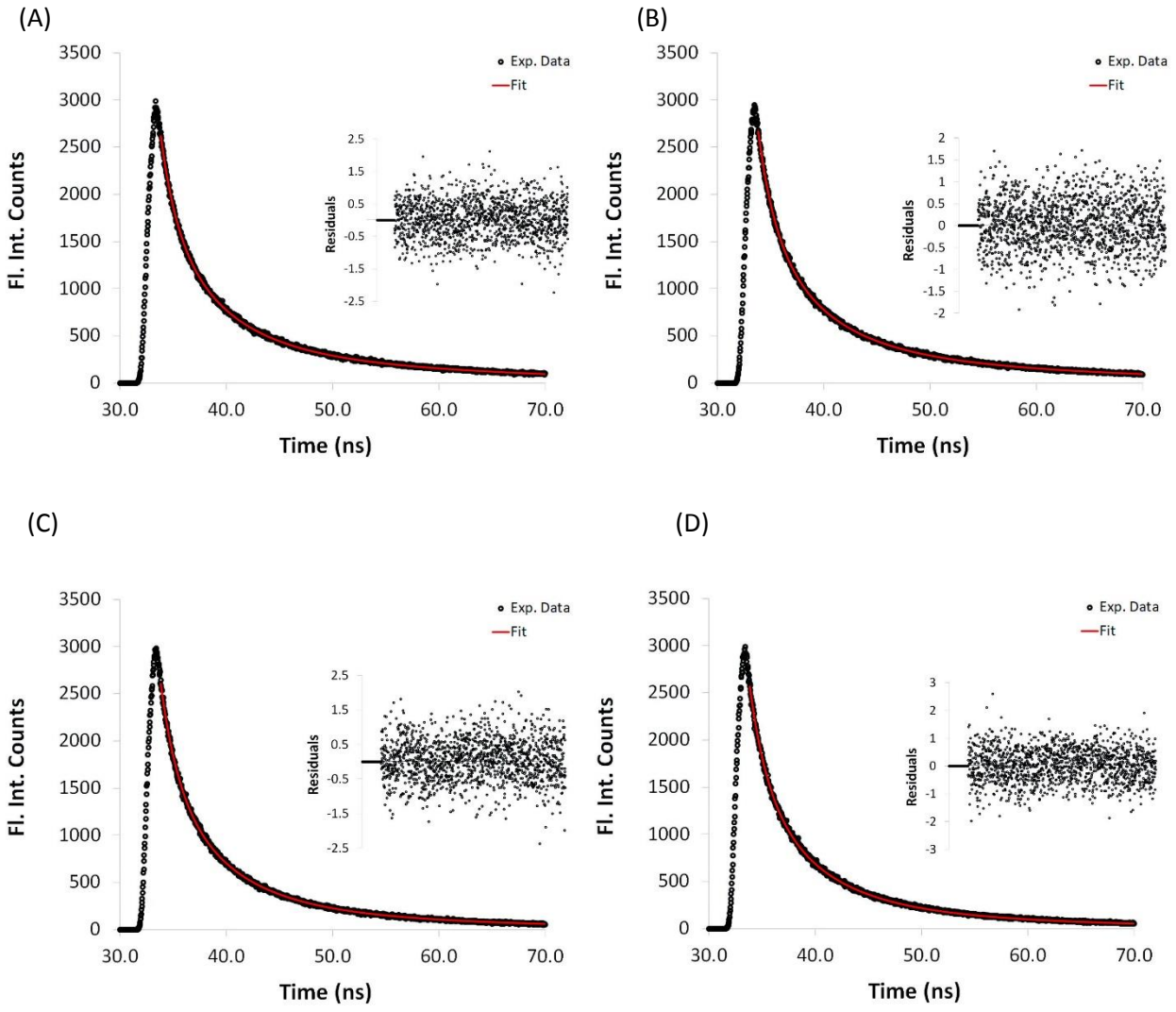


**Fig. S42** (A) Fluorescence lifetime (τ) of **QHC1** in DMSO using a 300 Nano laser and 400 Nano laser (A) and (C), respectively. Addition of two equivalents of $Zn(CH_3CO_2)_2$ using a 300 Nano laser and 400 Nano laser (B) and (D). Insert weighted residuals for each experiment (triplicate).

**Table S2** Fluorescence lifetimes of various reactive species (average of best three runs) using the 300 Nano laser.

| $\lambda_{em}$ | | $\tau_1$ | $\tau_2$ | $\tau_3$ | $\bar{\tau}$ | A | $\chi^2$ |
|---|---|---|---|---|---|---|---|
| 350 nm | **QHC1** | 5.2(6) | 20.8(8) | 1.5(1) | 6.7(5) | 7.5(5) | 1.05 |
| | | (36.8%) | (55.8%) | (7.3%) | | | |
| | $Zn(CH_3CO_2)_2$ | 5.2(6) | 20.2(8) | 1.5(1) | 6.7(5) | 9.05(5) | 1.01 |
| | | (36.1%) | (56.2%) | (7.8%) | | | |
| 400 nm | **QHC1** | 5.3(7) | 7.1(4) | 12.1(5) | 5.8(4) | 5.9(4) | 1.05 |
| | | (44.9%) | (21.4%) | (33.7%) | | | |
| | $Zn(CH_3CO_2)_2$ | 5.4(8) | 12.2(5) | 7.0(3) | 5.7(5) | 6.0(3) | 1.02 |
| | | (44.7%) | (34.2%) | (21.1%) | | | |

Note: lifetime-$\tau$, average lifetime- $\bar{\tau}$, pre-exponential factor-A, and Chi-squared-$\chi^2$. Parenthesis, relative amplitude.

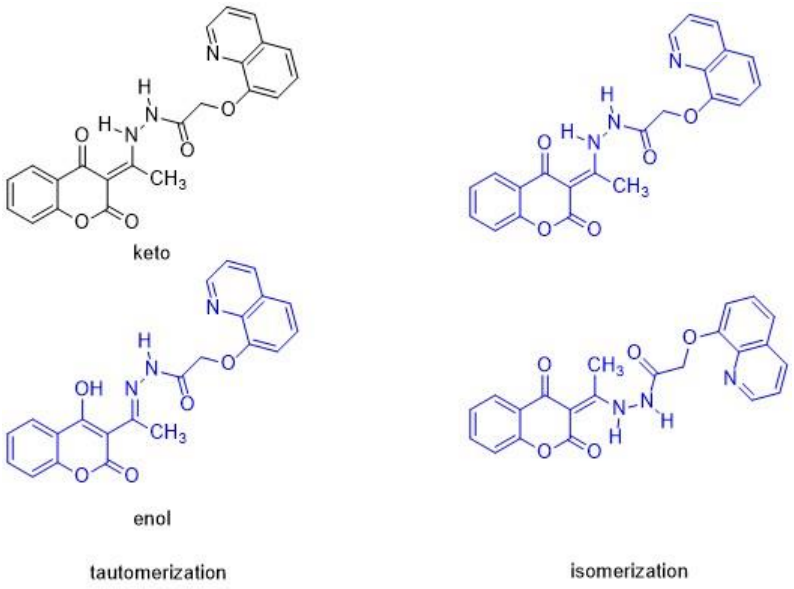


**Fig. S43** Potential tautomerization and isomers that are possible in solution giving rise to the various $\tau$.

# 7.0 Optisssscal Studies (UV-Vis and Fluorescence Spectroscopy) in Aqueous Solution

**Preparation of solutions:** A solution of **QHCX (X = 1 or 2)** is prepared by initially making a 3.0 mM stock solution in 100 % DMSO (5 mL). A specific volume was transferred from this stock solution to prepare a 50 μM working solution (5 mL) of **QHCX (X = 1 or 2)** in different DMSO and HEPES solvent ratios. Once transferred, the appropriate volume of HEPES buffer (25 mM, pH 7.4) is added to make the desired ratio in a 5 mL working solution. To prepare the stock titrant (10 mM), solutions of the metal(II) chloride salts (Cd(II) and Zn(II)) were made in DMSO. This was diluted to 0.1 $mol \cdot dm^{-3}$ in DMSO, whereby 1.0 μL aliquots (0.1 equivalent) were added to the cuvette containing 2.0 mL of 50 μM **QHCX (X = 1 or 2)**. The titrations were completed until no further spectral changes were observed.

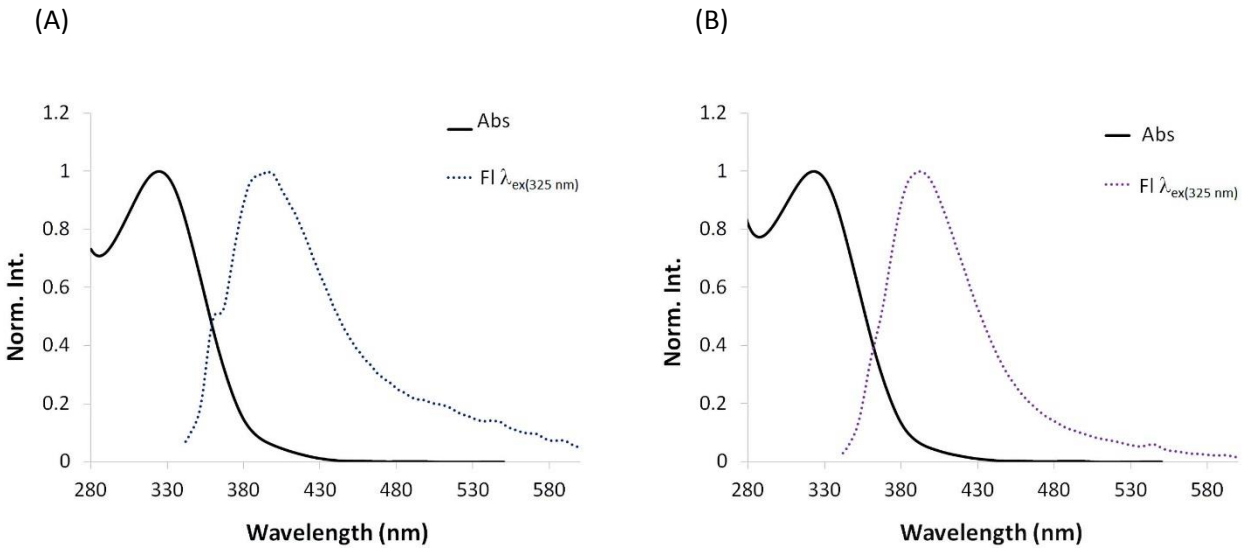


**Fig. S44 QHC2** (50 μM in 100% DMSO) (A) spectrum recorded within minutes of the sample prepared and (B) recorded after 24 hours.

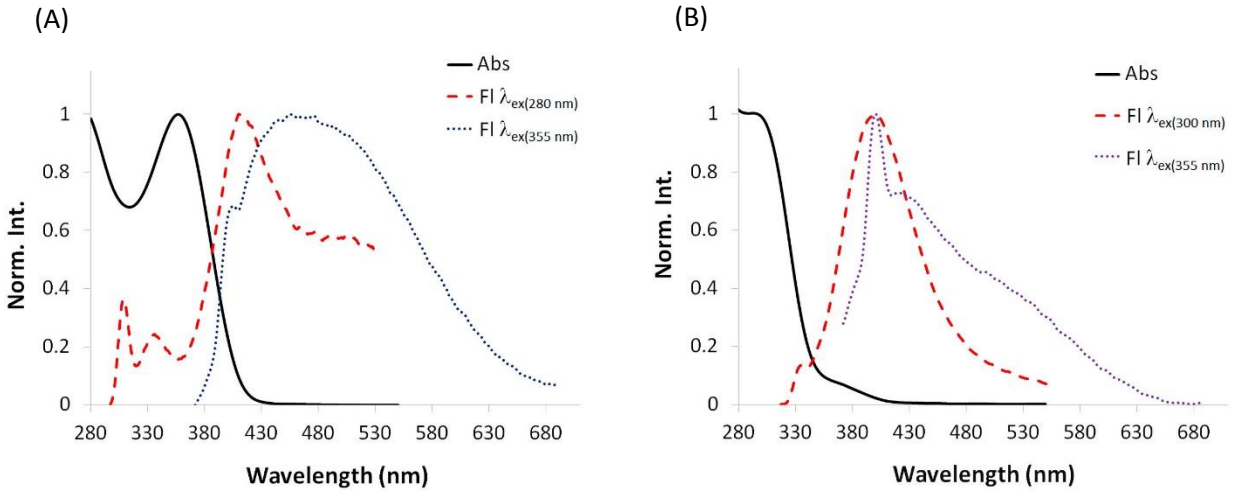


**Fig. S45 QHC2** (50 μM in 50:50 DMSO:HEPES) (A) spectrum recorded within minutes of the sample prepared and (B) recorded after 24 hours.

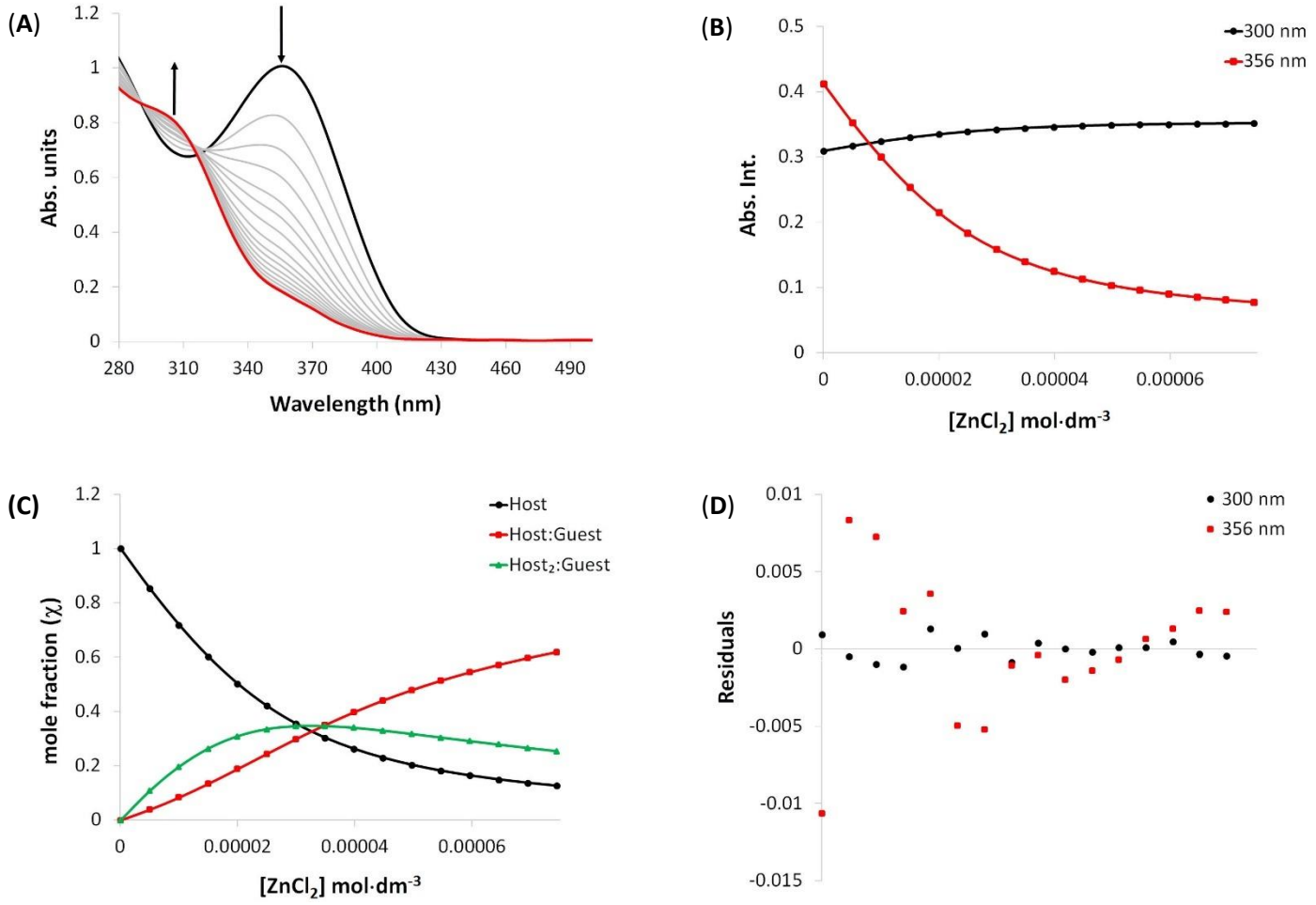


**Fig. S46** (A) Absorbance spectra of **QHC2** upon the incremental addition of $ZnCl_2$, up to 1.5 equivalents in DMSO:HEPES (50:50) (B) Nonlinear least squares binding isotherm (C) mole fraction ($\chi$) whereby the host represents **QHC2-**black circles, the guest is $Zn^{2+}$ ions and the host:guest complex ($K_{11}$) represents [Zn(**QHC2**)]$^{2+}$-red squares and host$_2$:guest signifies ($K_{21}$) [Zn(**QHC2**)$_2$]$^{2+}$-green triangles (D) residual plot from the experimental data. The data was calculated using Bindfit and the model was fitted to Nelder-Mead (non-cooperative).

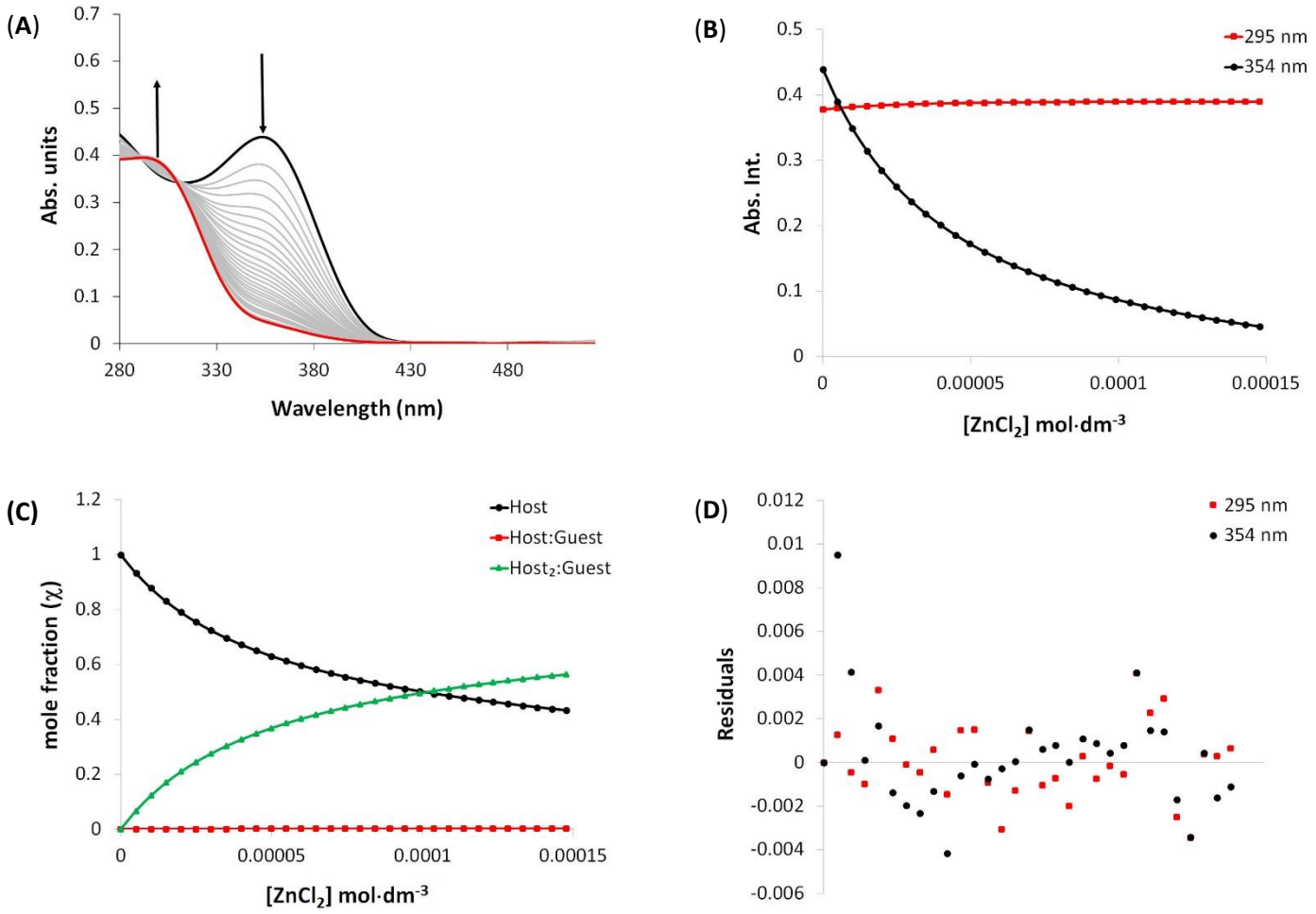


**Fig. S47** (A) Absorbance spectra of **QHC2** upon the incremental addition of $ZnCl_2$, up to 3.0 equivalents in DMSO:HEPES (25:75) (B) Nonlinear least squares binding isotherm (C) mole fraction ($\chi$) whereby the host represents **QHC2-**black circles, the guest is $Zn^{2+}$ ions and the host:guest complex ($K_{11}$) represents [Zn(**QHC2**)]$^{2+}$-red squares and host$_2$:guest signifies ($K_{21}$) [Zn(**QHC2**)$_2$]$^{2+}$-green triangles (D) residual plot from the experimental data. The data was calculated using Bindfit and the model was fitted to Nelder-Mead (full).

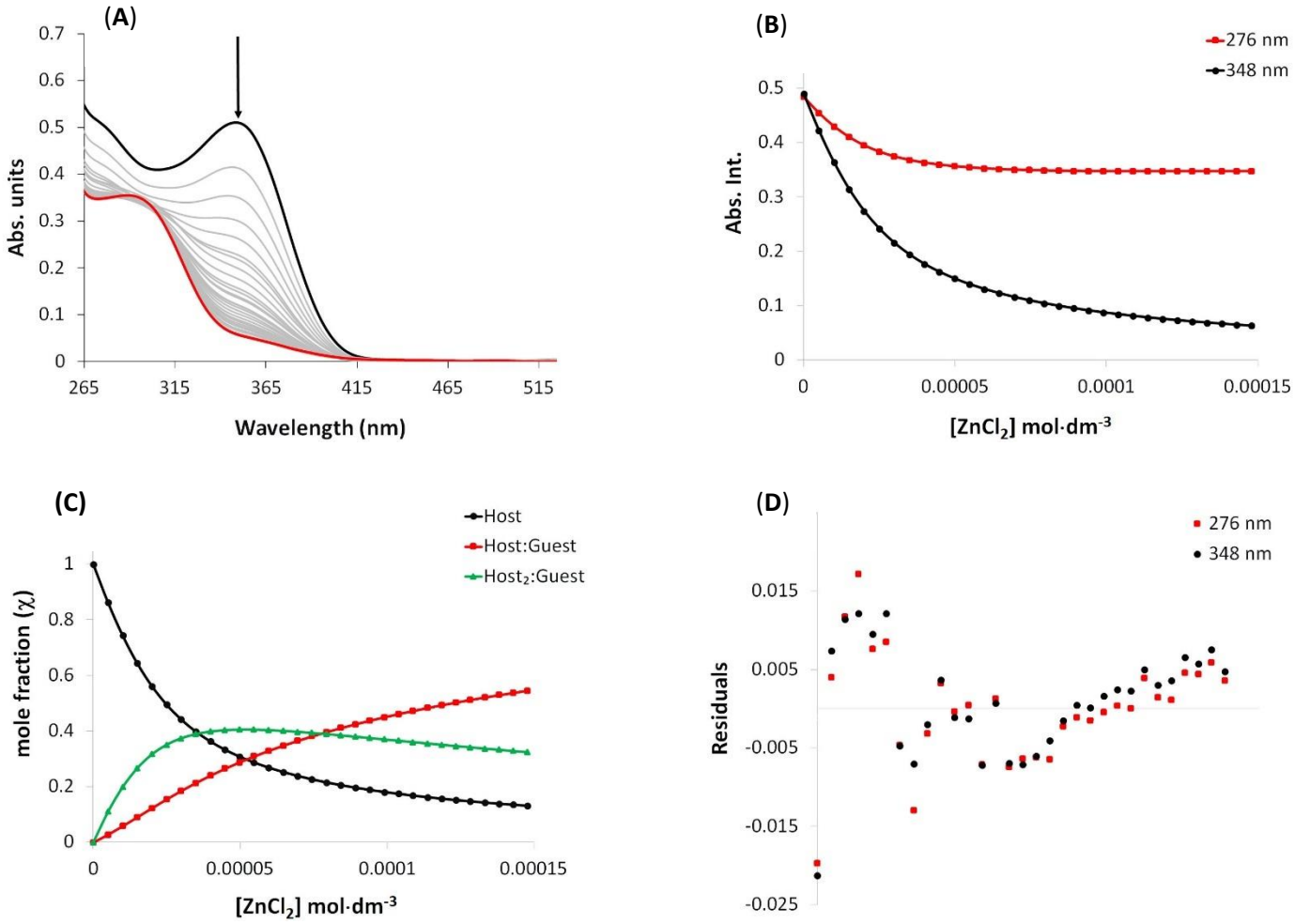


**Fig. S48** (A) Absorbance spectra of **QHC2** upon the incremental addition of $ZnCl_2$, up to 1.5 equivalents in DMSO:HEPES (5:95) (B) Nonlinear least squares binding isotherm (C) mole fraction ($\chi$) whereby the host represents **QHC2-**black circles, the guest is $Zn^{2+}$ ions and the host:guest complex ($K_{11}$) represents $[Zn(\mathbf{QHC2})]^{2+}$-red squares and $host_2$:guest signifies ($K_{21}$) $[Zn(\mathbf{QHC2})_2]^{2+}$-green triangles (D) residual plot from the experimental data. The data was calculated using Bindfit and the model was fitted to Nelder-Mead (full).

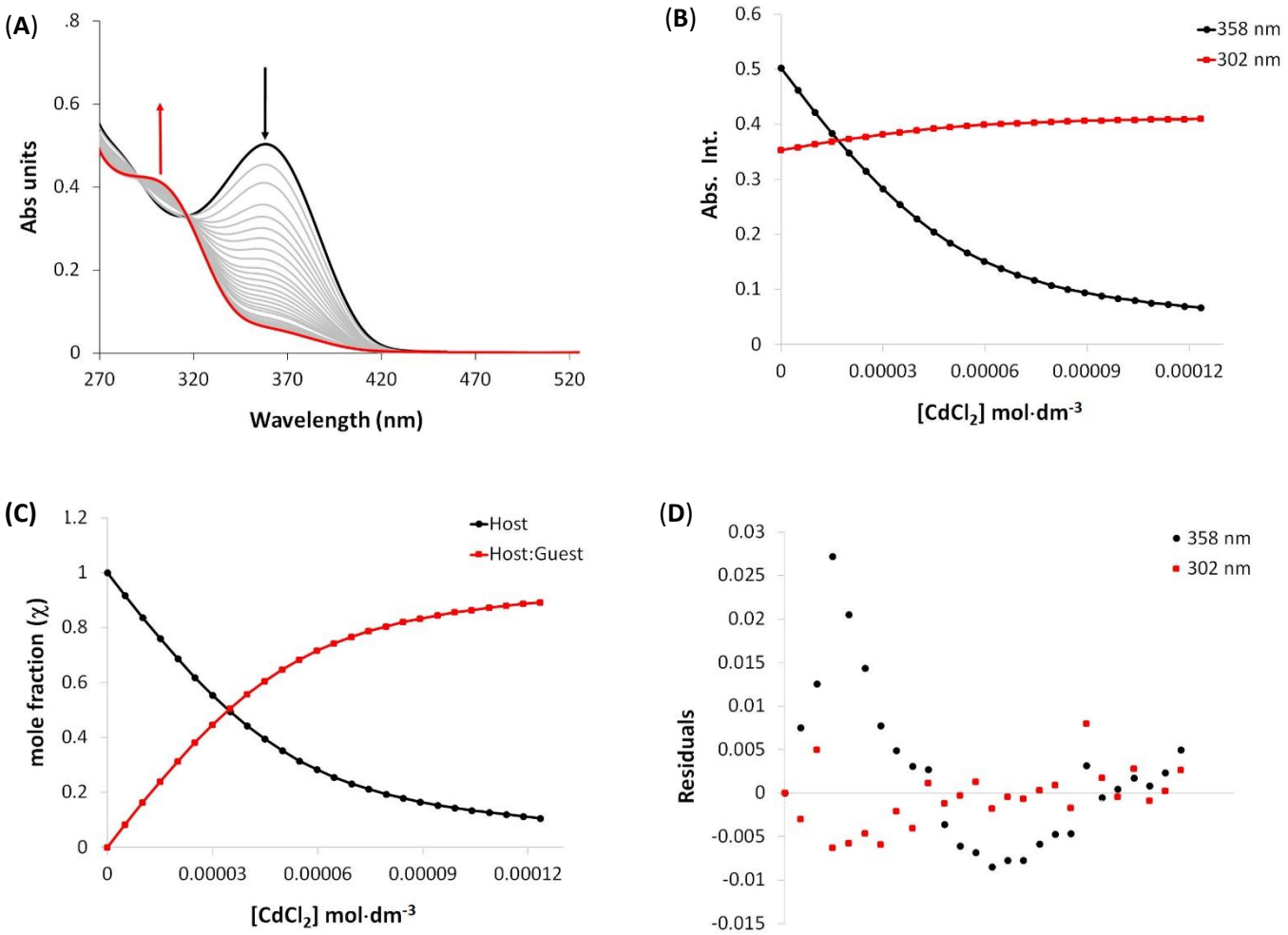


**Fig. S49** (A) Absorbance spectra of **QHC2** upon the incremental addition of $CdCl_2$, up to 2.5 equivalents in DMSO:HEPES (50:50) (B) Nonlinear least squares binding isotherm (C) mole fraction (χ) whereby the host represents **QHC2-**black circles, the guest is $Cd^{2+}$ ions and the host:guest complex ($K_{11}$) $[Cd(\mathbf{QHC2})]^{2+}$-red squares and (D) residual plot from the experimental data. The data was calculated using Bindfit and the model was fitted to Nelder-Mead (full).

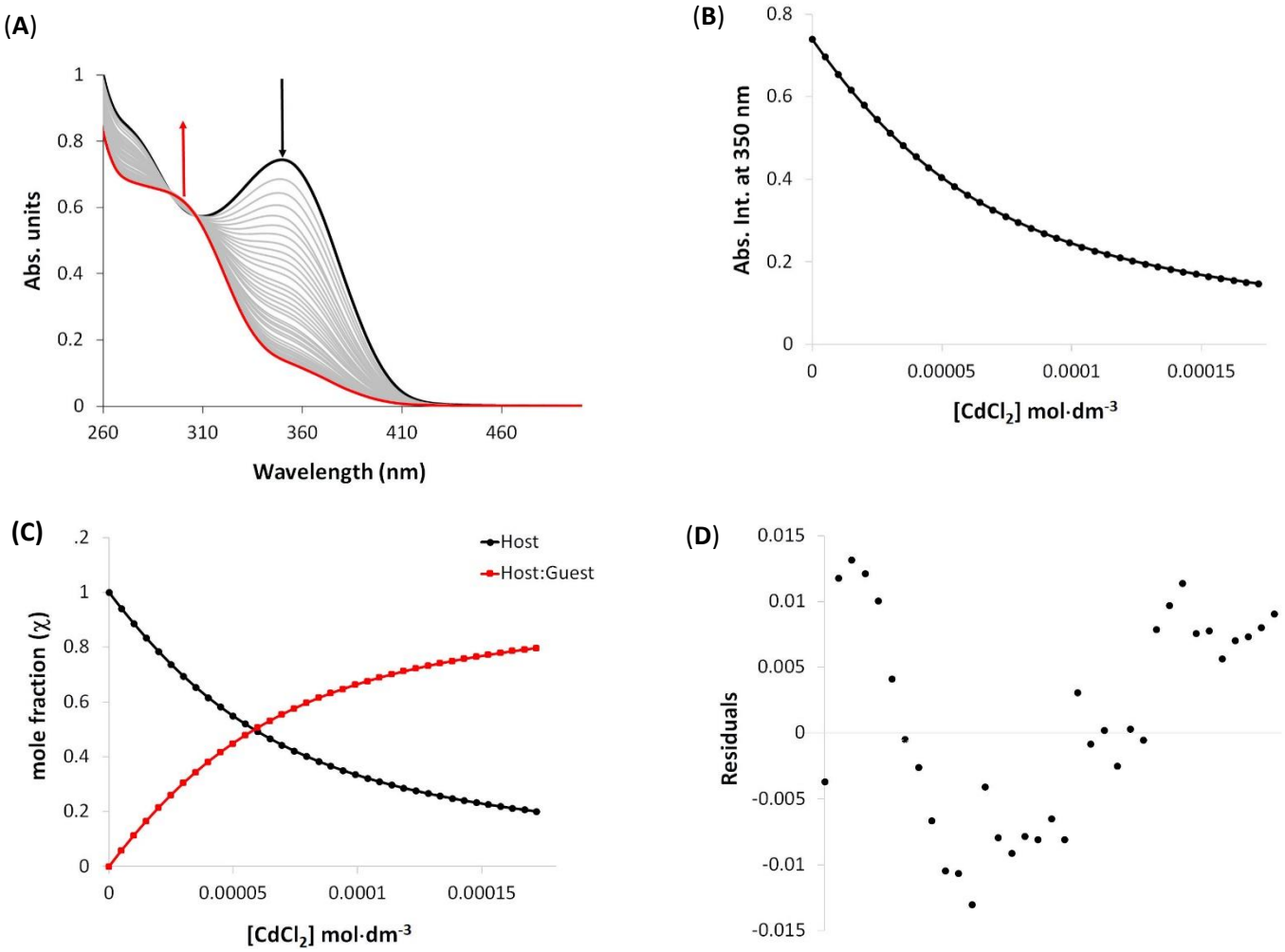


**Fig. S50** (A) Absorbance spectra of **QHC2** upon the incremental addition of $CdCl_2$, up to 3.5 equivalents in DMSO:HEPES (25:75) (B) Nonlinear least squares binding isotherm (C) mole fraction ($\chi$) whereby the host represents **QHC2-**black circles, the guest is $Cd^{2+}$ ions and the host:guest complex ($K_{11}$) $[Cd(\mathbf{QHC2})]^{2+}$-red squares and (D) residual plot from the experimental data. The data was calculated using Bindfit and the model was fitted to Nelder-Mead (full).

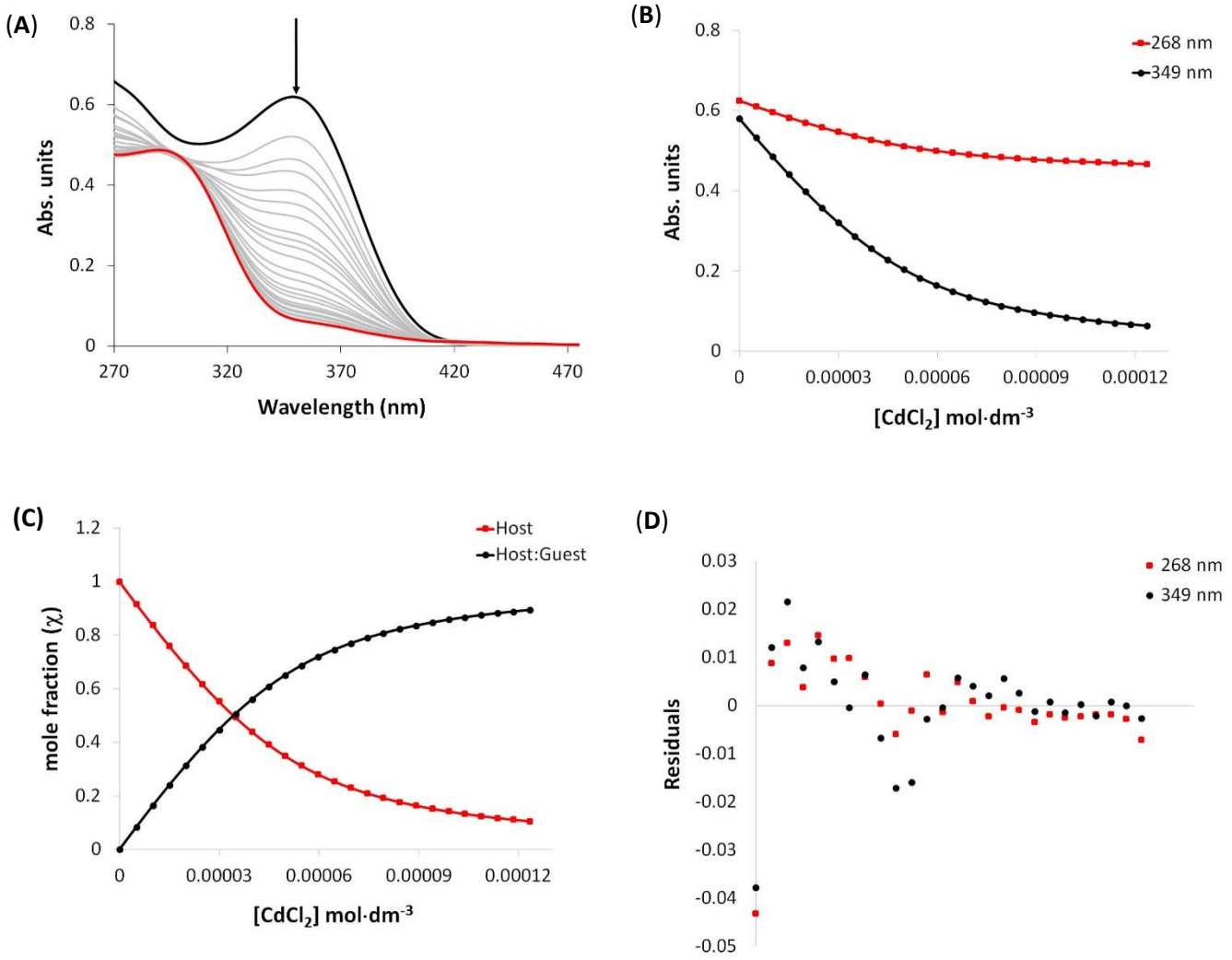


**Fig. S51** (A) Absorbance spectra of **QHC2** upon the incremental addition of $CdCl_2$, up to 3.5 equivalents in DMSO:HEPES (5:95) (B) Nonlinear least squares binding isotherm (C) mole fraction ($\chi$) whereby the host represents **QHC2-**black circles, the guest is $Cd^{2+}$ ions and the host:guest complex ($K_{11}$) $[Cd(\mathbf{QHC2})]^{2+}$-red squares and (D) residual plot from the experimental data. The data was calculated using Bindfit and the model was fitted to Nelder-Mead (full).

# 8.0 Fluorescence Lifetime Studies-Aqueous Media

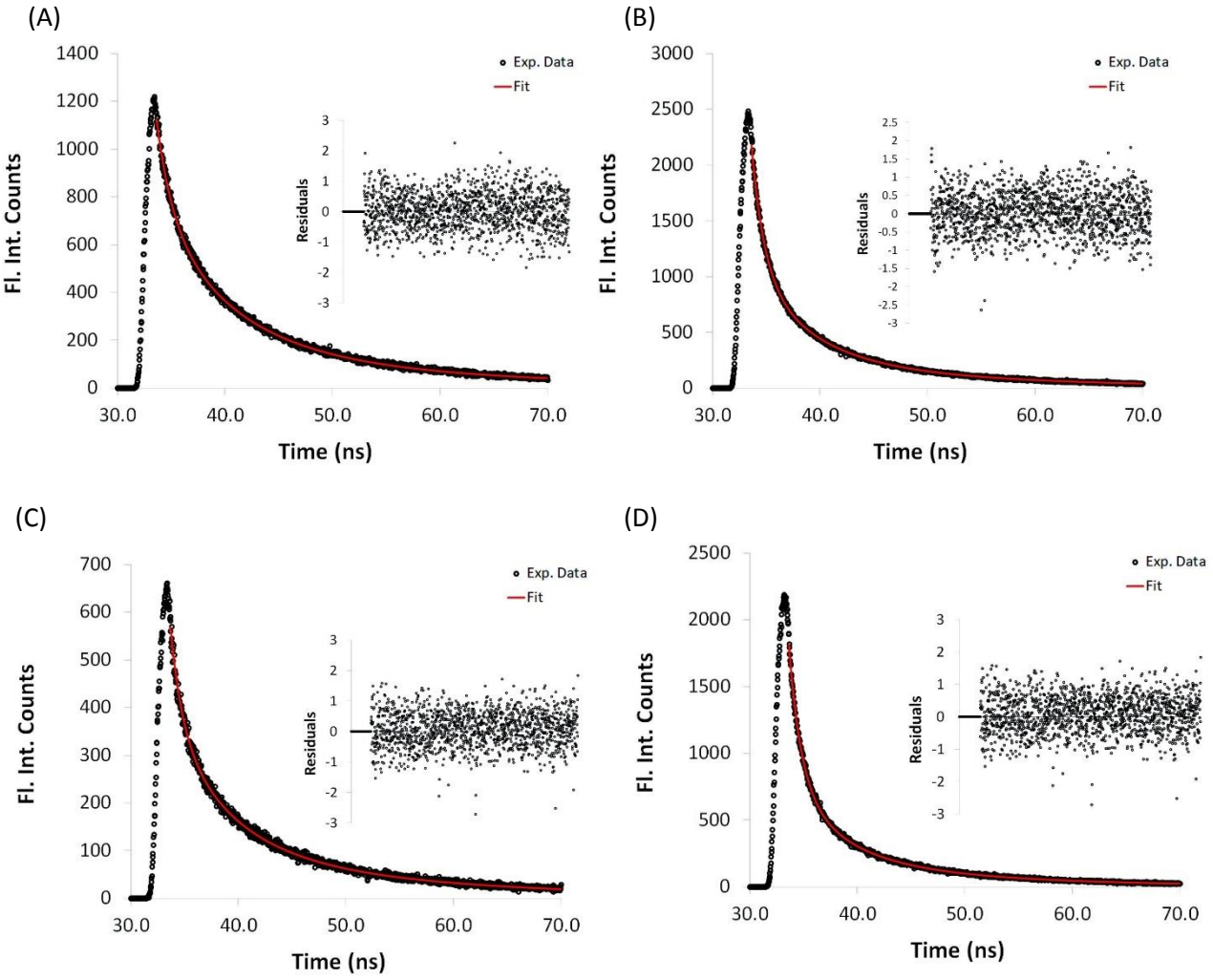


**Fig. S52** (A) Fluorescence lifetime (τ) of **QHC1** in DMSO:HEPES (50:50) using a 300 Nano laser and 400 Nano laser (A) and (C), respectively. Addition of two equivalents of $ZnCl_2$ using a 300 Nano laser and 400 Nano laser (B) and (D). Insert weighted residuals for each experiment (triplicate).

**Table S3** Fluorescence lifetimes (DMSO:HEPES (50:50)) of various reactive species (average of best three runs) using the 300 Nanolaser

| $\lambda_{ex}$ | | $\tau_1$ | $\tau_2$ | $\tau_3$ | $\bar{\tau}$ | A | $\chi^2$ |
|---|---|---|---|---|---|---|---|
| 350 nm | **QHC1** | 6.6(12) | 15.1(14) | 7.4(5) | 7.4(10) | 3.5(3) | 1.04 |
| | | (43.0%) | (35.1%) | (7.3%) | | | |
| | +$ZnCl_2$ | 5.13(12) | 12.5(11) | 7.2(6) | 6.3(10) | 2.3(3) | 1.06 |
| | | (36.0%) | (40.5%) | (23.5%) | | | |
| 400 nm | **QHC1** | 5.2(7) | 16.7(7) | 1.2(1) | 4.7(5) | 4.9(3) | 1.03 |
| | | (39.7%) | (47.5%) | (12.8%) | | | |
| | +$ZnCl_2$ | 4.6(9) | 14.7(7) | 1.1(1) | 3.9(6) | 3.1(3) | 1.09 |
| | | (34.5%) | (48.7%) | (12.4%) | | | |

Note: lifetime-τ, average lifetime- $\bar{\tau}$ , pre-exponential factor-A, and Chi-squared-χ2. Parenthesis relative amplitude

# 9.0 Molecular Modelling

**Table S4** Gibbs free energies for isomers of **QHC2** in the gas phase and a DMSO or aqueous solvent continuum (au) and their relative energies ($kJ \cdot mol^{-1}$)

| | G (au) | | | □G ($kJmol^{-1}$) | | |
|---|---|---|---|---|---|---|
| | gas | DMSO | Water | gas | DMSO | Water |
| A | -1427.94882 | -1427.97064 | -1427.98237 | 18.98 | 10.58 | 15.72 |
| B | **-1427.95605** | **-1427.97467** | -1427.98406 | **0.00** | **0.00** | 11.29 |
| C | -1427.94939 | -1427.96471 | -1427.97553 | 17.48 | 26.15 | 33.68 |
| D | -1427.95428 | -1427.96991 | **-1427.98836** | 4.65 | 12.50 | **0.00** |
| E | -1427.94954 | -1427.96478 | -1427.97558 | 17.09 | 25.96 | 33.55 |
| F | -1427.94929 | -1427.96472 | -1427.97519 | 17.75 | 26.12 | 34.57 |

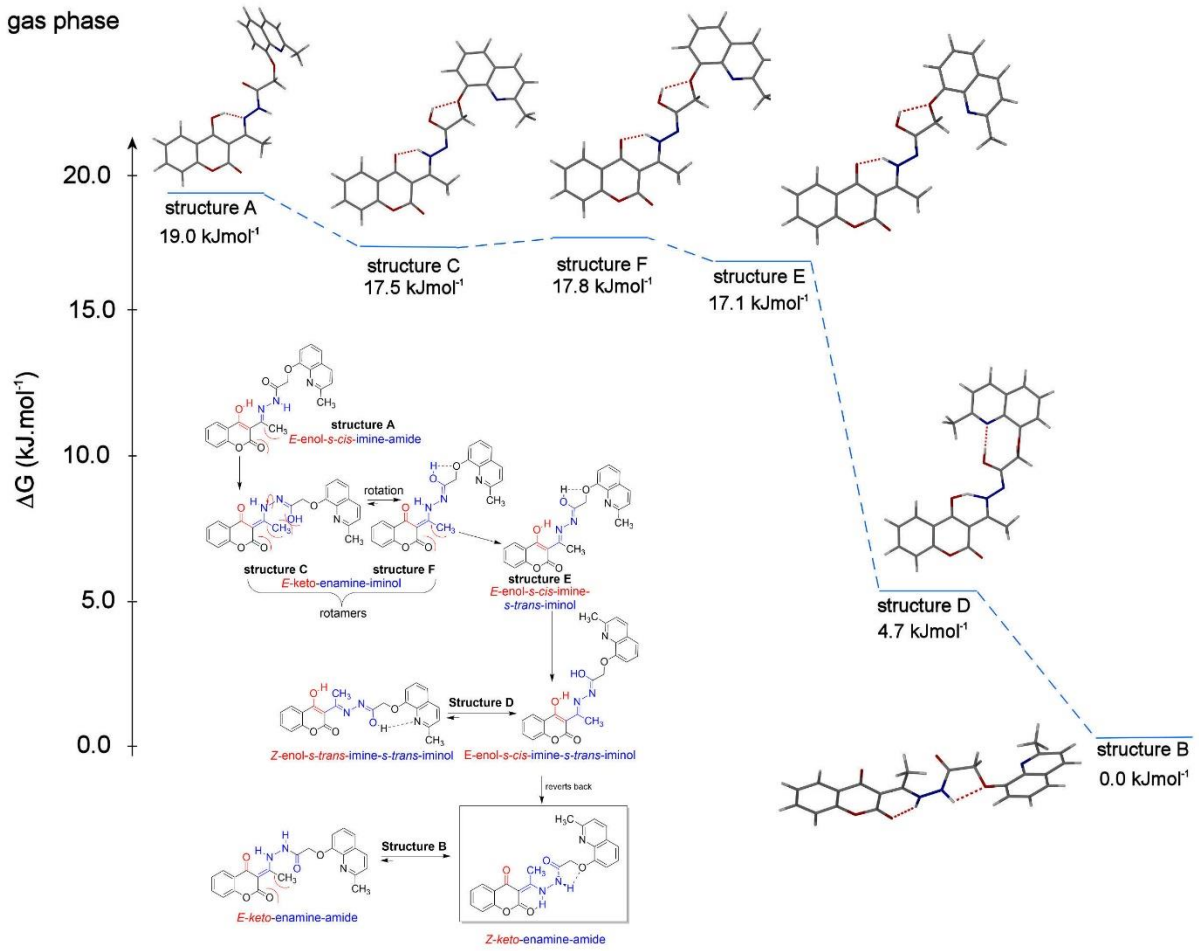


**Fig. S53** DFT calculations (DFT/B3LYP/6-31G*) of the potential isomers and tautomers of **QHC2** in the gas phase.

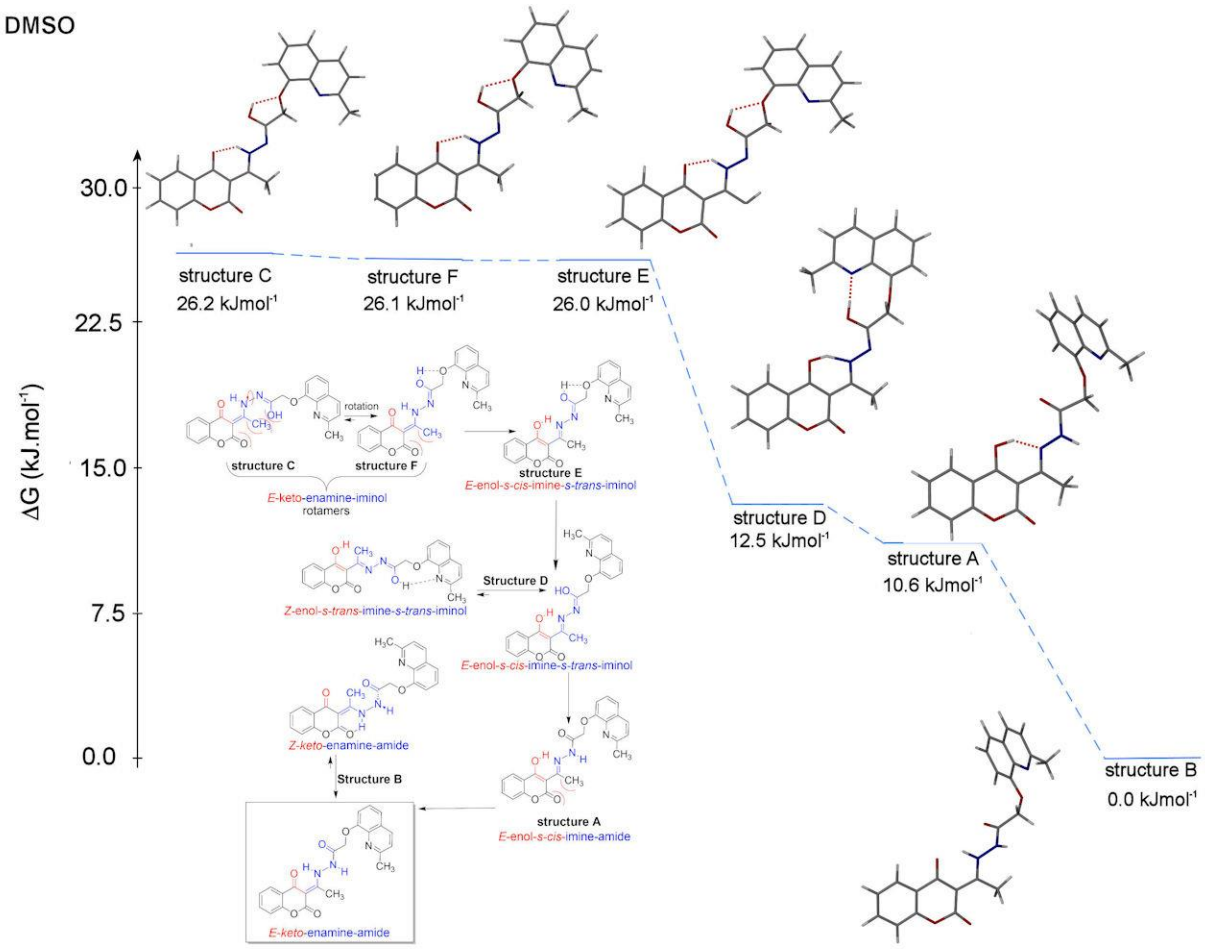


**Fig. S54** DFT calculations (DFT/B3LYP/6-31G*) of the potential isomers and tautomers of **QHC2** in a DMSO continuum.

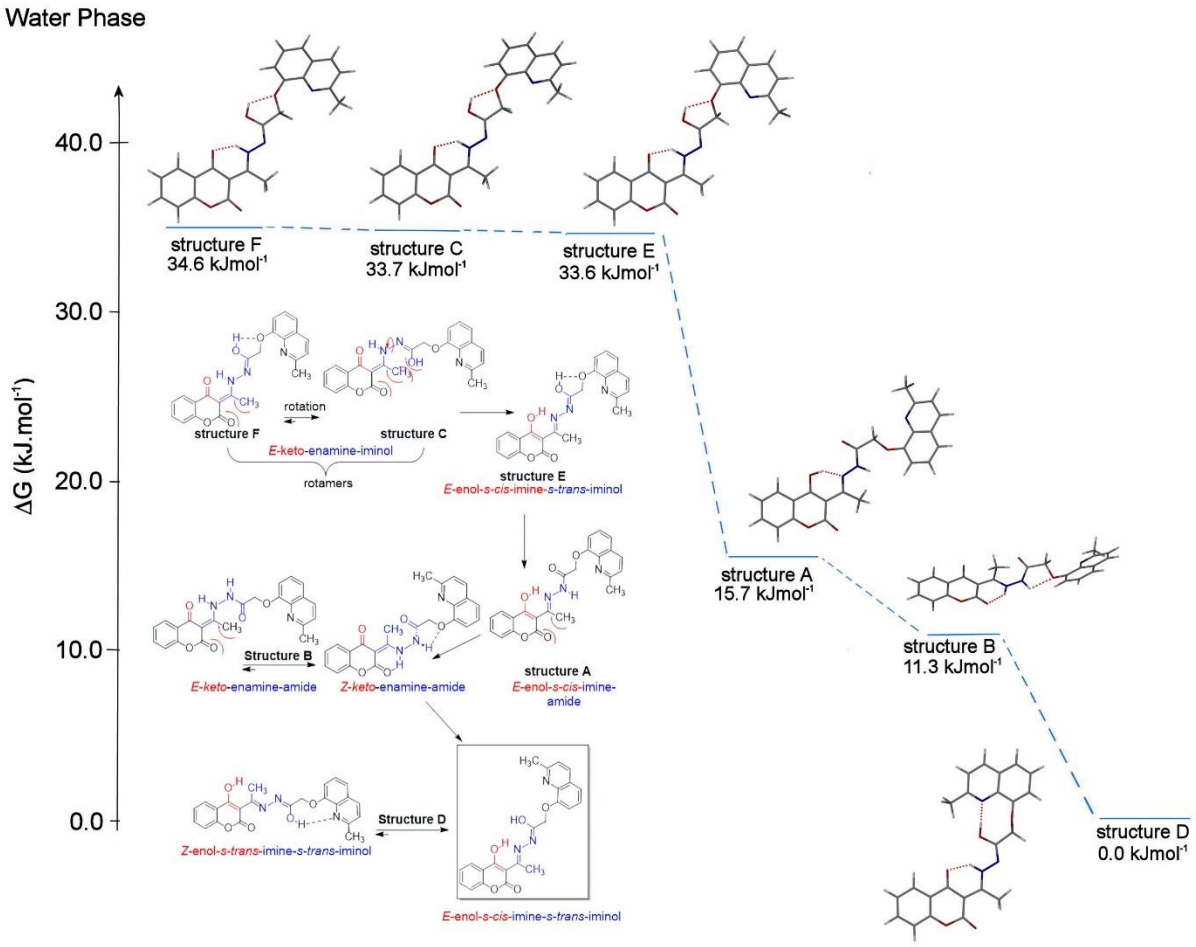


**Fig. S55** DFT calculations (DFT/B3LYP/6-31G*) of the potential isomers and tautomers of **QHC2** in the water continuum.

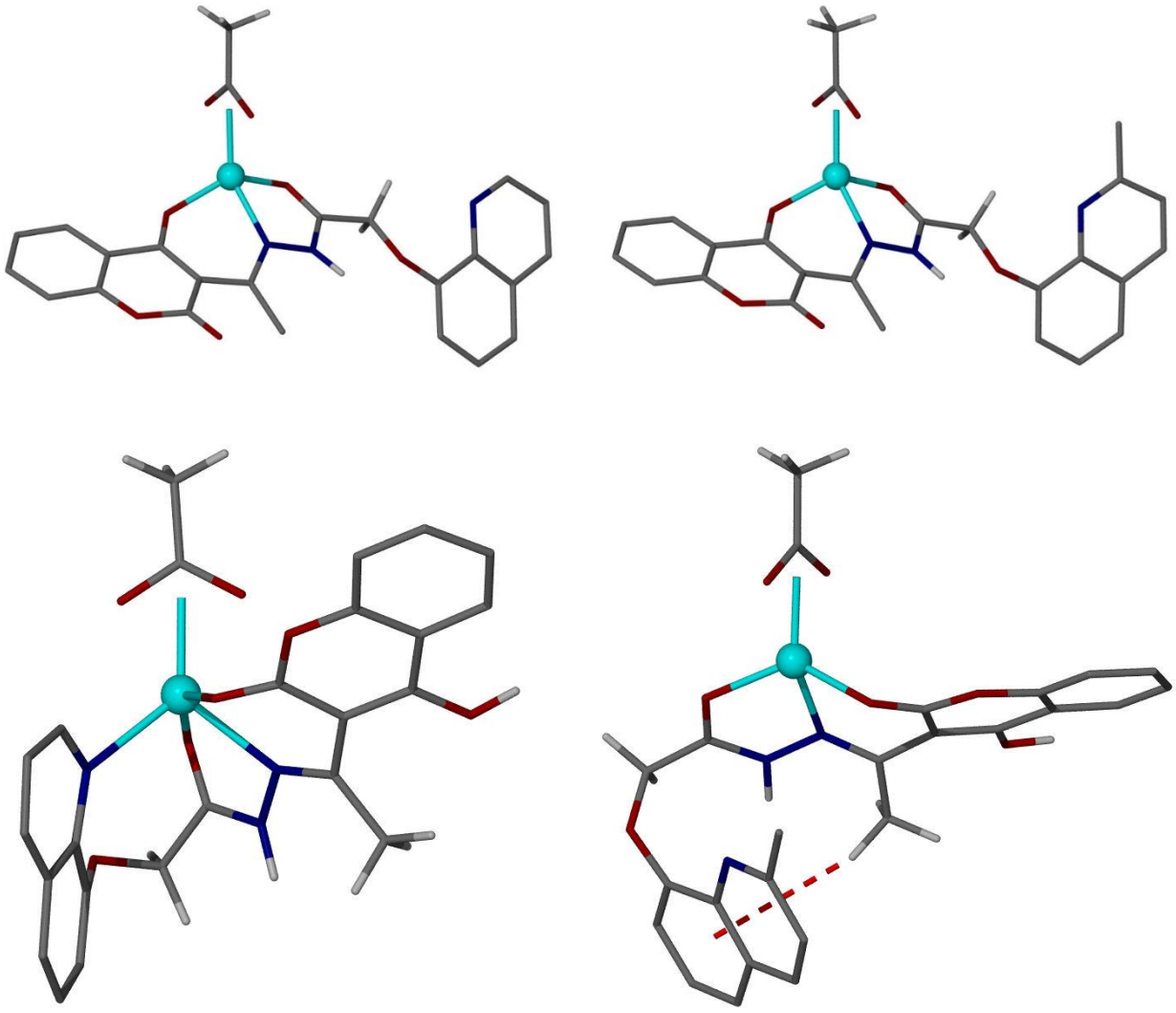

**Fig. S56** Minimized tetrahedral and trigonal pyramidal geometry (CN4 and CN5).

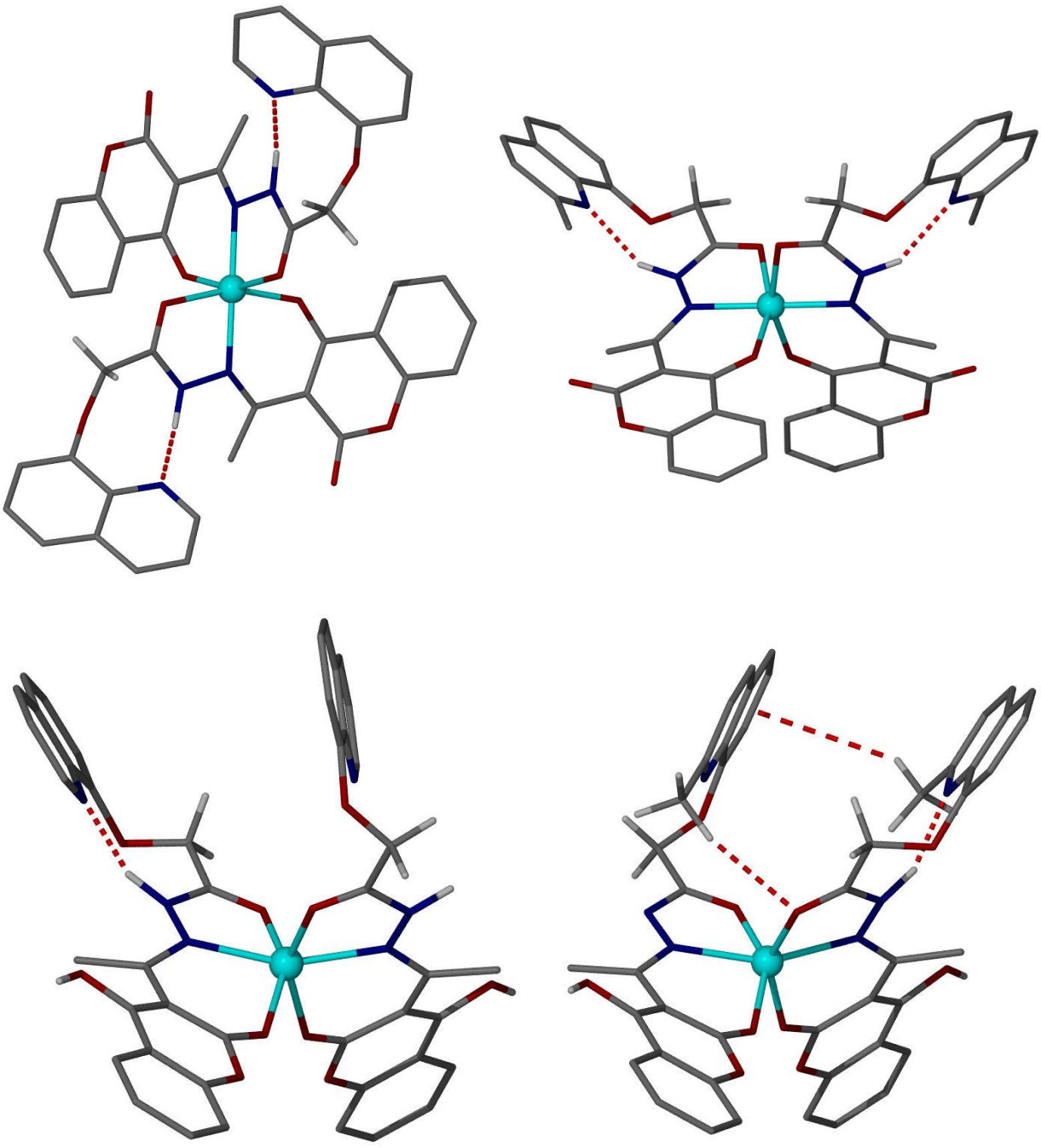

**Fig. S57** Minimized *syn* and *anti*-octahedral geometry (CN4 and CN5).

## 10.0 Cell Viability, Treatment, and Imaging

Human embryonic kidney (HEK293) cells were used to assess cytotoxicity. HEK293 cells were grown under standard conditions (37°C, 5% $CO_2$, DMEM media with 10% FBS and 1% antibiotic-antimycotic). Sensor dyes were incubated with cells for 24 h incubation period at concentrations that range from 500 ng·μL$^{-1}$ to 50 μg·μL$^{-1}$. Cell viability was evaluated with a CyQUANT LDH Cytotoxicity Assay Kit (Invitrogen) using a microplate reader (BioTek Synergy H1). In adherence to manufacturer protocols, both negative and positive controls are used in the assay. Experimental values were transformed based on two values: zero-cytotoxicity value (background) and 100% cytotoxicity value (cells treated with lysis buffer based on manufacturer protocol). Each experiment is represented by relative values based on the control values. The Tukey-HSD ANOVA statistical method was applied to determine significant differences.

For confocal imaging, HEK293 cells grown in a glass bottom culture vessel were incubated in sensor-dyes at 2.5 μg·mL$^{-1}$. Cells and sensor-dyes were incubated overnight. Prior to imaging, 10 μmol·dm$^{-3}$ of zinc chloride or cadmium chloride was added to the cells. Cells were washed with sterile PBS before imaging. Fluorescence associated with dyes in the absence or presence of either salt was observed with the Leica Stellaris STED confocal microscope

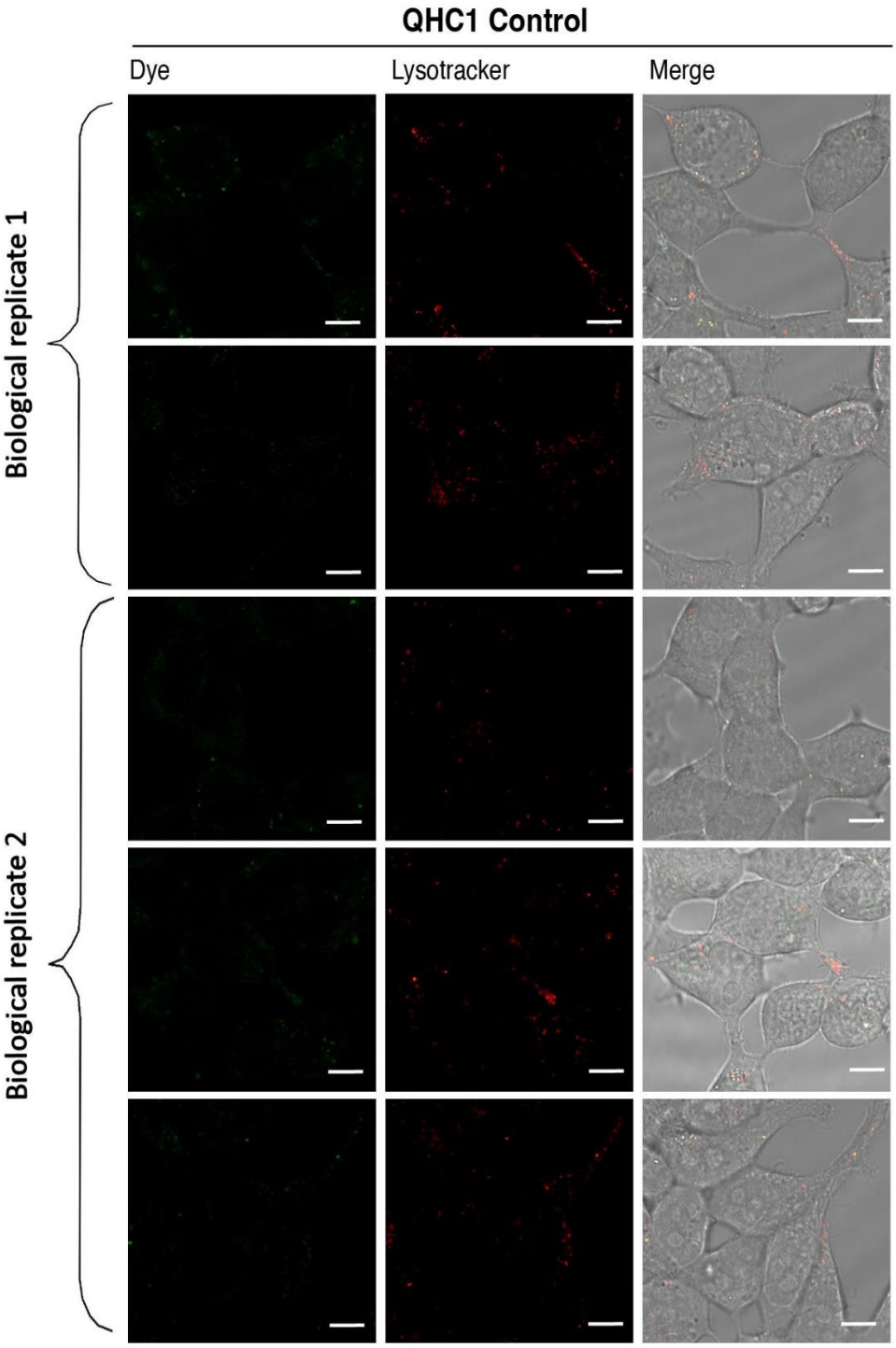


**Fig. S58** Fluorescence image of **QHC1** (2.5 μg·mL$^{-1}$) without $ZnCl_2$ or $CdCl_2$ in live HEK293 cells. Lysotracker deep red labels lysosomes in the middle track and last track is bright field showing the merge of dye and lysotracker. Minimal signal is seen in lysosomes for **QHC1** in cells loaded with probes alone. Scale bar = 5 μm.

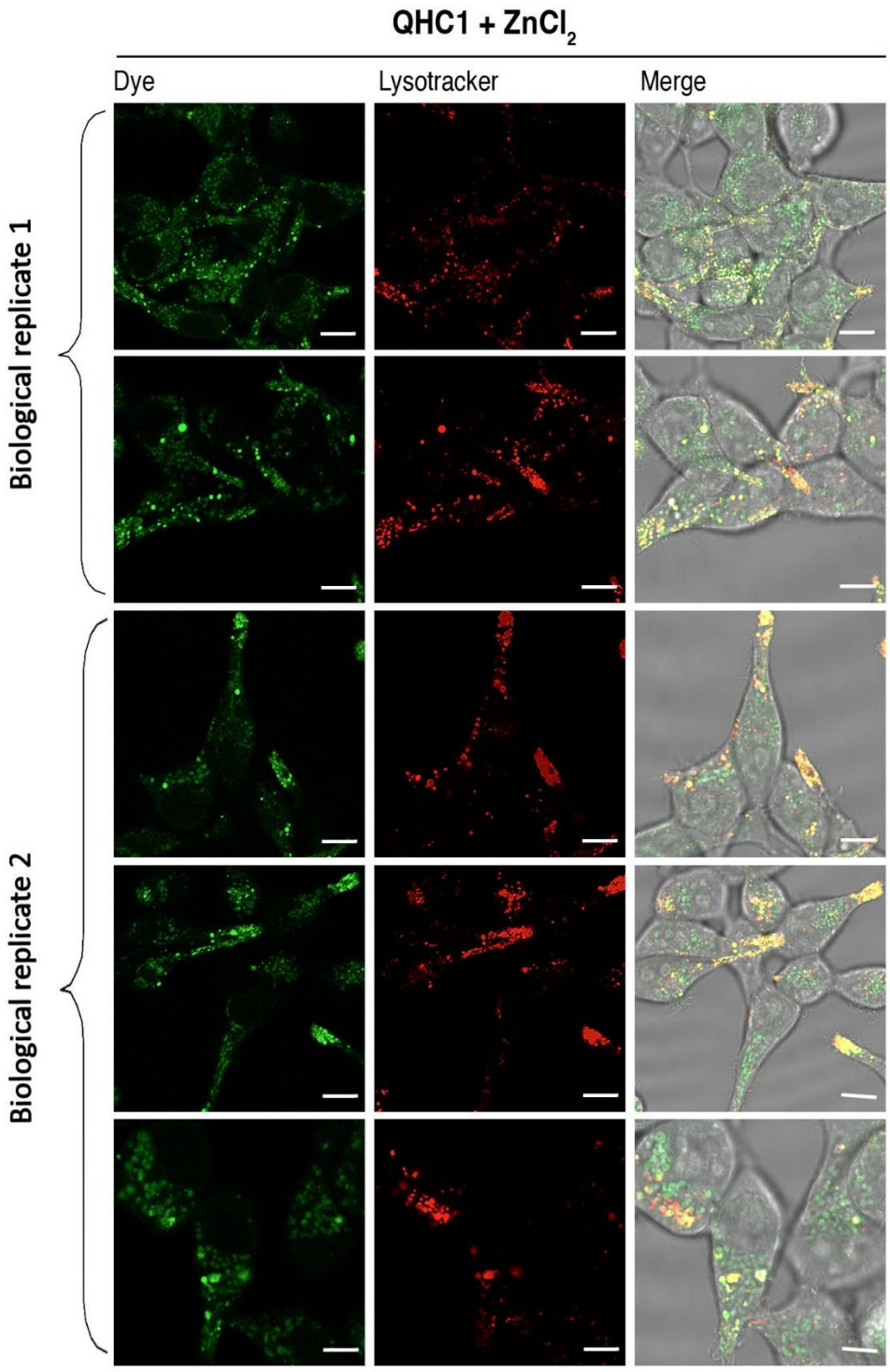


**Fig. S59** Fluorescence image of **QHC1** (2.5 μg·mL$^{-1}$) with $ZnCl_2$ (10 μmol·dm$^{-3}$) in live HEK293 cells. When $ZnCl_2$ is added, probes significantly accumulate in lysosomes. Lysotracker deep red labels lysosomes in the middle track and last track is bright field showing the merge of dye and lysotracker. Scale bar = 5 μm

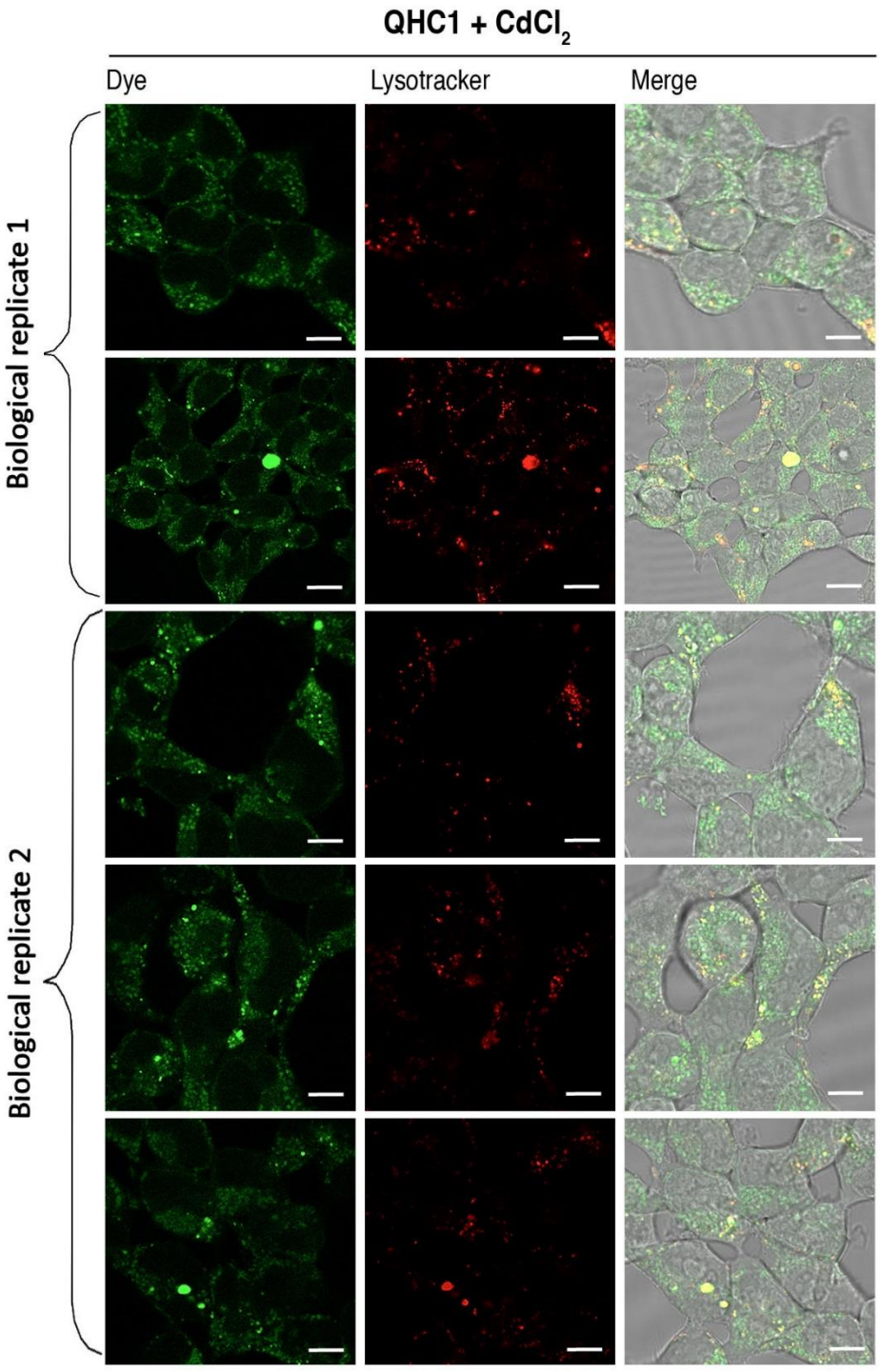


**Fig. S60** Fluorescence image of **QHC1** (2.5 μg·mL$^{-1}$) with $CdCl_2$ (10 μmol·dm$^{-3}$) in live HEK293 cells. When $CdCl_2$ is added, probes are significantly localized in the cytoplasm with some accumulation in lysosomes. Lysotracker deep red labels lysosomes in the middle track and last track is bright field showing the merge of dye and lysotracker. Scale bar = 5 μm.

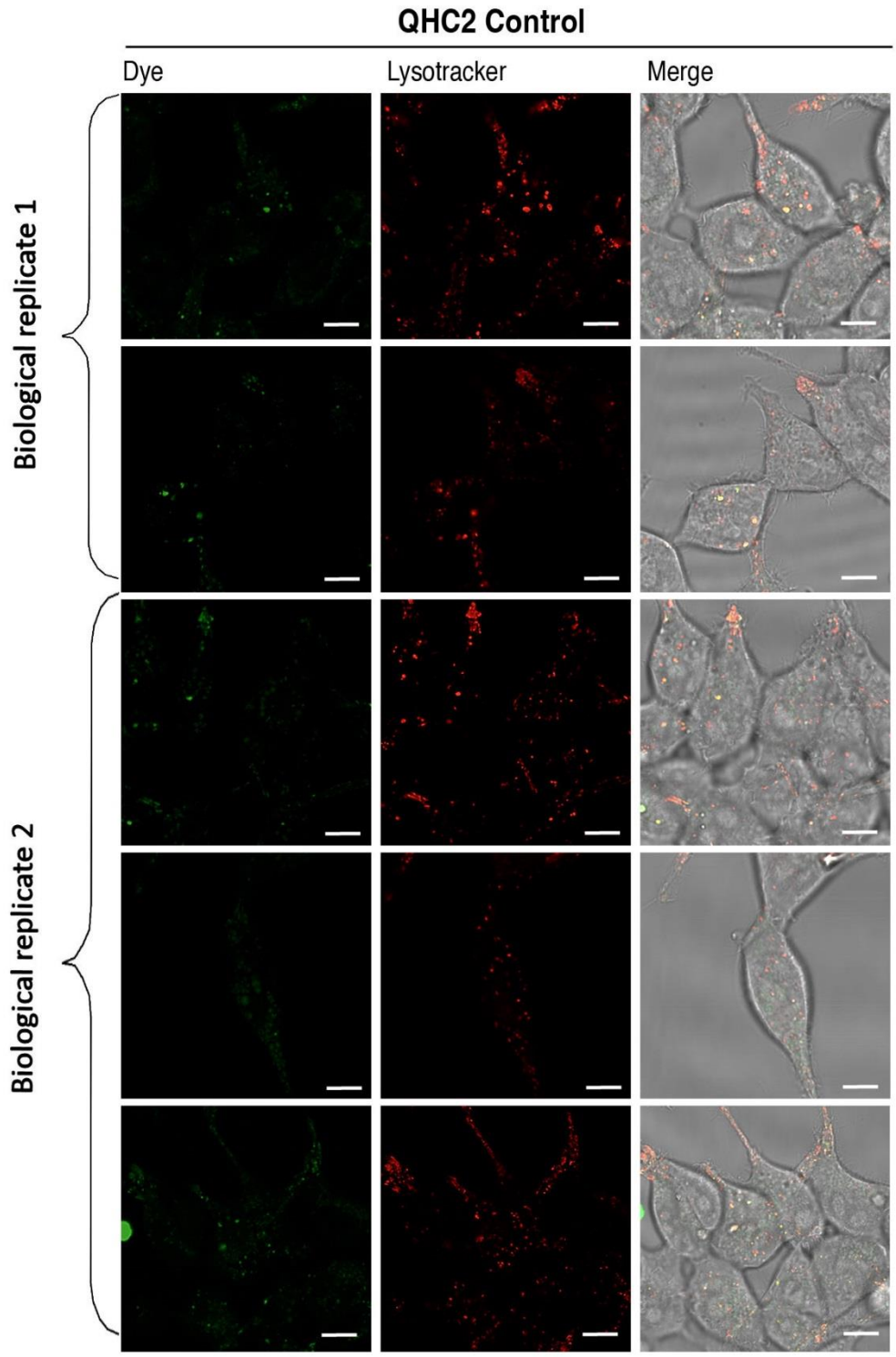


**Fig. S61** Fluorescence image of **QHC2** (2.5 μg·mL$^{-1}$) without $ZnCl_2$ or $CdCl_2$ in live HEK293 cells. Lysotracker deep red labels lysosomes in the middle track and last track is bright field showing the merge of dye and lysotracker. Minimal signal is seen in lysosomes for **QHC2** in cells loaded with probes alone. Scale bar = 5 μm.

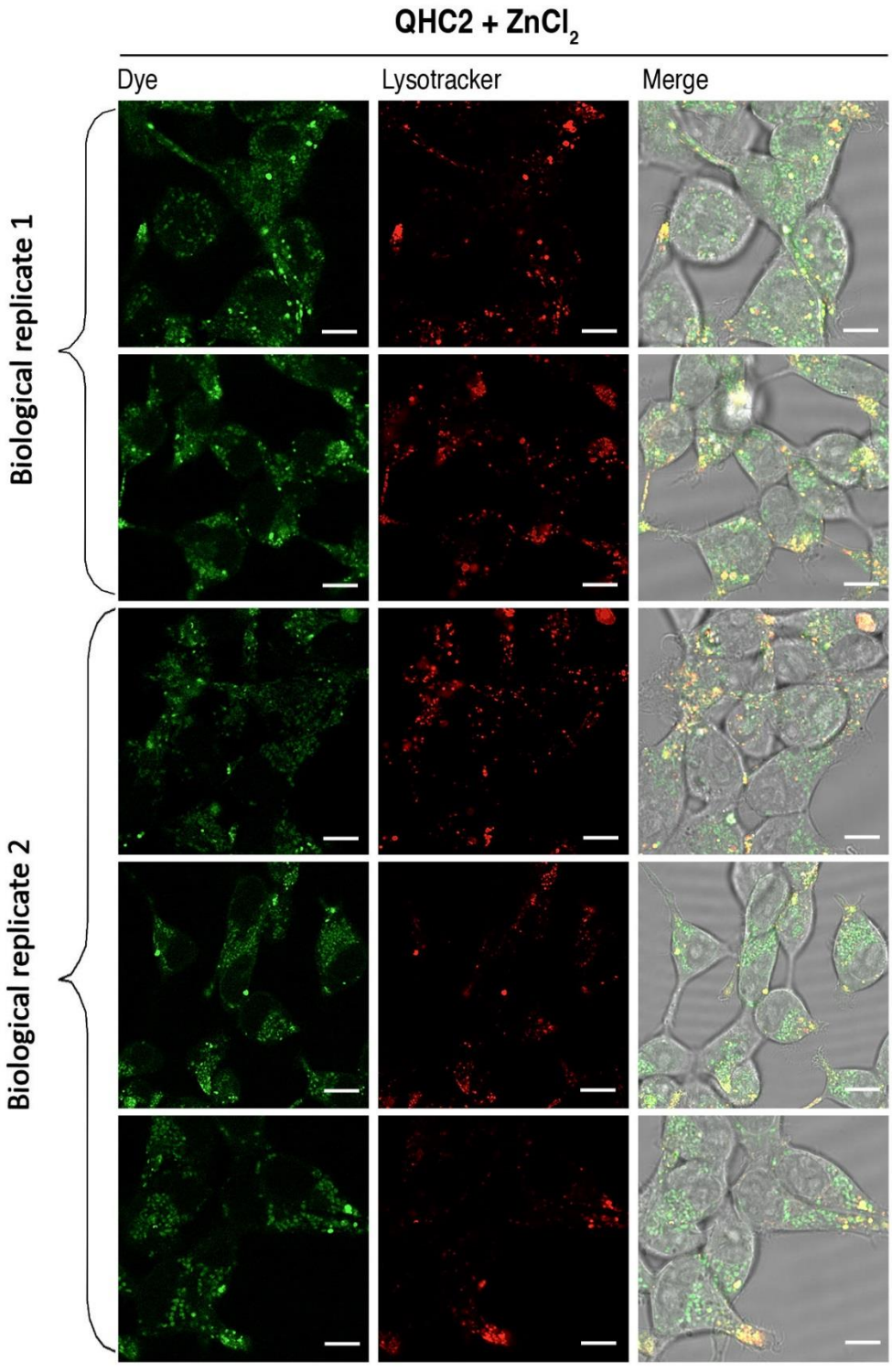


**Fig. S62** Fluorescence image of **QHC2** (2.5 μg·mL$^{-1}$) with $ZnCl_2$ (10 μmol·dm$^{-3}$) in live HEK293 cells. When $ZnCl_2$ is added, probes significantly accumulate in lysosomes. Lysotracker deep red labels lysosomes in the middle track and last track is bright field showing the merge of dye and lysotracker. Scale bar = 5 μm.

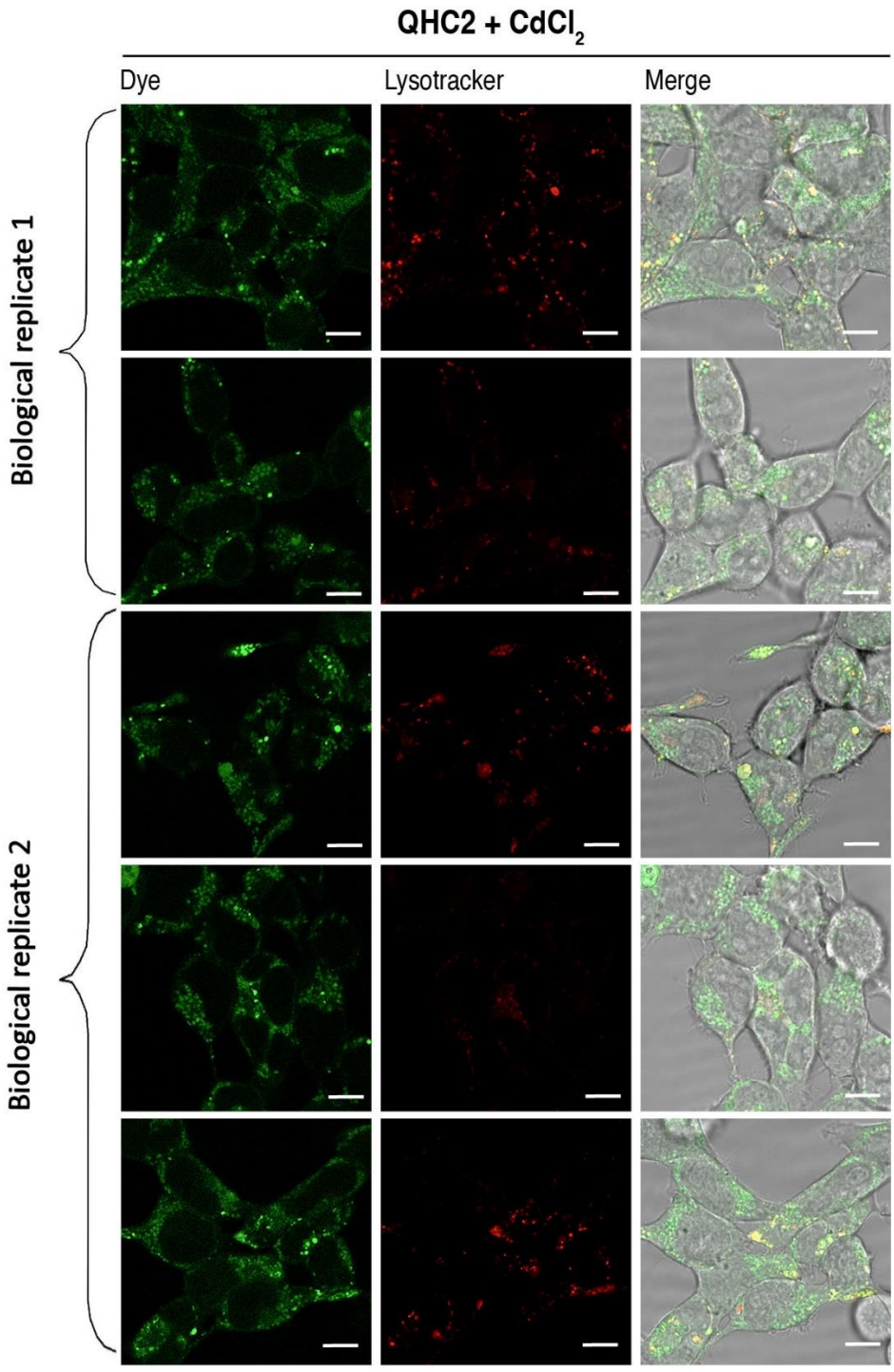


**Fig. S63** Fluorescence image of **QHC2** (2.5 μg·mL$^{-1}$) with $CdCl_2$ (10 μmol·dm$^{-3}$) in live HEK293 cells. When $CdCl_2$ is added, probes are significantly localized in the cytoplasm with some accumulation in lysosomes. Lysotracker deep red labels lysosomes in the middle track and last track is bright field showing the merge of dye and lysotracker. Scale bar = 5 μm.

## 11.0 References


1. W. I. Spartan ’20, Irvine CA 92612 USA, 2020.
2. M. Gardelly, B. Trimech, M. Horchani, M. Znati, H. B. Jannet and A. Romdhane, Anti-tyrosinase and anti-butyrylcholinesterase quinolines-based coumarin derivatives: synthesis and insights from molecular docking studies, *Chem. Afr.*, 2021, **4**, 491-501.
3. M. Zayene, F. K. Algethami, H. N. Abdelhamid, M. R. Elamin, B. Y. Abdulkhair, Y. O. Al-Ghamdi and H. B. Jannet, New synthetic quinaldine conjugates: Assessment of their anti-cholinesterase, anti-tyrosinase and cytotoxic activities, and molecular docking analysis, *Arabian J. Chem.*, 2022, **15**, 104177.
4. D. B. Hibbert and P. Thordarson, The death of the Job plot, transparency, open science and online tools, uncertainty estimation methods and other developments in supramolecular chemistry data analysis, *Chem. Commun.*, 2016, **52**, 12792-12805.
5. P. Thordarson, Determining association constants from titration experiments in supramolecular chemistry, *Chem. Soc. Rev.*, 2011, **40**, 1305-1323.